POLITECNICO DI TORINO

In collaboration with

University of Strathclyde

Civil Engineering Master

Degree Course

Master Degree Thesis

COLLAPSE FRAGILITY ASSESSMENT FOR STRUCTURES UNDER MULTIPLE EARTHQUAKES

Thesis Tutor

Prof. Ing. Paolo Castaldo

Candidate

Fabrizio Salvatore Stramaglia

Thesis Supervisor

Dr. Enrico Tubaldi

A.A. 2018/2019

...A mia madre

....A mio padre

ABSTRACT

Fragility analysis is crucial for the seismic risk assessment of a structure. Fragility models of works (structures and infrastructures) used nowadays are more likely to focus on the as-built condition, neglecting the possibility that they may be subjected to sequences of close multiple earthquakes sequences (such as mainshock-aftershock sequences) during their service life, and that the final structural damage may be related to the damage due to previous shakes. However, considering that this last scenario has a high probability of occurrence, and that in reality the buildings' performance may no longer be able to satisfy the initial seismic design requirements, it is important to include the effect of past earthquakes in the collapse fragility estimation of buildings.

This study contributes to deepen further this topic by developing methodologies which can simulate the real structural response and estimate collapse fragility when the structure is subjected to multiple stresses, taking into account, for each subsequent shock, the damage accumulated during previous earthquakes. These methodologies are applied in two cases of study: the first one is represented by a structure in which the application of cyclic loads (multiple earthquakes) does not contribute to reduce its stiffness; the second case is represented by the same structure in which however, this time, the transition from one earthquake to another leads to an accumulation of damage due to the dissipation of hysteretic energy and loss of stiffness.

Using the same methodologies, and so the same analyzes, different response parameters will be obtained in the two cases. The evaluation of fragility curves will allow to verify how, using this kind of analysis, the structural degradation affects the overall response again the application of these loads; in succession to this last check, the impact of previous shocks will be examined, in particular their degree of influence in the final collapse capacity of the structure.

Final results will confirm or not the efficiency of the methodologies used: if their estimate more or less reflects the real behavior of the structure in the same loading conditions, then these new fragility analyzes may be useful in the future in the decision-making processes related to the design of buildings in seismic area.

SOMMARIO

L'analisi sulla fragilità è fondamentale per la valutazione del rischio sismico di una struttura. I modelli di fragilità delle opere (strutture e infrastrutture) utilizzati al giorno d'oggi sono più propensi a concentrarsi sull'edificio nelle condizioni intatte, non tenendo conto della possibilità che possano essere sottoposti a sequenze di terremoti multipli ravvicinati (come ad esempio sequenze mainshock-aftershock) durante la loro vita utile, e che il danno finale della struttura possa essere correlato ai danni causati dalle scosse precedenti. Tuttavia, considerando che quest'ultimo scenario ha un'alta probabilità di occorrenza, e che nella realtà le prestazioni degli edifici potrebbero non essere più in grado di soddisfare i requisiti di progettazione sismica di partenza, è importante includere l'effetto dei terremoti dei precedenti nella stima della fragilità degli edifici.

Questo studio contribuisce ad approfondire ulteriormente la problematica sviluppando metodologie in grado di simulare la reale risposta strutturale e di stimare la fragilità a collasso quando la struttura è sottoposta a sollecitazioni multiple, tenendo conto, per ogni scossa successiva, del danno cumulato durante i terremoti precedenti. Queste metodologie vengono applicate in due casi di studio: il primo rappresentato da una struttura nel quale l'applicazione di carichi ciclici (terremoti multipli) non contribuisce a ridurne la rigidezza; il secondo caso è rappresentato dalla stessa struttura nel quale, questa volta, il passaggio da un terremoto all'altro comporta un accumulo di danno per dissipazione energetica e perdita di rigidezza.

Utilizzando le stesse metodologie, e quindi le stesse analisi, si otterranno parametri di risposta diversi nei due casi. La valutazione delle curve di fragilità permetterà di verificare se e come, utilizzando questo tipo di analisi, il degrado della struttura influenzi la risposta complessiva all'applicazione di tali carichi; in successione a tale controllo verrà esaminato l'impatto delle scosse precedenti, in particolare il loro grado di influenza nella capacità di collasso finale del struttura.

I risultati finali confermeranno o meno l'efficienza delle metodologie utilizzate: se la loro stima rispecchia più o meno il comportamento reale della struttura nelle stesse condizioni di carico, allora queste nuove analisi sulla fragilità potrebbero risultare utili in futuro nei processi decisionali relativi alla progettazione di edifici in zona sismica.

ACKNOWLEDGEMENTS

I would like to express profound gratitude to my supervisor, Prof. Ing. Paolo Castaldo, Associate Professor at the Department of Structural Building Engineering and Geotechnical in the Polytechnic University of Turin, for having significatively contributed to enrich my baggage of cultural experiences, allowing me to conclude this cycle of study in a foreign University and always giving me all necessary support before, during and after this beautiful experience .

I sincerely thank my co-supervisor, Dr. Enrico Tubaldi, Lecturer at the Department of Civil and Environmental Engineering in the University of Strathclyde, Glasgow (UK), for giving me the opportunity to cope an issue as interesting as particularly delicate, supporting me when I needed and always helping me with all necessary tools for the realization of the thesis project.

I thank all Professors I've had during my Master's Degree here at the Polytechnic University of Turin, having contributed to improve my civil engineer qualities, and whose courses will be the base for my future career in this field.

It's my duty to thank a special person, Francesco Di Bari, my dear friend, as well as my longtime colleague, with whom I had the immense pleasure of sharing every single moment in this course of studies, from the best to the worst one, personal and professional one; studying with him allowed me to become a better person, a great understanding is born due to the same passion for engineering and the same determination to complete all estabilished objectives, overcoming the many difficulties encountered during the journey and by carrying out professionally our work.

I would also thank my friends and colleagues, Maurizio, Alessio, Roberto, Loris, Nicola and Pierpaolo that help me and encourage me in my study as well as in my life and with whom I shared also funny moments.

Finally, I would also thank my parents and my beautiful girlfriend Veronica for their financial and mental support during my graduate study. It was their encouragement and inspiration that helps me to hardly work and get the degree.

RINGRAZIAMENTI

Vorrei esprimere profonda gratitudine al mio Relatore, il Prof. Ing. Paolo Castaldo, Professore Associato presso il Dipartimento di Ingegneria Strutturale e Geotecnica del Politecnico di Torino, per aver contribuito in modo significativo ad arricchire il mio bagaglio di esperienze culturali, permettendomi di concludere questo ciclo di studi in un Ente straniero e dandomi sempre tutto il supporto necessario prima, durante e dopo questa bellissima esperienza.

Ringrazio sinceramente il mio Co-Relatore, dott. Enrico Tubaldi, docente presso il Dipartimento di Ingegneria Civile e Ambientale all'Università di Strathclyde, Glasgow (Regno Unito), per avermi dato l'opportunità di affrontare un argomento tanto interessante quanto particolarmente delicato, supportandomi nei momenti di difficoltà ed aiutandomi sempre con tutti gli strumenti necessari per la realizzazione del progetto di tesi.

Ringrazio tutti i professori incontrati nel mio percorso di Laurea Magistrale al Politecnico di Torino, avendo contribuito a migliorare le mie qualità di ingegnere civile, ed i cui corsi saranno la base della mia futura carriera in questo campo.

È mio dovere ringraziare una persona speciale, Francesco Di Bari, mio caro amico, nonché il mio collega di vecchia data, con il quale ho avuto l'immenso piacere di condividere ogni singolo momento di questo corso di studi, dal migliore al peggiore, personale e professionale; studiare con lui mi ha permesso di diventare una persona migliore, una grande comprensione nasce dalla stessa passione per l'ingegneria e la stessa determinazione nel completare tutti gli obiettivi stabiliti, superando le molte difficoltà incontrate durante il viaggio e svolgendo professionalmente il nostro lavoro.

Vorrei anche ringraziare i miei amici nonchè colleghi, Maurizio, Alessio, Roberto, Loris, Nicola e Pierpaolo avendomi sostenuto nel percorso di studi come nella vita personale, e con cui ho condiviso soprattutto momenti indimenticabili.

Infine, vorrei ringraziare i miei genitori e la mia bellissima ragazza Veronica per il loro sostegno economico e soprattutto mentale, fondamentale per il raggiungimento dei miei obiettivi, professionali e personali. La loro presenza mi ha aiutato a lavorare duramente ed a conseguire la laurea.

TABLE OF CONTENTS

CHAPTER 1 INTRODUCTION…… 1

1.1 Historical and descriptive overview about the main topics of the problem…….. 1

1.2 Objectives and Scope of Research……..... 12

1.3 Organization of the thesis……..... 14

CHAPTER 2 OVERVIEW ON LITERARY BACKGROUND……. 16

2.2 Researches on SDOF Systems…….……..……..... 17

2.3 Researches on MDOF Systems……..…….....25

2.4 Briefing……. 28

CHAPTER 3 NON LINEAR DYNAMIC RESPONSE HISTORY AND COLLAPSE FRAGILITY EVALUATION…….....29

3.1 Introduction……..…..…… 29

3.2 Non Linear Dynamic Analysis: Approach 1……...….. 29

i) Mainshock Non Linear Incremental Dynamic Analysis…….....30

ii) Aftershock Non Linear Incremental Dynamic Analysis……..…… 31

3.3 Non Linear Dynamic Analysis: Approach 2……..... 31

3.4 Non Linear Dynamic Analysis: Approach 3……...…...……...… 32

3.5 Analytical Collapse Fragility Curves....……..... 33

3.5.1 Analytical Collapse Fragility Curves: Approach 1……. 33

i) Mainshock Collapse Fragility Curves…….....34

ii) Aftershock Collapse Fragility Curves…….....34

3.5.2 Analytical Collapse Fragility Curves: Approach 3……..... 35

i) Mainshock Collapse Fragility Curve.…….. 35

ii) Aftershock Collapse Fragility Curves……..37

3.6 Empirical Collapse Fragility Curves…..... 39

3.6.1 Empirical Collapse Fragility Curves: Approach 2……..... 39

i) Mainshock Collapse Fragility Curve……...39

ii) Aftershock Collapse Fragility Curves……..40

3.7 Input Ground Motions..... 40

3.7.1 PEER and NGA-West2 Database…….……42

CHAPTER 4 APPLICATIONS TO THE CASE OF STUDY: NON-DEGRADING SYSTEM…….…… 49

4.1 Introduction……..... 49

4.2 Non-Degrading System Construction……49

4.3 Structural Response Evaluation: Approach 1……...… 55

4.3.1 Mainshock Scenarios…….....56

4.3.2 Mainshock-Aftershock Scenarios…… 57

4.4 Analytical Collapse Fragility Curves: Approach 1……...…...… 59

4.4.1 Mainshock Collapse Fragility Curve……60

4.4.2 Aftershock Collapse Fragility Curves……..…….. 62

4.5 Structural Response Evaluation: Approach 3……..… 63

4.6 Analytical Collapse Fragility Curves: Approach 3……..…… 65

4.6.1 Mainshock Collapse Fragility Curve……..... 65

4.6.2 Aftershock Collapse Fragility Curves……..…… 68

4.7 Empirical Collapse Fragility Curves: Approach 2…….....75

4.7.1 Mainshock Collapse Fragility Curve…….……75

4.7.2 Aftershock Collapse Fragility Curves……..... 76

CHAPTER 5 APPLICATIONS TO THE CASE OF STUDY: DEGRADING SYSTEM..... 78

5.1 Introduction……..... 78

5.2 Degrading system: OpenSees……..…… 78

5.2.1 Creation of command files for the degrading system…… 80

5.3 Structural Response Evaluation: Approach 1…… 85

5.3.1 Mainshock Non Linear Incremental Dynamic Analysis……..…… 85

5.3.2 Mainshock-Aftershock Non Linear Incremental Dynamic Analysis...…… 87

5.4 Analytical Collapse Fragility Curves: Approach 1……..... 88

5.4.1 Case 1: Required Displacement…….89

i) Mainshock Collapse Fragility Curve…… 89

ii) Aftershock Collapse Fragility Curves……..... 91

5.4.2 Case 2: Park & Ang Damage Index……..... 92

i) Mainshock Collapse Fragility Curve……..... 92

ii) Mainshock-Aftershock Collapse Fragility Curves……..…… 94

iii) Aftershock Collapse Fragility Curves……..…… 95

5.5 Structural Response Evaluation: Approach 3……..……..... 97

5.5.1 Mainshock-Aftershock Non Linear Dynamic Analysis…… 97

5.6 Analytical Collapse Fragility Curves: Approach 3…….....98

5.6.1 Case 1: Required Displacement……..... 98

i) Mainshock Collapse Fragility Curve……...……..…… 98

ii) Aftershock Collapse Fragility Curves…… 100

5.6.2 Case 2: Park & Ang Damage Index……..... 105

i) Mainshock Collapse Fragility Curve……..... 105

ii) Mainshock-Aftershock Collapse Fragility Curves……..... 107

iii) Aftershock Collapse Fragility Curves…… 111

5.7 Empirical Collapse Fragility Curves: Approach 2……..……...114

5.7.1 Case 1: Required Dispacement…….....114

i) Mainshock Collapse Fragility Curves……..…….. 114

ii) Aftershock Collapse Fragility Curves…….....115

5.7.2 Case 2: *Park & Ang* Damage Index……...……... 116

i) Mainshock Collapse Fragility Curves…...……..……... 116

ii) Mainshock-Aftershock Collapse Fragility Curves…….....……... 117

iii) Aftershock Collapse Fragility Curves……..….... 118

CHAPTER 6 DISCUSSION OF RESULTS AND CONCLUSIONS…..... 120

6.1 Introduction……...….. 120

6.2 Aftershock Collapse Fragility Curves: Non Degrading System….....120

6.3 Aftershock Collapse Fragility Curves for Degrading System: Case 1……..... 123

6.4 Mainshock-Aftershock Collapse Fragility Curves: Degrading System.....125

6.5 Aftershock Collapse Fragility Curves for Degrading System: Case 2……..... 128

6.6 Summary and Concluding Observations……....….. 131

6.7 Suggestions for future works……...…… 134

CHAPTER 1 INTRODUCTION

1.1 Historical and descriptive overview about the main topics of the problem

Regardless their morphological nature, being both/either structural and/or infrastructural ones, reinforced concrete works are particularly vulnerable to multiple earthquakes. In particular, research conducted in this regard focused mainly on the evaluation of seismic effects of the structures under the strongest earthquake, in other words the earthquake with the highest seismic intensity, ignoring and perhaps underestimating the effects of the previous stress.

Effects that greatly influence the dynamic characteristics of the previously damaged structures and so their response after other earthquakes come: this is a case of structural stiffness and resistance degradation basically deriving from the accumulation of damages in the materials from construction in case of high-wide cyclical excursions.

An example is shown in Figure 1.1a, in which it is possible to observe the damage to the buildings following the so-called "Main Shock" of the Kobe earthquake in Japan. In fact it is impossible to predict the capacity of these buildings to tolerate further secondary shocks to the main one because in this case it has not been possible to define the dynamic characteristics and their resistance capacities.

Figure 1.1a Kobe earthquake - Damaged buildings (http://www.blueplanetheart.it)

Generally earthquakes are identifiable in the multiple regions of the world where there's the presence of fault systems with a particular distribution of horizontal actions, infact in that regions they are well "ramified". This branching distribution is the result of a process in which the fracture causing the first earthquake does not usually relieve all the tensions accumulated during the fault movement; so, in other points of the system making part of this "web", the increasing level of stresses brings to the accumulation of mechanical energy, causing sequential cracks which decline when the fault system reaches the stability; in this way sequences of multiple earthquakes are generated.

These sequences can be classified as: (1) Fore-, Main- and After-shock ones; or (2) sequences of indipendent earthquakes generated from fault segments casually distributed. An adjustment shake (commonly called "Aftershock") is a smaller earthquake that occurs after a previous one with greater magnitude, within the same area of the main earthquake (the so-called "Mainshock"). If an Aftershock has a magnitude greater than the main one, the Aftershock is re-defined as the Mainshock and the original main earthquake is re-cataloged as Foreshock (Figure 1.1b). it's simple to deduce the position of the Aftershock and the Mainshock epicentres, infact they occupy the entire fault-breaking area, exactly they occur either along their own fault plane or along other faults within the surface involved in the branching, and linked with their Fore- and Main- shocks.

Aftershock causes serious damages to the structures, sometimes also irreversible ones, first of all because they cannot be predicted in terms of position of the hit structures related to the main fount, in terms of starting action and energy content; second because they strike structures previously already damaged, with low rigidity and resistance. There's not a specific moment in which the Aftershock occurs subsequently to the Mainshock, but usually the range of time between in which both manifest is in the order of a couple of years, especially when earthquakes are located in the same specific region, as it has been told before; it could take either one day or one year or months before the aftershock occurs. For example the well known earthquake of Tohoku, in which a shock of magnitude 7.9 was recorded less than an hour after the main one having a magnitude 9.0; but also in Chile, where an earthquake of magnitude

7.2 manifested after 12 days, and in New Zealand, in which an aftershock of magnitude 6.3 was recorded more or less 4 months after the first one.

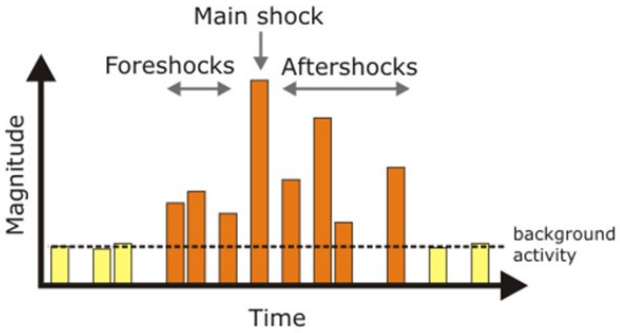

Figure 1.1b Classical earthquake sequence: fore-,main-,and after-shocks (http://www.geologypage.com)

On the other hand it has been sayed that These are generated in correspondence of fault segments casually distributed. But at the same time it might happen that more indipendent earthquakes, with their actions, build an environmental zone within the same seismic area, although they don't belong to the same fault areas: a clear example is represented by two earthquakes in Turkey, as it's possible to observe in Figure 1.1c; in particolar the 17th August at Kocaeli (magnitude of 7.4) and the 12th November at Duzce (magnitude 7.2) manifested in two different fault zones, the western extension and the eastern end of the North Anatolian fault system.

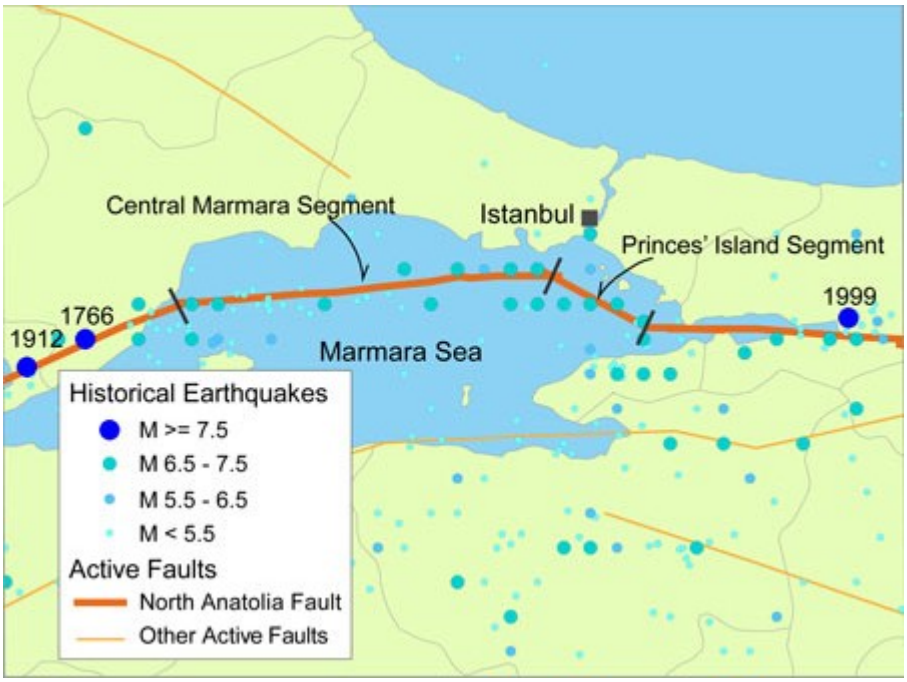

Figure 1.1c Kocaeli and Duzce independent earthquakes, with their epicentres and aftershocks (https://www.air-worldwide.com)

After buildings have been hit by multiple earthquake sequences, detailed field analysis have been conducted, with the conclusion that the main cause of the collapse of structures must be sought in the repeated shaking, infact their actions brought to the loss of structural rigidity and capacity resistance, result of damage accumulation eartquake after earthquake. It's right to suppose that intact structures, which suffer no damage during a great main shock, are more likely to collapse in this way, when the same buildings previously hit by the great main shock reach the failure few days later under short after shocks, like shown in Figure 1.1d.

Focusing on recent recorded earthquakes it's possible to find the same collapse procedure for many structures exposed before, always if in presence of repeated motions. These are the recorded cases, for instance, of the Umbria-Marche (Italy) in 1997, Kocaeli and Duzce (Turkey) in 1999, Chile (2012), Christchurch (New Zealand) in 2011 and 2012 and Tohoku (Japan) in 2011 and 2012.

Figure 1.1d Earthquake of Gediz, 1970: building hit only by the main-shock (*left*); the same one after an aftershock with smaller intensity (*right*) (https://www.cambridge.org)

September the 26th 1997 is a well known date for Italians because a sequence of powerful seismic events, made up of two dangerous main shocks respectively with

magnitude of 5.5 and 5.9, hit the Umbria-Marche countries, occurring at different moments, the first one at 00:33am and the second one at 09:42am. Subsequently, on October the 14th a dangerous after shock of magnitude 5.5 has been registered (Figure 1.1e).

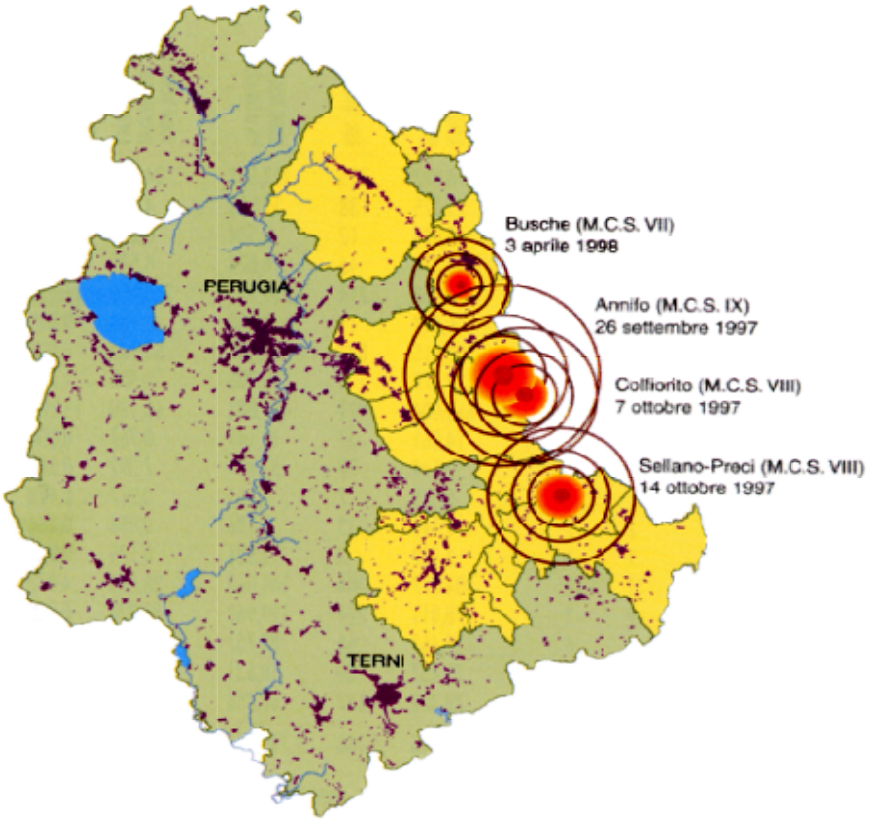

Figure 1.1e Seismic zone interested by earthquake sequences of 1997 in Umbria-Marche. Red circles shows their epicenter locations (http://prolabenergia.blogspot.com)

Regarding always the case of Umbria-Marche earthquake, San Francesco Church and Foligno Tower are perfect examples of buildings whose collapse verified not after the first shock but in the following shaking.

The roof of the Basilica di San Francesco reached the failure when the structure was hit by the second shock (magnitude of 5.9 at 09:42am); in Figure 1.1f the roof during the second earthquake is shown. Four priests inspected damaged producted by the first shock, but they lost their lives after the drop of rubble from the roof when the second shock occurred.

Figure 1.1f Bottom view showing the frescoed roof of the Basilica di San Francesco after the 09:42 event (https://it.wikipedia.org/wiki/Terremoto_di_Umbria_e_Marche_del_1997)

The collapse of Foligno Tower is the same described for the Basilica di San Francesco, always verified during the Umbria-Marche repeated earthquakes, but unlike the Church, the tower didn't collapse under the first and second shock on September the 26th, infact the tip of the tower reached the failure once the after shock on October the 14th manifested (Figure 1.1g).

Figure 1.1g Folgino bell tower after the two main shocks on September 26, 1997 (*left*) and after the shock on October 14, 1997 (*right*) (http://www.ansa.it/umbria/notizie/2017/09/19, https://tuttoggi.info)

In the previous Figure 1.1c the epicenter position of two of the most important earthquakes are illustrated whit their relatives after shock, in particolar the shock of magnitude 7.4 which hit Kocaeli and Sakarya counties in north-west of Turkey (August the 17th 1999), and the earthquake of magnitude 7.2 strucking Duzce (November 2012).

Most of structures reached the collapse during Duzce shaking, some of which were previously damaged during the first one (Kocaeli). In Figure 1.1h an example of These structures is represented.

Figure 1.1h Collapsed building in Duzce previously damaged in the Kocaeli event (https://www.air-worldwide.com)

The 2010 earthquake in Chile is particularly known for having recorded a considerable number of high intensity aftershocks within three days just after the main shock of magnitude 8.8 (Figure 1.1i), the actions of which significantly influenced the damaged structures, although the present discussion does not provide details about the possibility of surviving structures to the main shock and consequent failure during aftershocks.

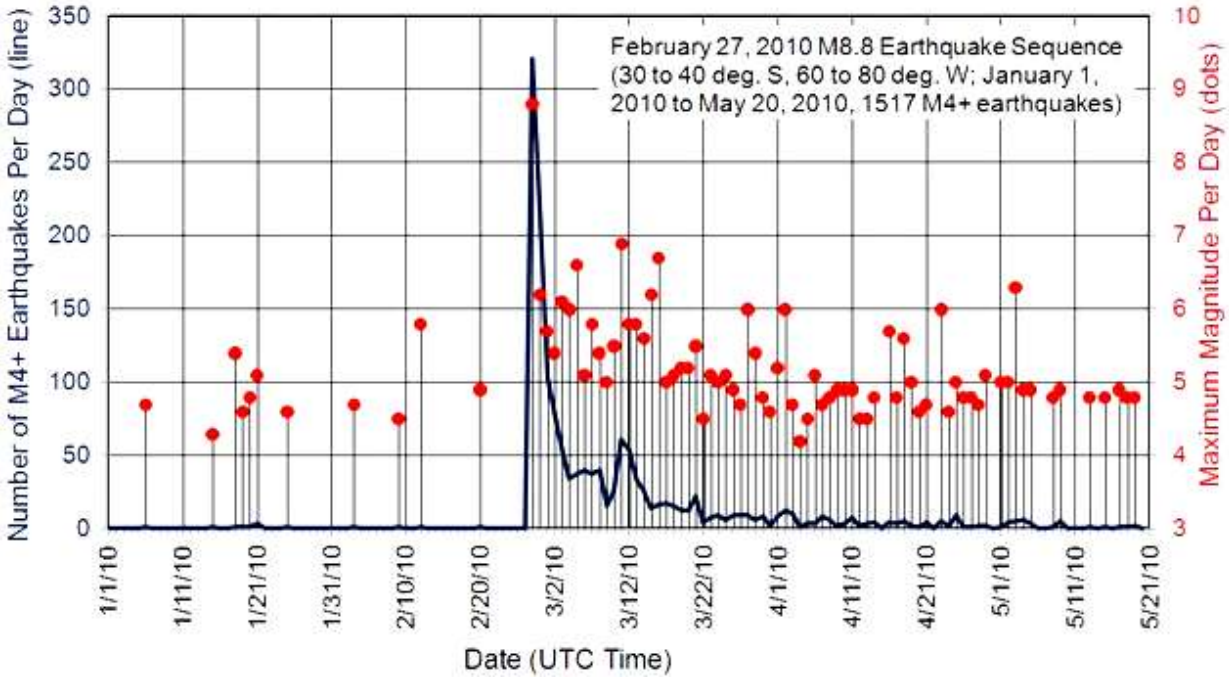

Figure 1.1i Time/Magnitude representation of the main shock and after shocks earthquakes in Chile (https://web.ics.purdue.edu)

Moving to New Zealand we have to remember the sequence of Christchurch, which began in September 2010 with the main magnitude of 7.1 occurred near Darfield, more or less 40 km from the city of Christchurch. In February 2011 there was a much more destructive aftershock because, despite the magnitude of this shock equal to 6.2 was lower than the previous one, in addition to hit the previously damaged structures (in September 2010), it generated directly in correspondence of Christchurch.

As a result, the loss of life stopped to 180 victims, and many buildings collapsed after the secondary shock, reporting significant damages, precisely because of the accumulation of damages from the main shock. In the subsequent aftershocks, in June (magnitude 6.0) and December (magnitude 6.0) 2011 no major damage was recorded.

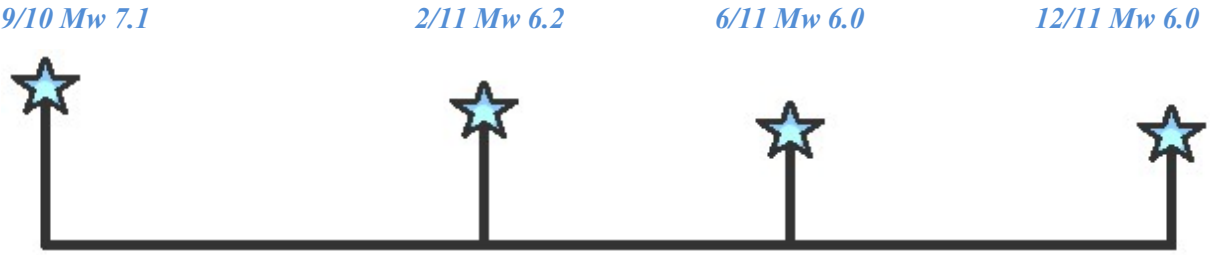

Figure 1.1m Christchurch sequence and magnitude of earthquakes

Figure 1.1n February 2011**:** Christchurch overview during the aftershock of magnitude 6.3 (https://www.tiziano.caviglia.name)

Figure 1.1o shows the territorial distribution of main shock and aftershocks in the recent earthquake in Tohoku on 11 March 2011 in Japan, with magnitude 9.0, in which aftershock entities caused the collapse of many buildings; for instance the secondary shock of magnitude 7.4 recorded few weeks later (April 7) in the city of Sendai. Also in this case it's possible to notice that, for one of the houses of that city, represented in Figure 1.1p, the collapse has been reached subsequently to the secondary earthquake of 7 April, not suffering any damage after the main shock of 11 March.

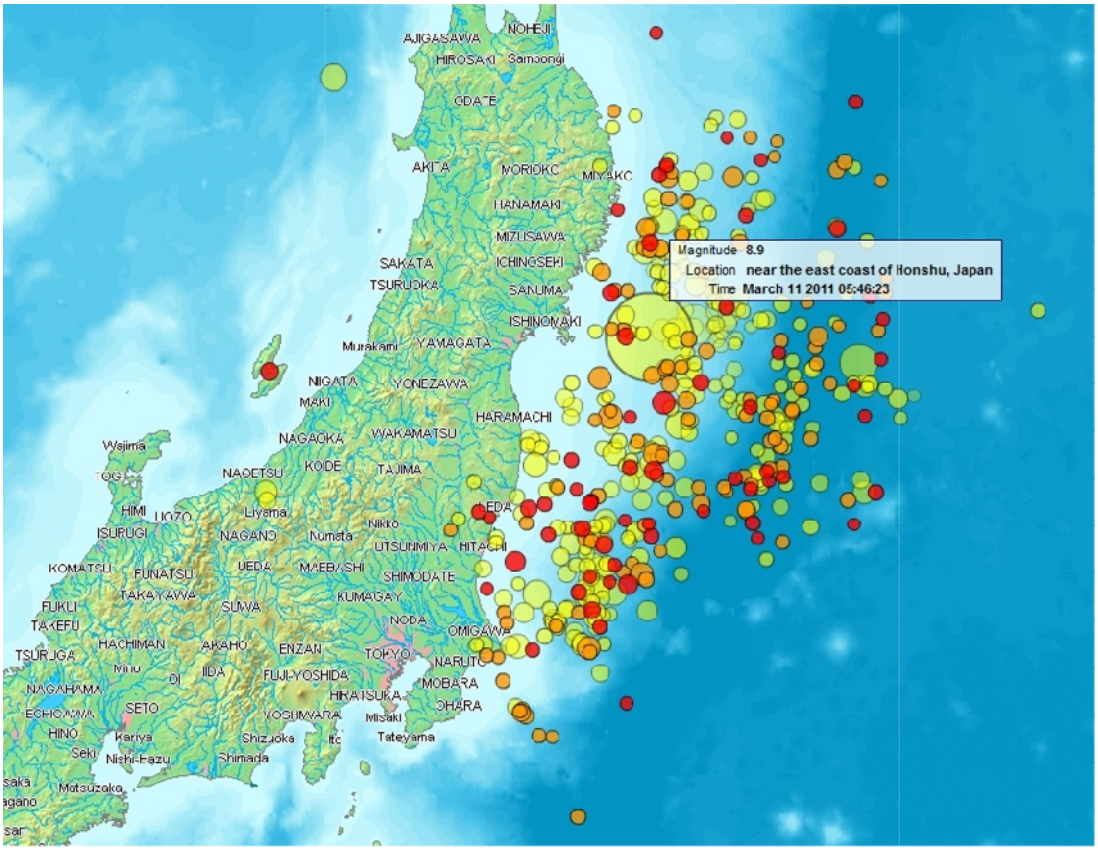

Figure 1.1o Tohoku earthquake, Japan: mainshock and aftershocks epicentral positions; circle size and colours identifies magnitudes (http://it.wikipedia.org/wiki/Terremoto_e_maremoto_del_Tohoku_del_2011)

Figure 1.1p Sendai, 7 April: collapse of a house after the aftershock
(http://www.asahi.com/special/gallery_e/view_photo_feat.html?jisin-pg/TKY201104120069.jpg)

Based on just exposed facts and really happened, it can easily be said that the collapse of structures is the result of the continuous accumulation of damage when these structures are subject to sequential earthquakes. Today, unfortunately, the effects of multiple stresses are not dealt in the different anti-seismic design codes; furthermore, given that the degradation of building materials, earthquake after earthquake in a sequence, represents the basis of the damage accumulation of the same ones, due to the complexity in implementing and defining a structural design model taking into account the degrading effect, this problem has been neglected or not sufficiently treated by previous designers.

The numerical calculation and design software currently available, capable of performing linear and nonlinear dynamic analysis of reinforced concrete structures (such as OpenSees) haven't got the degrading functionality necessary to simulate the actual behavior of a structure subjected to multiple shakings. So it would be necessary to create appropriate models to solve this problem, establishing a solid starting point that refers to a comprehensive literature able to cover all the points of this topic, and which continues the work done by previous researchers.

Talking in terms of safety, if a certain building has already been damaged by a previous earthquake, the risk associated with the damage will increase, so its

performance may not suit the requirement for future earthquakes. In order to provide an assessment of the behavior and reliability of buildings subject to multiple shocks, and taking into account the lack of sufficient tools to implement models of structures with degrading functionality (for example in building materials), this study focused on the development of analytical/probabilistic methodologies useful to the evaluation of fragility, applied respectively on intact and damaged systems, trying to consider, for this last one, also the degrading effect.

In reference to an element or a system, fragility is defined as the conditional probability of exceeding a certain limit state under given demand variables; lots of researches have been conducted developing the fragility models of various building systems, such as Hwang and Huo in 1994, Shinozuka et al. 2000 and Wen and Ellingwood in 2003.

Fragility models of both steel and concrete structures have been studied by past researchers, and, while the majority of the models gave importance to the reliability of the buildings in as-built condition, only a limited number of researches have been performed in the past with the intention of understanding the effect of main shock-aftershock sequences or multiple earthquake events on the seismic performance of steel and RC buildings (eg. Lee and Foutch, 2004; Li and Ellingwood, 2007; and Hatzigeorgiou and Liolios, 2010).

Luco et al. (2004) proposed an alternative methodology to compute the probabilistic residual capacity of main shock damaged buildings in terms of the ground motion intensity of an aftershock.

However, those researches focused on either the demand or capacity side without offering an overview of seismic fragility estimation. Kumar and Gardoni (2012) made up a seismic degradation reliability model of RC bridges subjected to multiple earthquakes and a general stochastic model useful to implement the deterioration process in engineering systems.

1.2 Objectives and Scope of Research

Basing on what previously sayd, this thesis aims to provide a contribute in the assessment of the fragility in structures subjected to multiple seismic events during the service life, precisely in case of mainshock-aftershock sequences, trying to include also the effect of the first shock to the overall damage evaluation; a comparison between fragility curves defined both for the non-degrading system and those defined for the degrading one will be made, in this last case taking into account the degrading properties of the system from the construction materials' point of view; in order to obtain these curves, the whole discussion is based on the achievement of two objectives, described below in order of importance.

The first main objective is to set up analysis procedures that are effective and appropriate for simulating the behavior of buildings, capable of providing results similar to those that represent the real response of a structure in the same situation. So, with the help of softwares MATLAB and OpenSees, three different design approaches are implemented to evaluate the non linear dynamic response history: the first one takes inspiration from the methodology developed by Raghunandan et al. (2015), infact it's an analytical method based on the non-linear incremental dynamic analysis (IDA) results; the second one is simpler than the previous one because it's always based on the non-linear dynamic analysis results, but in this case a multiple regression demand model is adopted, following the mythology purposed by J. Ghosh, J.E. Padgett and M. Sànchez-Silva (see the Bibliography Section); the third one is linked to the first one because, considering the results due to the same IDA of the first approach, a simple and mathematical evaluation of the ratio between favourable cases and possible cases has been done, referring to the probability that the seismic demand exceeds certain damage levels (structural capacities).

Considering the second method, the closed form expression developed by Tubaldi et al. (2016), in which a lognormal distribution of seismic demand, or structural response (including parameters due to the multiple regression) and structural capacity is assumed in the probability calculation; a similar lognormal distribution is at the base of another closed form expression used for the first method and elaborated by Murat

Serdar and Zekeriya Polat (see Bibliography Section) to calculate the probability of failure. The framework of this study is shown in the following Figure.

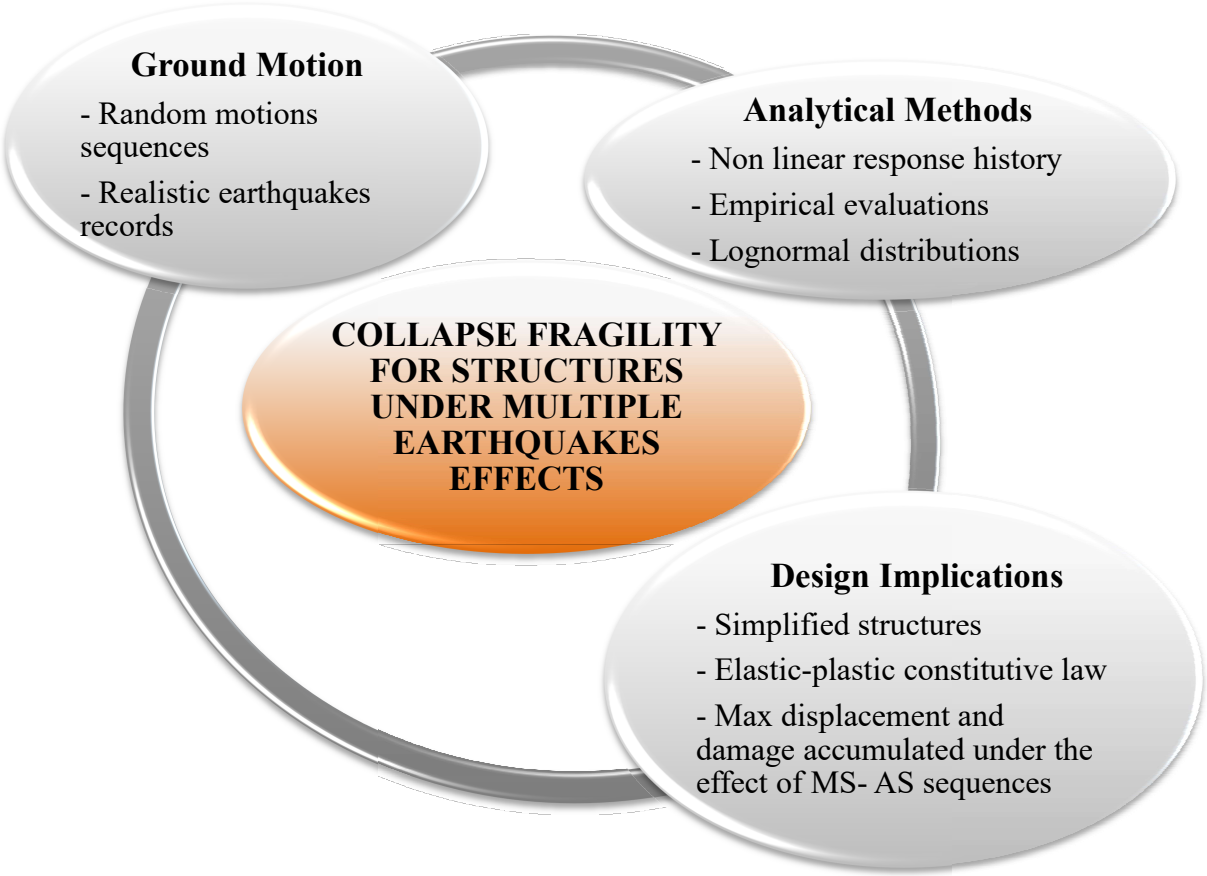

Representative earthquake sequences are created by combining ground motions recorded from seismic events really happened. Replicate and random motions sequences are used for the non-degrading case; the same ground motions, but with different sequence combinations, will be used for the degrading case.

The second objective is as important as the first one, although the study does not focus mainly on the topic that will be mentioned, but the concentration is addressed on methodologies previously announced; anyway it's important also to use an appropriate degrading model for the same structure, as a complement to the fragility analysis, that does not neglect the damage accumulated over time by past earthquakes. The main challenge of establishing a degrading material level based model is that, in all existing analysis tools, proper damage features of concrete and steel materials are not treated. This is due to the complexity of implementing these features in the material models

because they are computationally expensive and usually cause convergence problems when subjected to complex dynamic loading. So the numerical calculation and design software currently available don't consider the degrading functionality necessary to simulate the actual behavior of a complex MDOF structure subjected to multiple shakings: it is for these reasons that the structure analyzed is extremely simple; in fact, a system with a single degree of freedom (SDOF) has been chosen as case of study for testing the goodness of procedures used in the construction of fragility curves. Thanks to its elementary geometry, for an SDOF system it is easier to evaluate its response even when it is subject to complex load cycles and, referng to the available tools, it is also possible to avoid convergence problems.

Furthermore, in addition to the structural simplification, logical choices have also been made for construction materials, in fact, in substitution of the classic reinforced concrete, it has been decided to simulate the degradation in a system made only in steel and therefore, through the use of the design software OpenSees, a design model has been implemented, mainly based on the hysteretic uniaxial bilinear behavior easily verifiable in the steel and including the "pinching" effect in force and deformation.

The three analytical methodologies are applied both for the no-degrading and degrading issue and, once structural responses are evaluated for each approach, they will be elaborated in a post-processing phase, of a probabilistic nature, for constructing fragility curves in function of many different limit states; a final comparison will allow us to understand if the adopted calculation procedures can predict the real behavior of a building in multiple shocks scenarios in all cases that will be described, and to understand if the damage accumulation can affect the final response of the system, and in what entity.

1.3 Organization of the thesis

The script will have 5 main sections (section 2 to 6) after the Introduction Section 1 in which researches conducted on the topic are presented.

Section 2 discusses literary background that helps to understand how this problem has been faced from previous researchers; infact, referring to the seismic behavior of

different types of structures under the effects of multiple earthquakes, most of past theories will be exposed, highlighting characteristics of each one and their possible limits of applicability.

In Section 3 all methodologies set up are presented; it includes all precautions and design strategies taken into account for determining the structural response, for each method. These approaches will be the starting point for cases of study which they will be applied on, because they are based on the non linear dynamic response history evaluation, and they are equal for all them. Furthermore the source of Ground Motions and their selection criteria will be commented.

In Section 4 it's possible to find a description of the first case of study: the non degrading system; steps necessary to calculate the structural response, basing on the non linear dynamic response history evaluation exposed in the previous Chapter, are carried out. The probability of having only damaging Mainshock will be calculated, as well as, subsequently, the probability of having damaging Aftershock (a specific and most common case of multiple earthquake events) for different damage (capacity) levels; about this, fundamental hypothesis, assumptions and considerations will be done, as well as for the seismic demand.

In section 5 the same methods will be applied to the degrading system; also in this case the description of the case of study is presented, the implementation techniques are highlighted, and the structural response is determined. The estimate of probability of having damaging Aftershock in different damage (capacity) levels is carried out. Also in this case important assumptions on structural capacity and seismic demand will be done and; about this, in order to test the effectiveness of analyzes, many different damage indexes will be defined.

Section 6 is dedicated to the comparison between fragility curves obtained applying the three methods, distinctly for non-degrading and degrading system, in function of assumptions about the structural capacity made in sections 4-5. Summary of the research, conclusions and suggestions for future work of this study are presented.

CHAPTER 2 OVERVIEW ON LITERARY BACKGROUND

2.1 Introduction

The first important step in the evaluation and design of structures able to withstand more severe shocks over time was made following the earthquakes of Chile, Tohoku (Japan) and Christchurch; in this regard the researchers particularly focused on the problem by starting to develop new design methods.

The primary objective of modern design codes is to guarantee, for a generic structure in reinforced concrete or steel, adequate resistance to earthquakes with different intensity and different frequencies; in other words, in the current design codes, solutions are sought such that, in the case where earthquakes occur with small intensity but very frequent, earthquakes with moderate intensity but less frequent, and earthquakes with high intensity but rarely frequent, allow a sufficient strength, strength and ductility respectively to guarantee maintenance, damage protection, and collapse within the limit prevention states.

The current design rules consider the damage induced on a structure following a high-intensity earthquake, but at the same time they do not evaluate either the behavior or the effects of the accumulation of damage caused by earthquakes at small and medium intensity on the same structure previously damaged.

To consider the accumulation of damage, the researchers used simplified models, although they lack of important properties due to the degradation, as presented in this paper. In support of this, the works previously carried out came to a rather contradictory conclusion with the investigation reports presented in the previous Chapter: in fact it was concluded that if the structures are designed to withstand more damaging earthquakes then the accumulation of damage is irrelevant if the same structure is subject to multiple earthquakes. Totally the opposite of what has been highlighted in the first chapter, in which the really happened events showed cases of buildings collapsing under small aftershocks, although it remained intact after the main shock.

In this first part of the chapter the literature has been "dusted" in order to build the foundations for this study. The purpose of this “review” is to help: a) first of all

understanding the approaches used to evaluate the structural response after multiple earthquakes; b) identifying assumptions made in modelling the behavior of degrading systems; c) evaluating the results and conclusions of each study.

Unlike what this literature let understand, the objective of this discussion is to establish how it is possible to improve results of these researches, regardless of the case study which the methodologies are applied to, not the development of analytical methodologies (appropriate for this purpose) in function of the modeling of the structure. However, the utility in reading this chapter is that to understand how the problem has been dealt in the past and under what points of view.

Thanks for their simplicity, SDOF systems, characterized by different inelastic force-displacement and hysteretic relationships, have been considered by many researchers: for instance Mahin (1980), but also Aschheim et al. (1999), Amadio et al. (2003) and Hatzigeorgiou et al. (2009). Also MDOF systems were introduced as well as SDOF ones, for instance moment resisting steel (Fragiacomo et al., 2003; Ellingwood et al., 2007) and concrete frames (Hatzigeorgiou et al., 2010).

Several design methods were followed for studying both SDOF and MDOF systems; furthermore, in each study different ground motions' selection criterias were used: for example, some studies based on Gutenberg's mainshock-aftershock relationships for scaling their aftershock records (Ellingwood, 2007); real shakes, recorded on different stations during previous multiple earthquakes (Fragiacomo et al., 2003) and finally random sequences of earthquakes were adopted by Amadio et al. (2003), Mahin (1980), Hatzigeorgiou et al. (2009 and 2010). Great differences between results and conclusions for each study were observed, for the simple reason that different approaches and hypotheses have been used in the literature to model buildings and select the applied ground motions.

2.2 Researches on SDOF Systems

As already mentioned in the previous paragraph, SDOF systems, thanks to their simplicity in implementing the effects of degradation by means of force-displacement relations of hysteretic behavior, have been of great help in the analysis of the damage

caused to structures when subjected to repetead shakings: for them, a scheme with non linear degrading springs connected to concentrated masses were provided.

According to this, a brief description of the main movements, models and results obtained by previous researchers who studied the response of these systems to repeated shakings will be provided. For example Mahin (1980) studied the "effects of duration and aftershocks on earthquakes designed with inelastic response history". The hysteretic models used in this case were characterized by elastic-perfectly plastic constitutive law (non-degrading hypothesis).

However, in the carried out analyzes, the effects of P-Δ influenced the degradation of the rigidity referred to the entire system, during the application of the earthquake. Mahin used the main shock of the 1972 earthquake in Managua, with a Peak Ground Acceleration of 0.351g and the next two successive aftershocks with 0.120g and 0.277g of PGA respectively.

Figure 2.2a shows the cumulative ductility spectra due to the main and adjustment shocks. Looking this Figure it's possible to deduce that the main shock induced significant inelastic deformations if applied to the initially intact system (having initial period and force). Unlike the poor effects induced by the first aftershock, the second aftershock caused significant deformations over the elastic limit and an increase in the demand for ductility and energy dissipation of the system equal to twice the demand after the main shock.

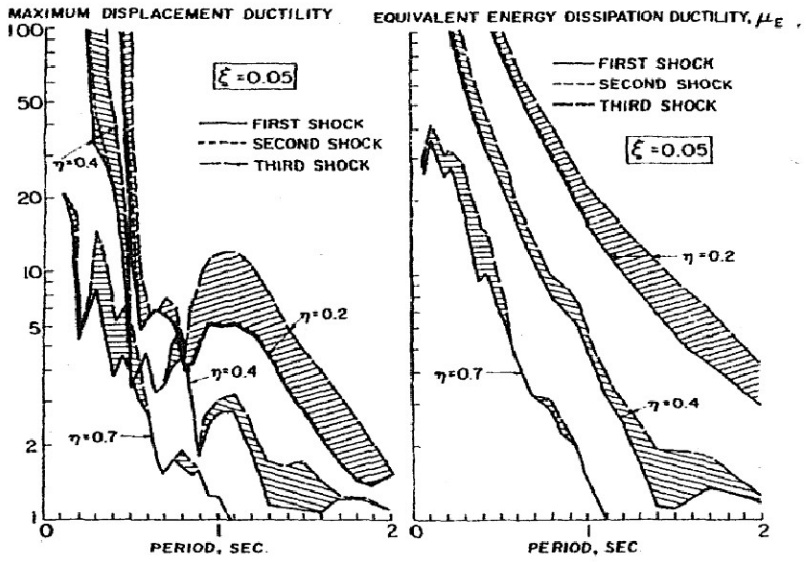

Figure 2.2a Aftershock effect on ductility for a SDOF system (Mahin, 1980)

Mahin concluded that aftershocks do not greatly affect the maximum displacements and damages of SDOF systems; in addition he recommends that further analysis should be conducted considering the effects of stiffness and deterioration of systems resistance on response in case of long-time earthquakes and / or aftershocks.

The first one who introduced degrading systems in his research was Aschheim (1999), with the aim of studying the "effects of the previous seismic damage on the response in simple degrading structures". Extending on a large scale, this study turned into the assessment of the effects of previous earthquake damage on the response (in terms of peak displacement) on over 20000 oscillators with a single d.o.f.

To implement the hysteretic behavior of these oscillators, the Takeda model shown in Figure 2.2b was used, modified with the addition of the "pinching" effect; each oscillator also possessed defined stiffness and strength; 18 ground motions with different frequency and duration contents complete the analysis.

The effects of the residual shifts deriving from a previous shaking haven't been taken into account in this study, as they are considered almost irrelevant on the response. As damage parameter, displacement ductility was chosen; the previous damage was simulated by varying the initial stiffness and the current displacement ductility in order to reach a pre-specified level of previous damage demand (PDD), then PDD values of 1, 2, 3, 4 and 8 are assumed.

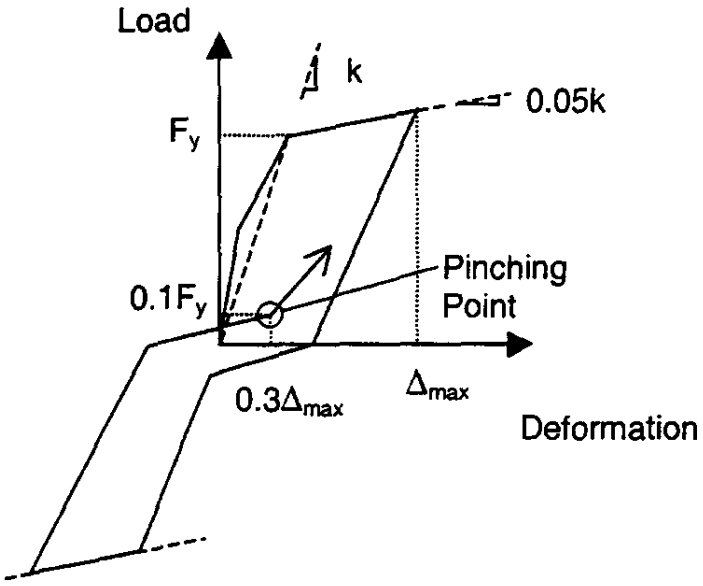

Figure 2.2b The Takeda model, whit the "pinching" effect and the degrading of strength (Aschheim,1999)

This analytical study ended with the result that the response, in terms of peak displacements, is slightly affected by the previous shock. Furthermore the study demonstrates that, during an event, the displacement response of initially damaged SDOF systems and their undamaged counterparts while experiencing the peak displacement are perfectly marche. To substain this statement, Figure 2.2c highlights outputs (displacements), in particular four SDOF systems with PDD values 1, 2, 4 and 8 (different initial damage parameters) were subjected to a ground motion. From the Figure it's possible to deduce that the responses matched when the displacements reached the peak value at time approximately equal to 5.6 s; infact, over that time, they almost matched for different PDD values.

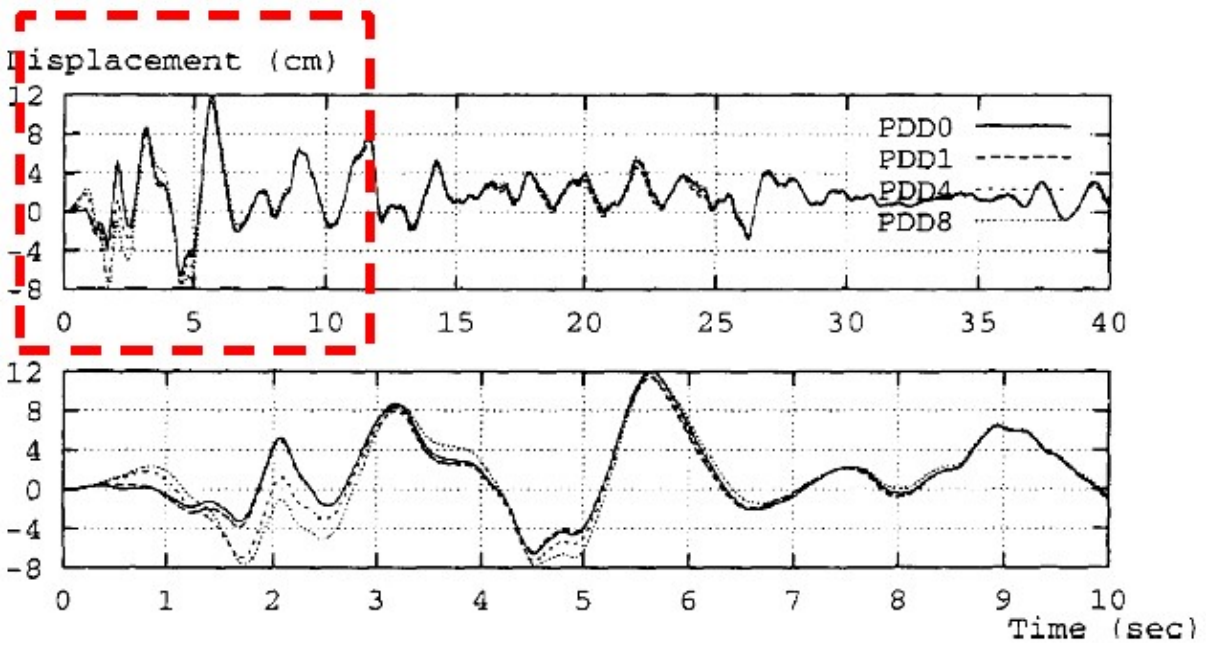

Figure 2.2c Displacement histories of the record, for the first 10 seconds, referring to oscillators with previous damage parameters equal to 0,1,4,8 (Aschheim, 1999)

Studying the behavior of SDOF non-linear systems when affected by multiple earthquakes, in 2003 Amadio et al. introduced a new design idea focusing on more than a "single damageability limit state". He used different hysteretic models represented in Figure 2.2d. Undamaged system was compared with damaged one and what emerges allowed us to say that the elastic-perfectly plastic system was the most vulnerable system under repeated earthquake sequences.

For the aforementioned systems with hysteretic behavior, identical sequences of multiple earthquakes were launched. To ensure that the system had the right relaxation time and subsequent complete rest, a time interval of forty seconds was considered sufficient. The accelerograms used were spectrum-compatible with the project response spectra and actual recordings of previous earthquakes (Figure 2.2e).

This research shows that several earthquakes could mean a significant accumulation of damage and at the same time a reduction of the response factor (q).

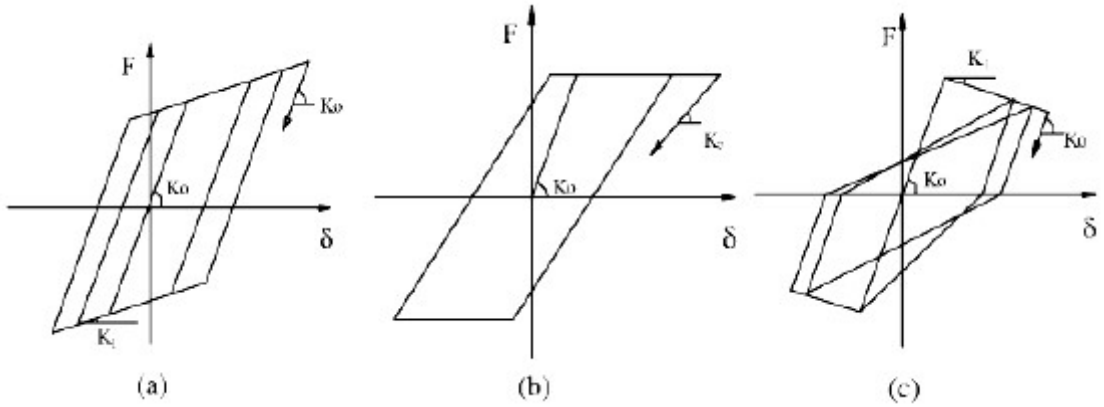

Figure 2.2d Hysteretic: a) Bi-Linear model; b) Degrading Stiffness models without Pinching; c) Degrading Stiffness and Strength models incuding Pinching for SDOF systems (Amadio et al., 2003)

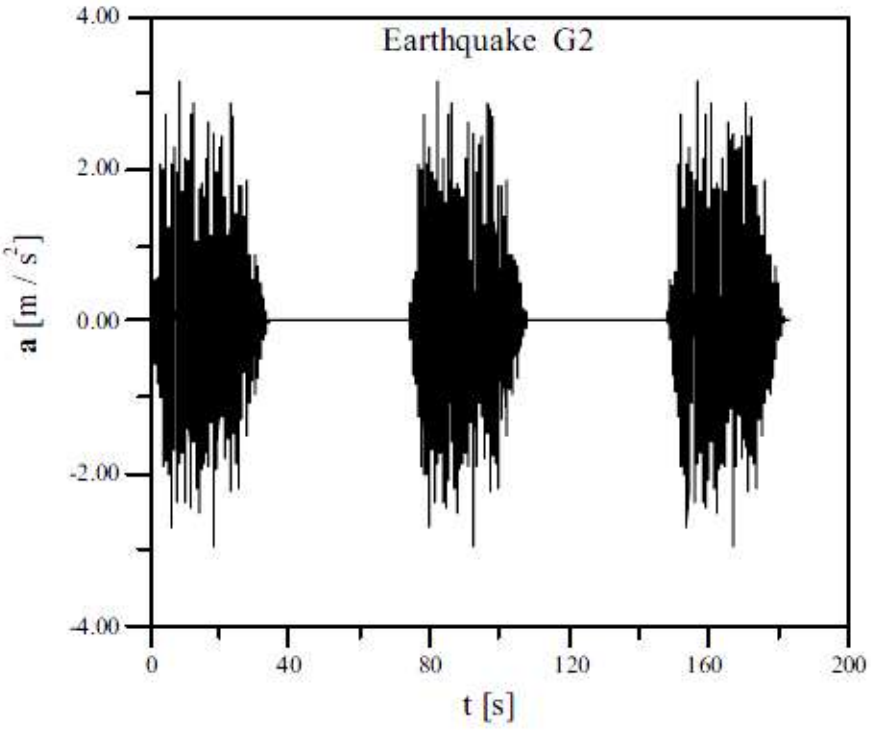

Figure 2.2e Sequence of three G2 earthquake ground motions (Amadio et al., 2003)

Looking at Figure 2.2f, ratios between force reduction factors q1 and q3 (calculated respectively for the first and third earthquakes) were appropriately reduced according to the different periods of the SDOF systems. Moreover, this study has shown that these simplified systems are not the most suitable for predicting the actual behavior of the structures for a series of reasons: the complex opening and closing mechanism of the plastic hinges is not present in their modeling; the interaction between the first and the highest modes of vibration is not considered; the effect of axial loads on the external piles is neglected. Therefore, given the low efficiency of SDOF systems in representing a complete response, more complex structural models from the point of view of materials and components were recommended, projected on future analyzes.

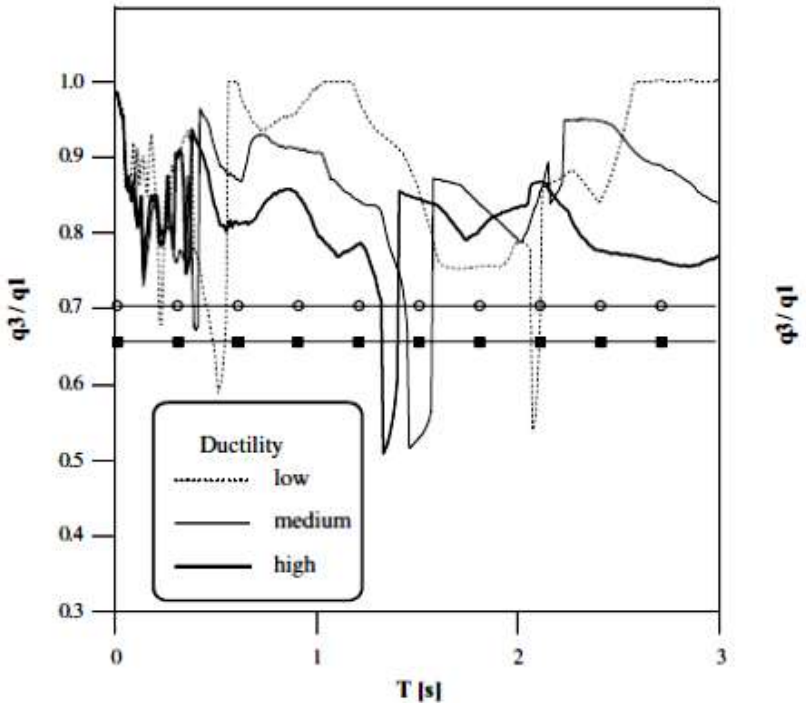

Figure 2.2f Different q ratios in function of fundamental periods of vibration. q1 and q3 are calculated after applying the first and the third earthquakes (Amadio et al., 2003).

In 2009 Hatzigeorgiou et al. contributed to the development of a new procedure for estimating the displacement ratio over the elastic limit of SDOF systems (u_{max}/u_{el}) in presence of multiple earthquakes, an innovation in the study of this topic, although from this analysis it's not possible to understand if the degrading effect is considered in modeling the system. Models he adopted were the traditional elasto-plastic ones

with linear hardening or softening, simple models that can accurately describe steel or reinforced concrete structures with predominantly flexural behavior.

In order to define expressions that best represent the inelastic displacement ratio, he considered the influence of the vibration period, the force reduction factor ($R = f_{el}/f_y$), site conditions, post-yield stiffness ratio ($H = K_t/K_{el}$), and viscous damping ratio (ξ) through extensive parametric studies and no-linear regression analysis.

The maximum displacement over the elastic limit was obtained by means of a non-linear dynamic chronological analysis. Statistical analysis included 5,644,800 inelastic analyzes of temporal history, studying 12,600 SDOF models excited by 112 worldwide seismic accelerogram records, in functions of the site conditions and the shear wave velocity. These studies broutgh to a series of conclusions, in particular it has been shown that the increase in force reduction factors R always leads to an increase in the inelastic displacement ratio and vice versa, as seen in Figure 2.2g

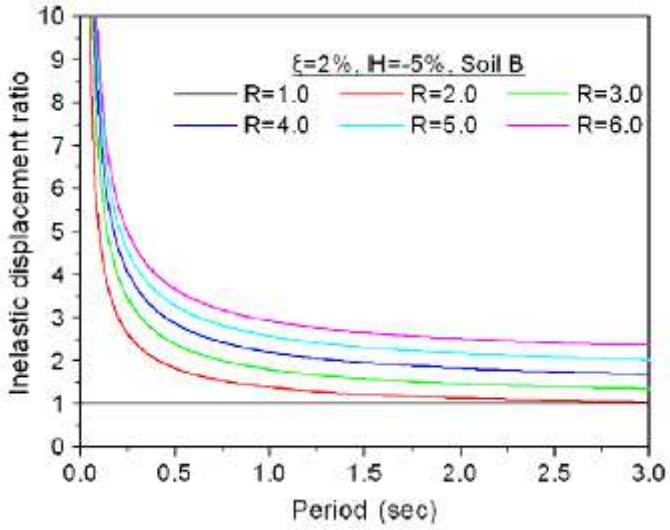

Figure 2.2g Influence of force reduction factors R, for a specific soil type and with defined values of viscous damping ratio (ξ) and post-yielding stiffness ratio H (Hatzigeorgiou et al., 2009)

These ratios are also extremely sensitive to the structural period of the SDOF system, in particular for short-term intervals; in fact, the shorter the period, the greater the relationship. In addition, looking the Figure 2.2h, it's possible to note that the drop in post-yield stiffness ratio is synonymous of higher displacement demands and vice versa. The effect is more marked for negative values of this parameter, in other words for softening cases.

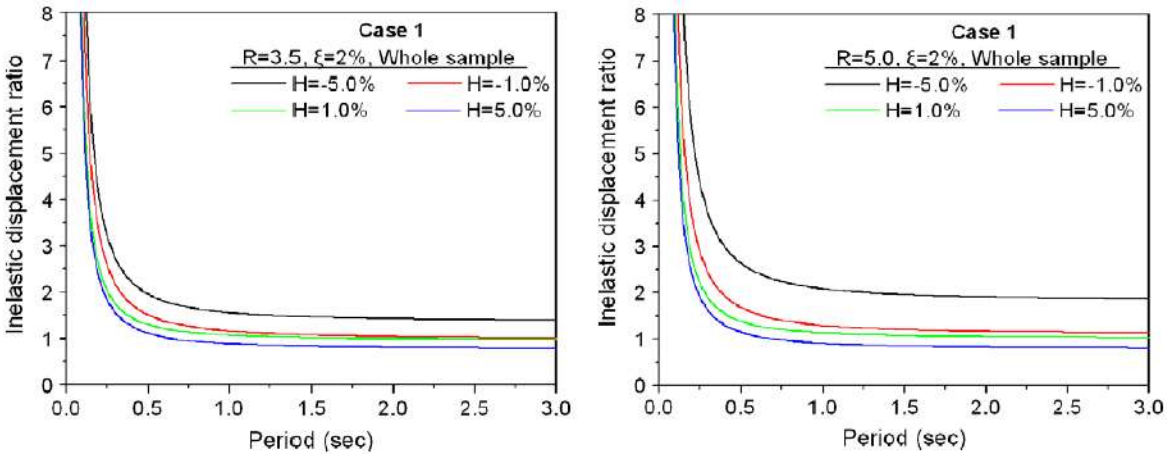

Figure 2.2h Influence of post-yielding stiffness ratios H, for a specific value of viscous damping ratio (ξ) and different force reduction factors R (Hatzigeorgiou et al., 2009)

The local site conditions (Figure 2.2j) and the viscous damping ratio (Figure 2.2i) slightly influence the inelastic displacement ratio and can be practically ignored.

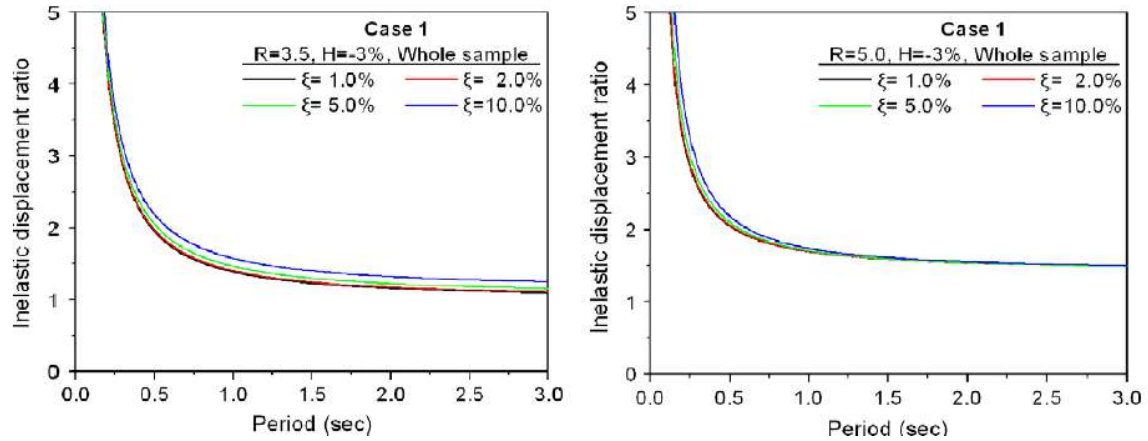

Figure 2.2i Influence of viscous damping ratios (ξ), for a specific value of H and different force reduction factors R (Hatzigeorgiou et al., 2009)

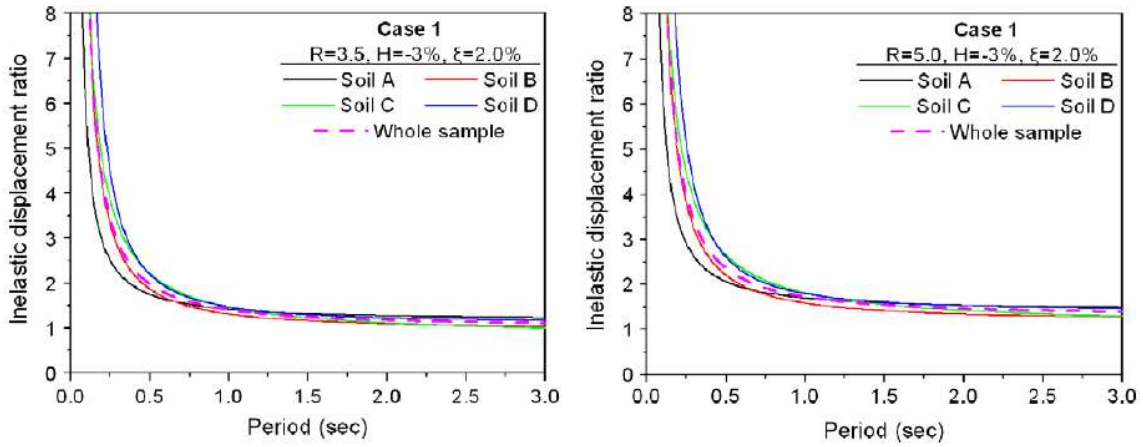

Figure 2.2j Influence of local site conditions, for specific values of H, ξ and different force reduction factors R (Hatzigeorgiou et al., 2009)

The most important result achieved in this study is that multiple earthquakes require greater displacement than individual seismic events ("design earthquake"). In fact, from the analyzes carried out, the inelastic displacement ratio seems to be increased by 100% or more compared to that obtained for the corresponding individual earthquakes.

2.3 Researches on MDOF Systems

Reinforced concrete and steel moment resisting frames under multiple earthquakes have been limitedly treated because it's difficult to set up analyzes able to simulate the real behavior of complex structures when subjected to these repeated cyclic loadings, consequently their degrading models cannot be easily incorporated in the study. However, referring to frame systems, all models carried out in literature were component level based degrading models, just for question of simplicity. These models includes moment-rotation relationships taking into account stiffness and strength degradation. Plastic hinges have been localized at beam-column connections, while the behavior of the rest of the structure was supposed to be elastic.

About steel frame structures, Ellingwood (2007) made researches on the "performance evaluation" and damage assessment under main shock-aftershock sequences. Making referrence to the Gutenberg/Richter relation for determining the magnitude of the aftershock based on mainshock ones, in this study identical earthquake sequences were used.

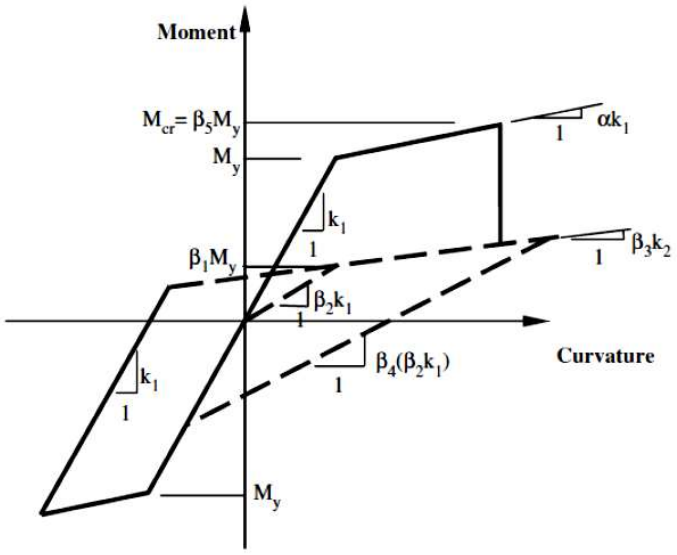

Figure 2.3a Damage welded connections, hysteretic behavior (Gross, 1998)

Looking the Figure 2.3a, frame connections have been modeled by moment-rotation relationships, taking in consideration the cracking of connection welds with a marked hysteretic behavior due to the applicaton of cyclic loads.

The damage accumulation has been determined as a normalized damage ratio between the number of fractured connections and the total number of connections. The main conclusion from this study is that the design hypothesis of the analysis, i.e. identical mainshock-aftershock sequences repeated over time, underestimate the damage in the aftershock because it depends significantly on the amplitude and frequency content of the aftershock ground motion. So this method of evaluation failed because of choices not particularly suitable to relate the damage due to the past earthquake with the damage the structure suffers in the aftershock. Figure 2-8 provides the damage pattern of steel frame connections under main shock and main-aftershock sequence of replicate ground motions. In Figure 2.3b the damage pattern of steel frame connections under mainshocks and sequences of replicate ground motions is represented; it's possible to observe that the additional damage induced these replicate ground motions is not considerable.

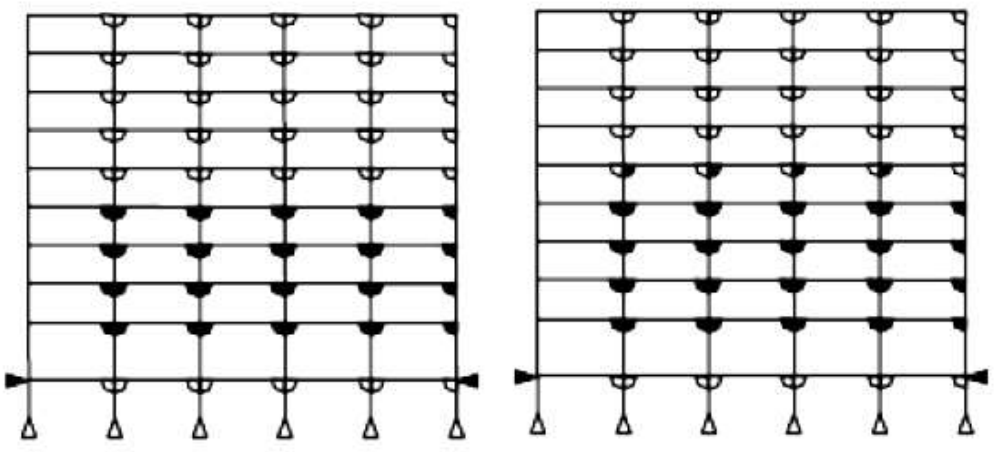

Figure 2.3b Damage level for the frame under mainshocks (left) and under mainshock-aftershock sequences (right) (Ellingwood, 2007)

A further study on the influence of repeated ground motions on the final response was conducted; the results are shown in Figure 2.3c, they show the effect of aftershocks' amplitude, function of the damage induced by main shocks on the additional damage induced to structures by the same aftershock.

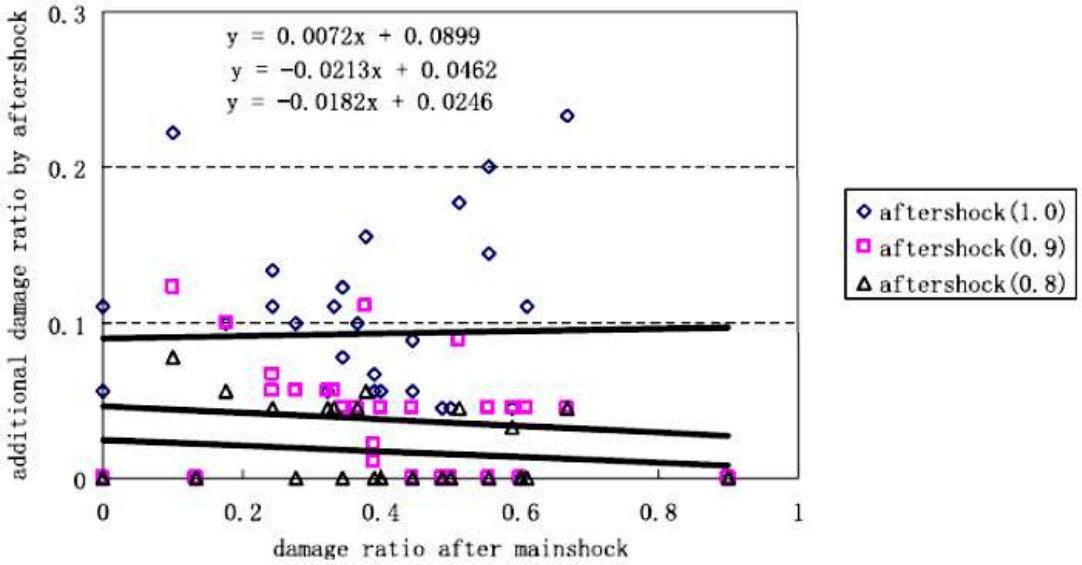

Figure 2.3c influence of aftershock in damage ratio and the damage ratio due to mainshock for a typical building (Ellingwood, 2007)

Hatzigeorgiou (2010) conducted a similar study applied in this case on reinforced concrete structures. Design approaches was the same of steel frame, i.e. component level based models assuming bi-linear moment-rotation relationships in correspondence of connections and including also P-Δ effects (geometric non-linearity). In Figure 2.3d analyzes are carried out, it's clear that residual displacements influences a lot the stiffness degradation of the whole frames, due to geometric non-linearity; in this study however the degradation of construction materials is not considered.

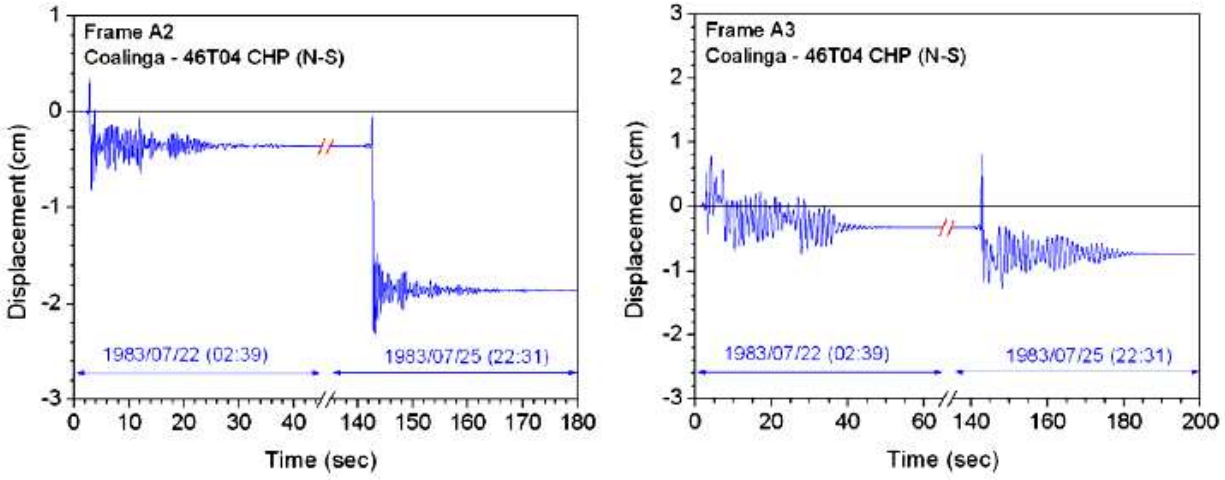

Figure 2.3d Permanent drifts in a reinforced concrete structure (Hatzigeorgiou, 2010)

2.4 Briefing

Analytical studies just presented are purely descriptive, and also represent a useful tool to introduce the analyzes that will be carried out in the following chapters, regadless the nature of the structure which they will be applied to. Because of the approximations on their modeling and schematization of procedures, over time discrepancies were observed in results, further marked by the different criteria for the choice of earthquakes, regardless of the different approaches followed.

About these approaches, the limits found mainly regards the modeling, however, in particular they were related to the accuracy in representing the degrading response of the structures, in fact SDOF systems were schematized with elastic springs, not inclined to consider the redistribution of forces during the earthquake because unable to predict locally the behavior of the material, the section and the element.

For the MDOF frame systems, results from past researches were used to idealize the moment-rotation relationship in the frame analyzes, and this revealed an inaccuracy in the results because this kind of choice did not depict the complex inelastic nature of the structure behavior, when it's subjected to repeated earthquakes.

It must be noted that this thesis, however, focuses on the development of methodologies that are able to predict the real behavior of the structures when exposed to multiple earthquakes, considering the damage due to the influence of previous earthquakes and verifying that the response assessment pathways used provide a correct estimate of collapse fragility, both in case the structure presents material degradation and not. Any limitations in the applicability of such methods will be due only and exclusively to errors found in the implementation codes, and not in the modeling of the system being tested.

CHAPTER 3 NON LINEAR DYNAMIC RESPONSE HISTORY AND COLLAPSE FRAGILITY EVALUATION

3.1 Introduction

During earthquake events, altough mainshock may cause small damages to a structure, subsequent aftershocks may be more dangerous. It's known that the magnitude of aftershocks are usually smaller than the mainshocks ones, but for their ground motion intensity is not always the same. Infact, due to the change in their location, function of the site, aftershocks may have a higher PGA than the mainshock ones, even longer duration, and very marked differences in energy content.

It is for this reason that, in the following approaches, a certain number of sequences is created randomly in such a way that, in a mainshock-aftershock sequence, the first eartquake may have its recorded peak ground acceleration smaller than the aftershock one and viceversa. In any case the main objective is always the same: making sure that shocks of a sequence are related, so investigating the collapse probability of the mainshock-damaged structure in aftershocks. Each methodology is explained in detail: analyzes which leads the structural response evaluation are exposed for each of them: they are the same for the non degrading and the degrading system, but the structural response will be recorded differently for each behavior in function of the non linear dynamic response history recorded, as described better in Chapter 4 and Chapter 5 ; then the probability of exceeding a certain damage level and finally the construction of fragility curves, equal for the intact and the damaged building. A second part of this Chapter is dedicated to the Ground Motions' selection, in particular the set used for analyzes is shown and the selection criteria of each earthquake are explained, making also an overview on databases in which ground motions have been found and from which their time series have been extracted.

3.2 Non Linear Dynamic Analysis: Approach 1

In a seismically active region, structures may be subjected to mainshock–aftershock phenomena or other sequences, leaving no time for repair or retrofit between the

events; based on the non linear dynamic analysis results, collapse fragility curves are generated for intact and damaged buildings (Raghunandan et al., 2015).

Mainshock–aftershock sequences for this analysis are generated using a set of 30 ground motions (exposed in the second part of this Chapter), applied as both mainshocks and aftershocks (Raghunandan et al., 2015).

i) Mainshock Non Linear Incremental Dynamic Analysis

The analyses of structural response in mainshock and aftershock sequences are organized around IDA. In IDA, the non-linear building is subjected to a ground motion having a particular intensity (quantified in terms of PGA), and its response (for instance the maximum displacement) is recorded; in subsequent analyses, the ground motion is scaled to a higher intensity, and the structural response is recorded again (Raghunandan et al., 2015).

This process of scaling the ground motion and recording structural behavior is continued until the structure collapses (Raghunandan et al., 2015), which is indicated by dynamic instability reached by the system in correspondence of the maximum scaling factor of PGA. The collapse capacity associated with each record, infact, is defined by the maximum displacement that the system reaches when the record is scaled at most; the range of scale factors which each record is scaled with, from the lowest value to the highest, is quantified in terms of g and it is sampled in steps of 0.1g starting from 0 and reaching 2g: each ground motion is scaled in a crescent way from 0 to 0.1g and the response is recorded, subsequently from 0.1g to 0.2g and the new response is recorded, until arriving to 2g, limit which the collapse of the system is supposed within.

Through the scaling process, IDA provides insights about structural behavior under rare, high-intensity ground shaking, for which few recordings are available; to account for the effect of record-to-record variability on structural response, IDA is repeated for multiple ground motions (Raghunandan et al., 2015) applied as mainshocks. The structural response will be represented by the maximum displacement recorded in the intact configuration (or in the mainshock) for the system.

ii) Aftershock Non Linear Incremental Dynamic Analysis

In aftershock analysis, the system is subjected to a mainshock–aftershock sequence. The mainshock record is scaled, the response of the structure is recorded, and, subsequently, an aftershock record is applied to the mainshock-damaged structure (Raghunandan et al., 2015). The scale factor on the mainshock record represents the initial damage level of the structure, in other words, once the damage (structural response) for the intact structure has been recorded by launching Mainshock Non Linear Incremental Dynamic Analysys, ground motion intensities corresponding to a specific initial damage state are extracted through an interpolation between mainshock sampled intensities and the damage: these will be scale factors for mainshocks.

A period of 4s is added between the mainshock and aftershock ground motions to represent the situation in which the structure comes to rest after the first event, but is not repaired (Raghunandan et al., 2015). Aftershock analysis is repeated considering the same structure and mainshock–aftershock sequence, increasing the intensity of the aftershock ground motions (by scaling the aftershock record) until the mainshock–aftershock sequence causes the collapse of the system (Raghunandan et al., 2015).

The scale factors on aftershock records are the same used for the evaluation of structural responses under the only mainshock effect (the range from 0 to 2g with steps of 0.1g). The intensity of the scaled aftershock ground motion in the sequence quantifies the collapse capacity of the mainshock-damaged building (Raghunandan et al., 2015). In this study, 500 artificial mainshock–aftershock sequences are created by combining randomly each of the 30 ground motions applied as mainshocks with the same 30 ground motions randomly applied as aftershocks.

In this case the stuctural response will be represented by the maximum displacement recorded in the damaged configuration (or in the aftershock) when the system is already damaged by past earthquakes (or by mainshocks).

3.3 Non Linear Dynamic Analysis: Approach 2

For this approach, the procedure of the structural response evaluation, i.e. the maximum displacement, is the same of Approach 1, both for the intact configuration

(or in the mainshock) and for the damaged configuration (or in the aftershock) when the system is already damaged by past earthquakes (or by mainshocks); it is different from the other two only in the construction of fragility curves, i.e. a different study for the collapse fragility based on a different definition of the probability is conducted, but this is based on non linear IDA results of the Approach 1.

3.4 Non Linear Dynamic Analysis: Approach 3

The system is subjected to a mainshock–aftershock sequence. There are many difference respect to the Approach 1, infact it is based on results of an Incremental Dynamic Analysis; this means that mainshocks are scaled in function of the initial damage level, aftershocks are applied to the damaged structure and they are scaled of 0.1g in a crescent way from 0 to 2g.

In this case each mainshock record is scaled with one only intensitiy that is not sampled, but it is randomly taken from the range [0;2g]; then the response of the system is recorded and and subsequently an aftershock record is applied to the mainshock-damaged structure; the aftershock record is scaled with one only intensity, not sampled, casually taken from the same range [0;2g]. The period addedd between the mainshock and the subsequent aftershock ground motion is always of 4s to represent the situation in which the structure comes to rest after the first event, but is not repaired (Raghunandan et al., 2015).

The intensity of the scaled aftershock ground motion in the sequence quantifies the collapse capacity of the mainshock-damaged building (Raghunandan et al., 2015). The artificial mainshock-aftershock sequences are always 500, and they are created by combining randomly each of the 30 ground motions applied both as mainshocks and aftershocks, but combinations are different from the ones used in the Approach 1.

The structural response will be represented by the maximum displacement recorded both in the intact configuration (or in the mainshock) and in the damaged configuration (or in the aftershock) when the system is already damaged by past earthquakes (or by mainshocks).

3.5 Analytical Collapse Fragility Curves

As part of the research of a method for constructing quantitative fragility curves, i.e. associating a numerical value at each level of damage, analytical type methods are placed, which provide many indexes (such as required ductility, displacement, interstorey drifts, dissipated energy) as the main parameters for the assessment of the structural damage.

Fragility curves are distributions of conditional cumulative probability, they express the probability of overcoming or equaling a certain level of damage conditioned to the extent of the earthquake intensity, which is expressed through the PGA. The term fragility $P_{f,PL}$ is introduced by the following expression (Diego Debortoli, 2013)

$$P_{f,PL}(i) = P[D > d_{PL}/i]$$

where D is the damage function (or *seismic demand*). So the fragility is the probability, conditioned to the intensity of the earthquake (i), that the function of damage exceeds or equals a given PL (or *structural capacity*).

In constructing fragility curves a critical aspect is the division of damage levels, infact the level of damage that a certain structure can suffer for a given waiting seismic action is related to its strategic importance in emergency conditions: generally, for structures of fundamental importance, only a slight damage is allowed, while in other cases higher damage levels are tolerated. This consideration is closely linked to the effectiveness of fragility curves as a useful tool to the priority planning for buildings adjustment and reinforcement of existing ones. Under no circumstances the collapse is allowed.

3.5.1 Analytical Collapse Fragility Curves: Approach 1

The damage function is a random one, whose randomness could derive from uncertainties about materials and seismic actions, consequently it is assumed that fragility curves can be expressed in the form of two-parameter lognormal distribution functions. Based on this assumption, the cumulative probability of the occurrence of

damage D, equal to or higher than damage level d_{PL}, is expressed as (Zekeriya Polat, 2006)

$$P[D > d_{PL}/X] = \Phi\left(\frac{lnX - \lambda}{\xi}\right) \quad (1)$$

where Φ is the standard normal distribution, X is the lognormal distributed ground motion index (PGA), and λ and ξ are the mean and standard deviation of ln X (Zekeriya Polat, 2006).

i) Mainshock Collapse Fragility Curves

Once the damage index is chosen for evaluating the structural damage D after the first shock, a damage limit d_{PL} is defined, associated to a specific Performance Level. The probability of the occurrence of damage D, equal to or higher than damage level d_{PL} is calculated with Eqn.(1), where X are mainshock sampled intensities [0:0.1g:2g], λ and ξ are respectively the mean and the standard deviation of ground motions intensities extracted for the damage level d_{PL}: once the damage function D (the *seismic demand*) is obtained through IDA for each sampled value of mainshock intensities, a vector containing ground motions intensities corresponding to the d_{PL} (the *structural capacity*) is defined through the interpolation of the vector cotaining mainshock sampled intensities and vectors of D.

Plotting the probability that the damage D equals or exceeds a damage limit d_{PL} in function of the mainshock sampled intentities, the fragility curve is built.

ii) Aftershock Collapse Fragility Curves

For the damaged system the collapse fragility curve is calculated based on the aftershock collapse capacities obtained for each of the 500 mainshock–aftershock sequences (Raghunandan et al., 2015) in which the mainshock damage corresponds to an initial damage level for the system $d_{PL,in}$.

In this case D is the damage function (or *seismic demand*) in the damaged configuration (aftershock). Given an initial damage $d_{PL,in}$ for the structure and subsequent limit damage levels $d_{PL,i}$, the cumulative probability of the occurrence of

damage D, equal to or higher than damage levels $d_{PL,i}$, is expressed as (Zekeriya Polat, 2006)

$$P_i[D > d_{PL,i}/X] = \Phi\left(\frac{lnX - \lambda_i}{\xi_i}\right)$$

X are aftershock sampled intensities [0:0.1g:2g] while λ_i and ξ_i are respectively the mean and the standard deviation of ground motions intensities extracted for each of the damage level $d_{PL,i}$: once the damage function D (the *seismic demand*) is obtained through IDA, a number of vectors equal to the subsequent limit damage levels ones, containing respectively ground motions intensities corresponding to each $d_{PL,i}$ (or *structural capacities*), are defined through the interpolation of the vector cotaining aftershock sampled intensities and vectors of D obtained for each artificial sequence.
Fragility curves are built plotting the probability P_i that the damage D occurs or exceeds damage levels $d_{PL,i}$ conditioned from the aftershock sampled intentities, considering an intial damage level for the system $d_{PL,in}$.

3.5.2 Analytical Collapse Fragility Curves: Approach 3

For this kind of approach a similar procedure for the construction of the fragility curves will be presented below, both for single shock scenarios and mainshock-aftershock sequences, which provides the definition of a *Probabilistic Seismic Demand Model (PSDM)*

i) Mainshock Collapse Fragility Curve

It is divided into the following steps:
- Values that represent the maximum response of the structure to the mainshocks are calculated through non linear dynamic analyzes (Section 3.3); the same damage index chosen in the first approach is also used in this case for the evaluation of structural damage D, in order to make a correct comparison of final results obtained by applying all approaches.
- it is assumed that the seismic demand is described by a logonormal distribution, as well as for the first approach, but in this case it is quantified by a parameter *IM*

Intensity Measures, usually expressed in PGA or Sa. Therefore, for a single shock event, the damage index or the *Engineering Demand Parameter* (*EDP*) is calculated with the following expression (J. Ghosh, J. E. Padgett, and M. Sànchez-Silva, 2015):

$$EDP = a\ IM^b$$

In the bilogarithmic plane, this espression defines a *linear PSDM*:

$$ln(EDP) = ln(a) + b\ ln(IM)$$

(J. Ghosh, J. E. Padgett, and M. Sànchez-Silva, 2015) for a single shock situation, because *EDP* is linear function of *IM* in the transformed space, then the damage *D* will be linearly dipendent on *IM*, so damage *D* can be dscribed with the following relation (J. Ghosh, J. E. Padgett, and M. Sànchez-Silva, 2015)

$$ln(D) = a + b\ ln(IM)$$

- Coefficients *a* and *b* are calculated by linear regression on the whole data set represented in the *ln (IM) - ln (EDP)* plane, i.e. we calculate the standard deviation β of the demand values respect to the average value λ given by the regression line for each value of *IM* (Cornell et al., 2002).
- Once the linear regression coefficients *a* and *b* are determined, it is possible to trace the fragility curve for each *PL* as a cumulative logonormal distribution, where the probability of exceeding each *PL* given the seismic action is:

$$P_{f,PL}(IM) = P[EDP > d_{PL}/IM]$$

For single shock scenarios a unique Performance Level (or structural capacity) is defined for the system, corresponding to a limit damage level d_{PL}; the probability of exceeding this d_{PL} is calculated through a closed form expression (Tubaldi et al., 2016)

$$P\,[D > d_{PL}/IM] \ = \Phi\left(\frac{ln(a) + b\ ln(IM) - ln\,(d_{PL})}{\beta_{lnEDP/IM}}\right)$$

$\Phi(\cdot)$ is the standard normal cumulative distribution function (Tubaldi et al., 2016), while $\lambda = ln(a) + b\ ln(IM)$ *is* the expected median value calculated on the regression

line for each *IM*: median value in this case is equal to the average value because, with the hypothesis that, for each value of *IM*, the data distribution is of Gaussian type, median and mean are coincident. $\beta_{lnEDP/IM}$ is the standard deviation calculated on the whole data set represented in the bilogarithmic plane with respect to the median value given by the regression line. Usually the hypothesis of homoscedasticity is associated to the use of this approach, it means that the standard deviation of the *EDP* is assumed constant with respect to *IM* as $\beta_{lnEDP|IM} = \beta$ (Tubaldi et al., 2016).

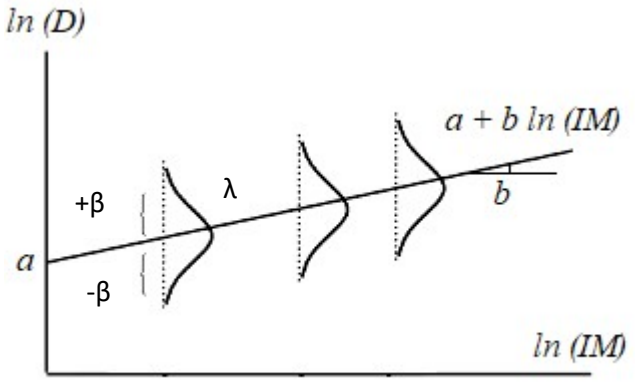

Also in this case the fragility curve is obtained plotting the probability that the damage *EDP* (the requred ductility) equals or exceeds the damage level d_{PL} in function of the mainshock intentities.

ii) Aftershock Collapse Fragility Curves

For the construction of aftershock fragility curves values that represent the maximum response recorded in the damaged configuration, when the system is already damaged by past earthquakes, are calculated through non linear dynamic analyzes (Section 3.3); the damage index is always the same chosen for the first approach.

Unlike single shocks, the evaluation of the damage index under multiple earthquakes is more complex because it depends on the history of shock occurrences. A consideration that could be done about this lies in the fact that, for multiple earthquakes scenarios, the damage *D* is calculated for all seismic shakes involved in the sequence; of course it will solely depends on the strongest shock in the history of the sequence (J. Ghosh, J. E. Padgett, and M. Sànchez-Silva, 2015) which the system

is subjected to, but, regardless this, the damage index after 2 earthquake shocks can be described as a multilinear regression model, consedering that

$$D_2 = f(D_1, IM_2)$$

IM_2 are Intensity Measures which aftershocks are scaled with, D_1 is the damage index evaluated after the system has been subjected to mainshocks and D_2 is the one calculated for the damaged system at the second shock (the seismic demand for the aftershock); so D_2 is evaluated with a *multilinear Probabilistic Seismic Demand Model (PSDM),* considering a multilinear regression built taking into account the relation written above, infact (J. Ghosh, J. E. Padgett, and M. Sànchez-Silva, 2015):

$$ln(D_2) = a + b\, ln(IM_2) + c\, ln(D_1) + d\, ln(D_1)\, ln(IM_2)$$

where *a, b, c, d* are regression coefficients, in particular *d* is the coefficient defining the interaction. Generally this multilinear regression model with interaction can be seen as an extension of the model presented in single shock treatment because the damage index of the structure after the 2 shocks naturally depends on how "weak" the structure has become after being exposed to the previous shock, quantified by D_1 (J. Ghosh, J. E. Padgett, and M. Sànchez-Silva, 2015).

Coefficients *a*, *b, c, d* are calculated by applying the multiple regression on the whole data set represented in the $ln(IM_2) - ln(D_2) - ln(D_1)$ plane, ie we calculate the standard deviation β of the demand values D_2 respect to the median value given by the regression line for each value of IM_2 *and* D_1.

For the damaged system, collapse fragility curves are calculated by considering the aftershock collapse capacities obtained for each of the 500 mainshock–aftershock sequences; it is supposed that the damage level reached by the structure during the first shock (the initial Performance Pevel) corresponds to a limit damage level $d_{PL,in}$.

D_2 is the seismic demand represented by the structural damage recorded by the system in the damaged configuration (aftershock). Given the initial limit damage and subsequent limit damages $d_{PL,i}$, the cumulative probability of the occurrence of damage D_2, equal to or higher than damage levels $d_{PL,i}$, is given by the following expression

$$P_i[D_2 > d_{PL,i}/IM_2] = \Phi\left(\frac{ln(median/d_{PL,in},IM_2) - ln(d_{PL,i})}{\beta}\right)$$

The term $ln(median/d_{PL,in}, IM_2)$ represents the expected median value of the seismic demand D_2 calculated on the regression surface for each IM_2 and considering a $d_{PL,in}$, so the probability is calculated for each mainshock-aftershock sequence and for each subsequent limit damage level. Plotting each probability in function of Intensity Measures, fragility curves are obtained.

3.6 Empirical Collapse Fragility Curves

Considering the same damage index used for Approach 1 and 3, collapse fragility curves are built by exploiting the classical definition of *mathematical* probability, due to Bernoulli and Laplace: the probability of an event is defined as the ratio between the number of favorable cases and the number of possible cases, supposed all equally possible.

Referring to an event, the number of all possible cases is known, subsequently the number of favorable cases is determined (i.e. those cases which verify the event for which the probability is to be calculated), finally the ratio between the number of favorable cases and the number of possible cases is calculated.

3.6.1 Empirical Collapse Fragility Curves: Approach 2

i) Mainshock Collapse Fragility Curve

D is the damage function (or seismic demand) evaluated in the undamaged configuration (mainshock) through non linear IDA (see Section 3.2). The limit damage level, associated to the relative performance level, is fixed d_{PL}

$$P = \frac{1}{N} P\ (D \geq d_{PL})$$

Referring to the event that the damage D equals or exceeds the limit damage d_{PL}, the number of possible cases which this event may realize is given by the total number N of earthquakes which the system is subjected to.

Given that the structural reposnse is due to an IDA analysis, the damage D is associated to a specific shock ad to a specific intensity level, so numerically the number of favorable cases is obtained simply by counting how many of these values of damage D exceed d_{PL}. Representing the probability in function of mainshock sampled intensities, the fragility curve is built.

ii) Aftershock Collapse Fragility Curves

The collapse fragility is evaluated always by considering the collapse capacities of the damaged system in the aftershock, for each of the 500 mainshock–aftershock sequences; the damage level reached by the structure during the first shock (the initial Performance Pevel) corresponds always to a limit damage level $d_{PL,in}$. Given the initial limit damage and subsequent limit damages $d_{PL,i}$, the mathematical probability of the occurrence of damage D, equal to or higher than damage levels $d_{PL,i}$, is given by the following expression

$$P_i = \frac{1}{N} P_i \, (D \geq d_{PL,i})$$

D is the seismic demand in the damaged configuration (aftershock) obtained through non linear IDA (see Section 3.2).

Referring to the event that the damage D equals or exceeds subsequent limit damages $d_{PL,i}$, the number of possible cases N which this event may realize is given by the total number of sequences which the system is subjected to, i.e. 500. The counting procedure is the same as described for mainshock scenarios, with the unique difference that this procedure is repeated as many times as the subsequent limit damage levels $d_{PL,i}$ are. Plotting the mathematical probability in function of aftershock sampled intensities, fragility curves for the damaged system are otained.

3.7 Input Ground Motions

Selecting ground motions is a fundamental step for reaching the final objective: obtaining fragility curves. Multiple earthquakes sequences used for these analyzes are generated using a set of 30 ground motions (Table 3.7a), casually applied as both

mainshocks and aftershocks. These 30 ground motions are recorded from California earthquakes, they are as-recorded (unscaled), with a peak ground accelerations varying between 0.04 and 0.63 g, the moment magnitude Mw is within 6.5–6.9, all recorded on firm soil (USGS type C, B or D) (Vamvatsikos et al., 2006) and at firm sites with closest distance to fault rupture (R) between 15 and 33 km (Raghunandan et al., 2015).

No	Event	Station	$\phi^{\circ *}$	Soil†	$M^{\ddagger}$	$R^{\S}$ (km)	PGA (g)
1	Loma Prieta, 1989	Agnews State Hospital	090	C, D	6.9	28.2	0.159
2	Northridge, 1994	LA, Baldwin Hills	090	B, B	6.7	31.3	0.239
3	Imperial Valley, 1979	Compuertas	285	C, D	6.5	32.6	0.147
4	Imperial Valley, 1979	Plaster City	135	C, D	6.5	31.7	0.057
5	Loma Prieta, 1989	Hollister Diff. Array	255	—, D	6.9	25.8	0.279
6	San Fernando, 1971	LA, Hollywood Stor. Lot	180	C, D	6.6	21.2	0.174
7	Loma Prieta, 1989	Anderson Dam Downstrm	270	B, D	6.9	21.4	0.244
8	Loma Prieta, 1989	Coyote Lake Dam Downstrm	285	B, D	6.9	22.3	0.179
9	Imperial Valley, 1979	El Centro Array #12	140	C, D	6.5	18.2	0.143
10	Imperial Valley, 1979	Cucapah	085	C, D	6.5	23.6	0.309
11	Northridge, 1994	LA, Hollywood Storage FF	360	C, D	6.7	25.5	0.358
12	Loma Prieta, 1989	Sunnyvale Colton Ave	270	C, D	6.9	28.8	0.207
13	Loma Prieta, 1989	Anderson Dam Downstrm	360	B, D	6.9	21.4	0.24
14	Imperial Valley, 1979	Chihuahua	012	C, D	6.5	28.7	0.27
15	Imperial Valley, 1979	El Centro Array #13	140	C, D	6.5	21.9	0.117
16	Imperial Valley, 1979	Westmoreland Fire Station	090	C, D	6.5	15.1	0.074
17	Loma Prieta, 1989	Hollister South & Pine	000	—, D	6.9	28.8	0.371
18	Loma Prieta, 1989	Sunnyvale Colton Ave	360	C, D	6.9	28.8	0.209
19	Superstition Hills, 1987	Wildlife Liquefaction Array	090	C, D	6.7	24.4	0.18
20	Imperial Valley, 1979	Chihuahua	282	C, D	6.5	28.7	0.254
21	Imperial Valley, 1979	El Centro Array #13	230	C, D	6.5	21.9	0.139
22	Imperial Valley, 1979	Westmoreland Fire Station	180	C, D	6.5	15.1	0.11
23	Loma Prieta, 1989	Halls Valley	090	C, C	6.9	31.6	0.103
24	Loma Prieta, 1989	WAHO	000	—, D	6.9	16.9	0.37
25	Superstition Hills, 1987	Wildlife Liquefaction Array	360	C, D	6.7	24.4	0.2
26	Imperial Valley, 1979	Compuertas	015	C, D	6.5	32.6	0.186
27	Imperial Valley, 1979	Plaster City	045	C, D	6.5	31.7	0.042
28	Loma Prieta, 1989	Hollister Diff. Array	165	—, D	6.9	25.8	0.269
29	San Fernando, 1971	LA, Hollywood Stor. Lot	090	C, D	6.6	21.2	0.21
30	Loma Prieta, 1989	WAHO	090	—, D	6.9	16.9	0.638

Table 3.7a Ground motions used to generate mainshock-aftershock sequences that will be applied in the following analyzes (Vamvatsikos et al., 2006)

Ground Motions have been selected making reference to real earthquake recordings, in order to adequately represent the seismic hazard of the site. In fact, following the Eurocode 8 directives, their choice is perfectly consistent with the seismogenic characteristics of the source, the soil conditions, the magnitude, the distance from the source and the maximum horizontal acceleration expected at the site.

3.7.1 PEER and NGA-West2 Database

The platform from which their response spectra and their time series have been extracted is the web-based Pacific Earthquake Engineering Research Center (PEER) ground motion database; infact, in this database, motions as-recorded are present, according to what previously sayd about selection criterias.

With PEER Database it's possible to obtain different outputs by considering lots of characteristics and properties of an earthquake, infact it is mainly based on the NGA-West2 Earthquake Source Table, which contains the list of all seismic events available in PEER Database with all their characteristics and data necessary to extract, as it has been sayd before, response spectra and time series. NGA-West2 includes a very large set of seismic events recorded in worldwide shallow crustal earthquakes in active tectonic regimes post 2003 (https://ngawest2.berkeley.edu/).

Since 2003, infact, numerous well-recorded events have occurred worldwide, including the 2003 Mw 6.6 Bam (Iran), 2004 Mw 6 Parkfield (California), 2008 Mw 7.9 Wenchuan (China), 2009 Mw 6.3 L'Aquila (Italy), 2010 Mw 7.2 El Mayor-Cucupah (California and Mexico), 2010 Mw 7 Darfield (New Zealand), 2011 Mw 6.2 Christchurch (New Zealand), and several well-recorded shallow crustal earthquakes in Japan, among other events; the NGA database has been extensively expanded to include the recorded ground-motion data and metadata, in these and other recent events. The updated database has a magnitude range of 3 to 7.9, and a rupture distance range of 0.05 to 1533 km (Timothy d.Ancheta et al., 2013).

The estimated or measured time-averaged shear-wave velocity in the top 30 m at the recording sites (*Vs30*) ranges from 94 to 2100 m/sec. The database includes uniformly processed time series as well as response spectral ordinates for 111 periods ranging from 0.01 to 20 sec and 11 different damping ratios (Timothy d.Ancheta et al., 2013).

So NGA-West2 is simply a great table including data about real seismic events: infact each of them is listed in function of all properties described in the Earthquake Source Table (Table 3.7.1a), for instance the seismic source, including earthquake origin date and time, moment magnitude, hypocenter location, focal mechanism, occurrence of primary surface rupture, and tectonic environment, among other metadata.

Column	Column Name (units)	Description
A	EQID	An arbitrary unique ID assigned to each earthquake for identification.
B	Earthquake Name	The common name of earthquake. The earthquake name may include the general area or country where earthquake occurred. In the case of multiple earthquakes in the same general area/country (for example there are eight earthquakes in the source table that are located in Imperial Valley, CA), a number was used to distinguish between these events.
C	Earthquake Magnitude	Moment magnitude. When the moment magnitude was not available the surface wave, local or duration magnitude was used.
D	Magnitude Type	If the listed earthquake magnitude is NOT a moment magnitude, this column identifies the type of magnitude ML = local magnitude MS = surface-wave magnitude Mb = body wave magnitude U = unknown magnitude type (-999) = unknown
E	Finite Fault Flag	If 1, a geometric representation of the ruptured area was developed using observed surface rupture, published slip model(s), aftershock distribution (and time after mainshock), etc.
F	Hypocenter Latitude (deg)	Hypocenter latitude adopted by NGA-West2 project
G	Hypocenter Longitude (deg)	Hypocenter longitude adopted by NGA-West2 project
H	Hypocenter Depth (km)	Hypocenter depth (km) adopted by NGA-West2 project
I	Total Fault Length (km)	The total length of the rectangular fault (including all fault segments for multiple-segment (complex) ruptures
J	Total Fault Width	The maximum width of the rectangular fault (including all fault segments for
K	Total Rectangular Fault Area (km*km)	The total area of the rectangular fault (including all fault segments for multiple-segment (complex) ruptures
L	Number of fault segments	Number of segments. Nearly all faults have a single rectangular fault. The maximum is 12.
M	Fault Segment Number	Segment number. Nearly all faults only have a single segment number (1).
N	Strike of fault segment (deg)	Strike angle of the fault plane used to approximate the causative fault surface. 0° <= Strike <= 360°. Convention of fault strike, dip, and rake follows that described in Aki and Richards (1980, p106) (see Figure 2.1)
O	Dip of fault segment (deg)	Dip angle of the fault plane. 0° <= Dip <= 90°. (see note above)
P	Segment Fault Length (km)	Length of the rectangular fault segment. (see Figure 2.1)
Q	Segment Fault Width (km)	Down-dip width of the rectangular fault segment. (see Figure 2.1)
R	Rake Angle (deg)	Rake is the angle measured on the fault plane counterclockwise from the reference strike direction to the average slip direction (see Figure 2.1). -180° <= Rake <= 180°
S	Latitude Fault Segment Upper Left Corner (deg)	Convention of fault upper left corner (ULC) follows that described in Aki and Richards (1980, p106)
T	Longitude Fault Segment Upper Left Corner (deg)	Convention of fault upper left corner (ULC) follows that described in Aki and Richards (1980, p106)
U	Depth of Fault Segment Upper Left Corner (km)	Convention of fault upper left corner (ULC) follows that described in Aki and Richards (1980, p106)

Table 3.7.1a The Earthquake Source Table of NGA-West2 from which it's possible to collect data to use in PEER database for obtaining selected ground motions (Timothy d.Ancheta et al., 2013)

Just to give an example of how ground motions and time series are generated from PEER database using data from NGA-West2 Earthquake Source Table, let's consider the set of 30 selected ground motions previously illustrated in Table 3.7a, in particular the last one event: Loma Prieta, 1989. About that seismic event, as well as the other ones, it's sufficient to consider only it's name (Loma Prieta, 1989) and the station where it has been recorded (WAHO), then we enter in the NGA-West2 Earthquake Source Table with these informations and, once the corresponding row has been found, in parallel we move on PEER Database (Figure 3.7.1a).

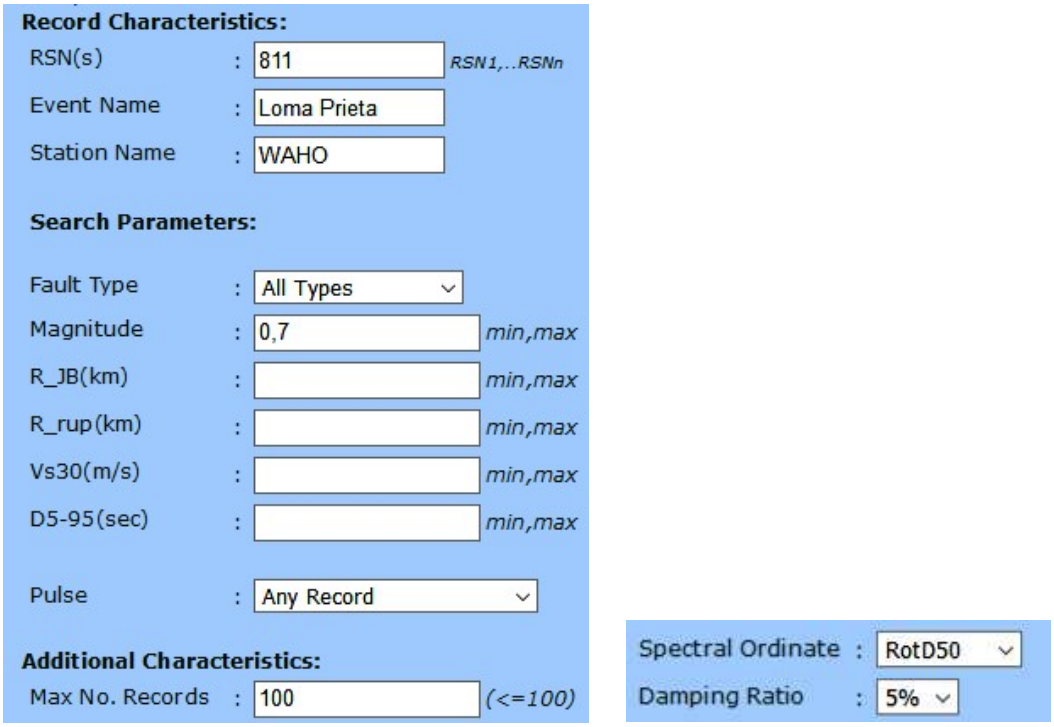

Figure 3.7.1a PEER Database interface

Starting from above we have the Record Sequence Number, a number which identifies the record position inside of the NGA-West2 Earthquake Source Table; after there's the Event Name and the Station Name which are already known; it's not necessary to insert parameters like Fault Type, Pulse, R_jB, R_rup, Vs30, D5-95 and Max No. Records because their values will be given back in the research's results.

The damping ratio used for these analyzes is 5%, a value included also in the range of Database available values (0.5, 1, 2, 3, 5, 7, 10, 15, 20, 25, 30%); furthermore, in correspondence of Spectral Ordinate, RotD50 is selected: it represents 50th percentile

or median amplitude of response spectra over all non-redundant rotations, used in the development of the updated ground motion prediction equations.

Finally, for completeness, the record's Magnitude Range could also be inserted, but it's not necessary because the precise value of magnitude will also be given back in the research's results, and obviously it is the same as the one we read in Table 3.7a or in NGA-West2 Earthquake Source Table referring to that specific earthquake. The response spectrum for the 1989 Loma Prieta earthquake is shown in Figure 3.7.1b.

Figure 3.7.1b Response spectrum in terms of pseudo-acceleration ($\omega^2 S_d$) for the 1989 Loma Prieta earthquake, source: WAHO, California

A first result is the response spectrum for the researched motion, in terms of pseudo-acceleration; the Scale Factor is intentionally set equal to 1 and, referring to this important detail, it's a duty to underline that analyzes for the estimation of the fragility aim to evaluate the behavior of a structure at the limit state of collapse, when subjected to sequences of multiple earthquakes, and so ground motions are not selected for calculating seismic actions useful for designing a new structure or checking an existing one. Therefore it is not necessary to respect the compatibility spectrum condition of

the mean response spectrum with the elastic response spectrum defined as representative of the seismicity of the site where the structure is located.

This is the reason why there is no need to apply any scaling factor or to define an elastic design response spectrum. Figure 3.7.1c shows response spectra for the 30 selected earthquakes

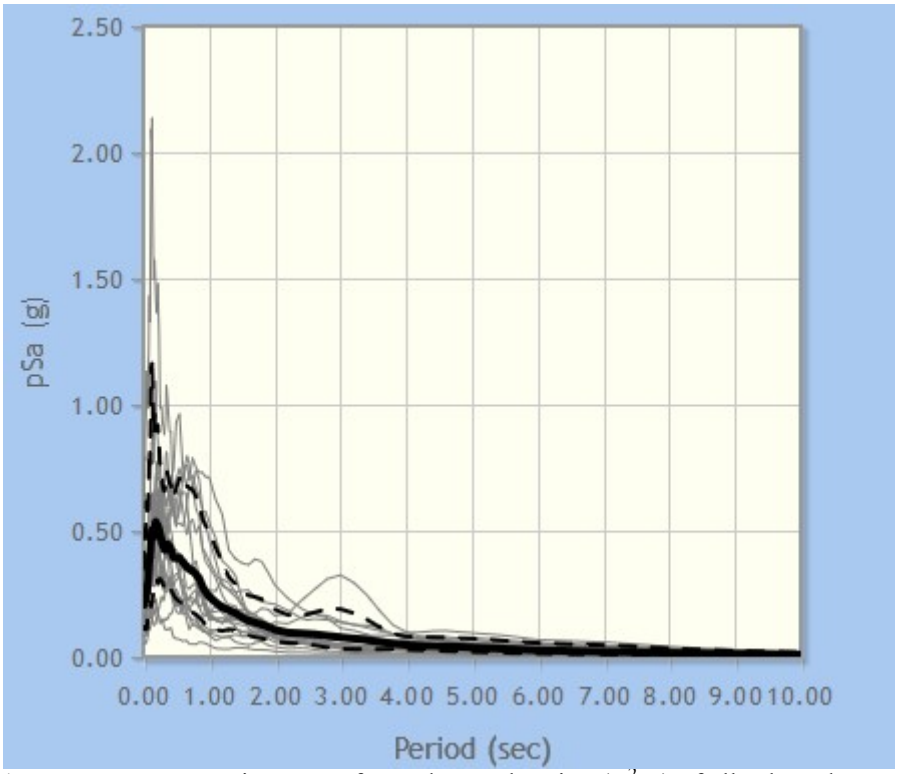

Figure 3.7.1c Response spectra in terms of pseudo-acceleration ($\omega^2 S_d$) of all selected ground motions, with representaton of mean (thick line), mean+σ (upper) and mean-σ (below)

In addition to the response spectrum, the research provides time histories for displacements, velocities and accelerations, defined along the three main directions: the horizontal two and the vertical one. For the representation of time series shown in Figure 3.7.1d the direction along which, for acceleration time series, the maximum PGA is developed (value equal to the one referred to the same event carried out in Table 3.7a), has been considered; in this case the 2nd Horizontal (max recorded PGA for H2 equal to 0.64 ≈ 0.638). This procedure is executed for all ground motions listed in Table 3.7a: once time series in three directions are generated, the only one that will present the maximum PGA equal to the value read in that table will be selected for the subsequent analyzes, for each event.

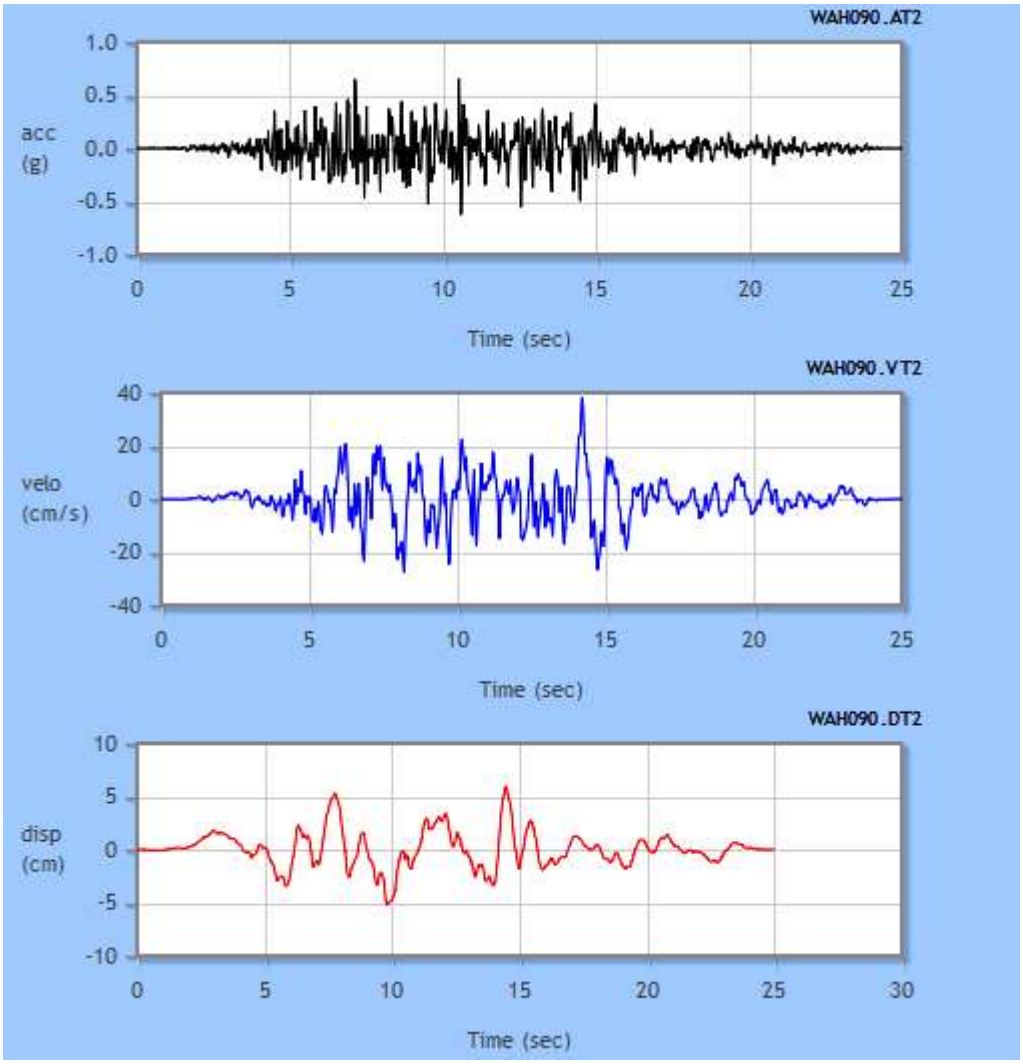

Figure 3.7.1d Time series representations for accelerations (g), velocities (cm/s) and displacements (cm), 1989 Loma Prieta eartquake, source: WAHO, California

In the upper right corner of each time series it's possible to observe a code: it is different for each recording direction, and it represents the name of the text file containing time series, duration, RSN and the number of steps in recording; a string with eight characters in which the first four are riserved for an abbreviation of the station name. The final three characters are reserved for the station azimuth (e.g., up, 090, 180). The extension of the text file describes the information contained within. For example the acceleration, velocity, and displacement text files have the extensions AT2, VT2, and DT2.

As evidenced in Table 3.7a there are repeated seismic events, this means that these earthquakes are considered both in the two horizontal directions H1 e H2, infact the

magnitude is the same, but the PGA and the station azimuth (φ) changes. In Figure 3.7.1e analytical results are illustrated and, in addition to give back parameters not inserted in input process (such as Mechanism/Fault type, Vs30, etc.) and to confirm the real earthquake magnitude read in Table 3.7a for the same event (6.93), there's the possibility to download text files for displacement, velocities and accelerations in all directions. In this case only the text file referred to accelerations (Acc. Files Names in the Figure), in all directions (H1, H2 and Vertical), have been downloaded and, for the subsequent analyzes, only the text file containing the maximum PGA value equal to the one read in Table 3.7a for the same earthquake will be selected, for the specific example the text file referred to the direction H2. In support of this selection, the value of station azimuth in the name of text file (090) is perfectly equal to the value carried out in Table 3.7a for the 1989 Loma Prieta earthquake (φ = 90°).

Result ID	Comp.	Record Seq. #	MSE	Scale Factor	Tp(s)	D5-75(s)	D5-95(s)	Arias Intensity (m/s)	Event	Year	Station	Mag
1	RotD50	811	-	1.0	-	8.0	11.0	6.3	Loma Prieta	1989	WAHO	6.93

Mechanism	Rjb(km)	Rrup(km)	Vs30(m/s)	Lowest useable freq(Hz)	Initial-Search SF	H1 Acc. File Name	H2 Acc. File Name	Vertical Acc. File Name
Reverse Oblique	11.03	17.47	388.33	0.1	1.0	LOMAP_WAH000.AT2	LOMAP_WAH090.AT2	LOMAP_WAH-UP.AT2

Figure 3.7.1e Downloadable text files and analytical results for the 1989 Loma Prieta eartquake, source: WAHO, California

Fragility analyzes will be conducted with the help of software MATLAB, so a MATLAB Code has been created, including a function named readPEER able to read ground motion data included in text files downloaded from PEER database.

CHAPTER 4 APPLICATIONS TO THE CASE OF STUDY: NON-DEGRADING SYSTEM

4.1 Introduction

Basing on design implications which each analysis introducted in Chapter 3 requires, in the following Chapter the evaluation of the Non Linear Dynamic response history is provided, in order to investigate the effect of multiple earthquake loadings on the structural response of non degrading systems, i.e. structures with non degrading behavior in terms of construction materials. The software MATLAB is the only tool used for this purpose.

As mentioned in the introductory Chapter, the model used as case of study is a SDOF system, infact, thanks to its elementary geometry, for an SDOF system it is easier to evaluate its response even when it is subject to complex load cycles. Prior to conducting all analyzes, properties of the system are carried out: to determine the dynamic characteristics in terms of fundamental period of vibration no Eigen value analysis has been conducted, first of all because modal shapes are not object of interest in this discussion, but also because, for a system like a single degree of freedom one, it's easier to choose a priori a value of T rather than finding it through a dynamic analysis, and verify afterwards the correctness of its estimate by checking results. In this way the it can be set up and modified in the best way possible in such a way that the structural response lead to a fragility estimation more similar to what it could be expected in a real case in the same conditions.

Ground motions represented in Section 3.7 are used, and the structural response captured from the non-degrading system is provided, both when it's subjected only to one shock and to the effect of mainshock-aftershock sequences. Finally fragility curves are built for each approach and for both cases just described.

4.2 Non-Degrading System Construction

The SDOF system has been chosen also because in the next Chapter the same procedures will be applied to the case in which the structure presents a degrading

behavior. So, given that the final comparison will focus on results obtained, for the same approaches, in two different behavioral cases but on the same system, and given that modern available tools are not able to provide a correct description of what really happens in a complex MODF system subjected to multiple earthquakes (not neglecting its natural propensity to accumulate damage shock by shock), the SDOF system will be used as unique case of study for both situations, avoiding possible convergence problems; it's a duty to remember that the modeling of the system is not the main topic of this discussion, infact it is only the practical application of methodologies set up; however a general brief description of this model is carried out for having a complete overview of all what needed for conducting this study.

The traditional starting point of any discussion of structure dynamics is the so-called simple oscillator, that is a system with a single degree of freedom. The simple oscillator is an ideal model consisting of a concentrated mass *m* which can move in one direction, constrained by a spring with stiffness *k* (Figure 4.2a).

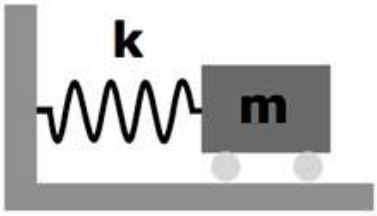

Figure 4.2a Simple Oscillator (Donato Sabia, 2016)

Many real structures can be schematised in this way, for example a hanging tank (Figure 4.2b): this is the one chosen for analyzes conducted in this treatment.

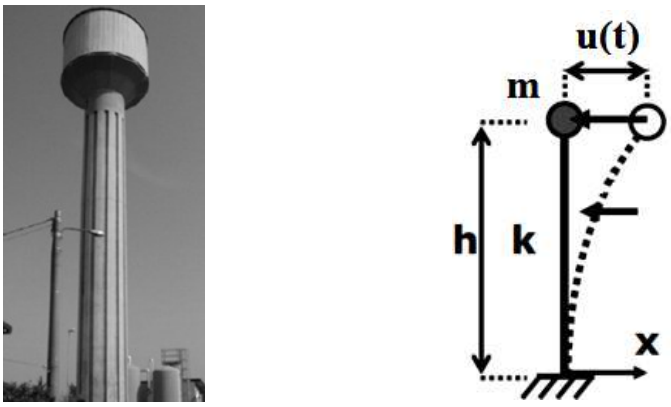

Figure 4.2b Hanging tank (*left*) and calculation model (*right*) (Donato Sabia, 2016)

In these cases the spring of the model represents the stiffness of the drum of the tank, which reacts to a horizontal displacement with a proportional force; the stiffness k is the force that produces a unit displacement, that is the relationship applied between force and consequent displacement. Obviously, the transition from the real object to the model requires a series of simplifications, such as considering the tank shaft to be free of mass. It should also be noted that the tank has, from the static point of view, more than one degree of freedom because both the horizontal displacement and the rotation of the nodes are permitted.

From the dynamic point of view, however, the scheme can be considered with a single degree of freedom; in fact, having considered the mass as concentrated in a point, it is indifferent to the rotations and undergoes only the effect of horizontal displacement (the vertical one is considered null, due to the high extensional stiffness of the drum). The analysis of the dynamic behavior of a simple oscillator starts from the hypothesis that the spring has a linearly elastic behavior.

In real constructions this is plausible when the oscillations are of modest amplitude and therefore for earthquakes with low peak acceleration. Realizing structures that are maintained in the elastic field also for the strongest earthquakes would be possible, but it is not convenient from the economic point of view. It is therefore necessary to analyze, immediately after, the behavior of the scheme once the elastic limit has been exceeded.

The real behavior is quite complex, with a progressive degradation of the stiffness and with a reduction of the resistance in successive loading and unloading phases. The analysis is however carried out, for simplicity, with the hypothesis that the relationship between force and displacements is elastic up to a given value and then perfectly plastic, without resistance degradation (Figure 4.2c), so the model for the SDOF system is non-linear, for the precision a geometric non-linearity due to the coming in a plastic phase over the elastic limit

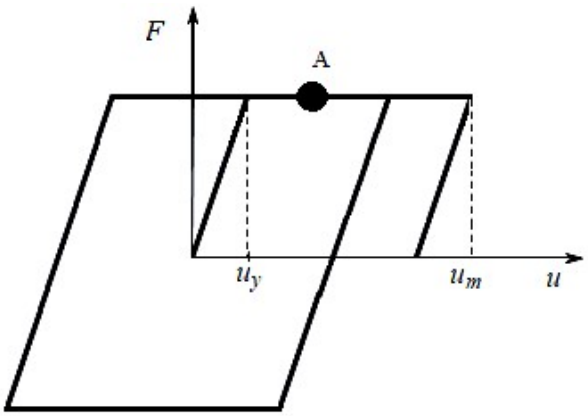

Figure 4.2c Relationship between force and displacement for the SDOF system

The maximum displacement reached u_m pictured in Figure 4.2c represents the seismic demand of the structure when subjected to multiple earthquakes, it is the structural response that will be calculated differently in function of the approach used.

This is a non-degrading system because, looking Figure 4.2c, the reloading phase, representing the coming of the aftershock, passes again through the point A; it means that there's no strength loss and also no rigidity loss because there's no variation of slope in the graph from a cycle to the other.

Let's imagine to impose a horizontal shift to the mass of the simple oscillator and then leaving it free. The mass will oscillate with a well-defined *T* period, with a behavior similar to that of other objects closer to daily experience, such as pendulums.

The mathematical treatment of the free motion of a simple oscillator requires the writing of a relation that expresses, in the generic instant t, the equilibrium between the return force and the inertial action (dynamic equilibrium). If we indicate *u(t)* the horizontal displacement of the mass, the elastic return force is *-ku* (the minus sign indicates that the force acts opposite to the displacement, to bring the mass back to its initial position). The inertial force is instead given by the product between mass *m* and acceleration *u* (second derivative of the displacement). The differential equation of dynamic equilibrium is therefore

$$m\ddot{u}(t) + ku(t) = 0$$

The solution of this equation, with the condition of having an initial displacement u_0, is

$$u(t) = u_0 \cos(\omega t)$$

that is a harmonic function with an angular frequency

$$\omega = \sqrt{\frac{k}{m}}$$

and period

$$T = \frac{2\pi}{\omega} = 2\pi\sqrt{\frac{m}{k}}$$

The free oscillation period T (also called own period of the the system), or the frequency f which is its inverse, containing the information relating to both mass and stiffness, expresses a sort of "dynamic stiffness" of the system.

In reality it is noted that the motion of a simple oscillator does not continue to infinity: its amplitude decreases gradually, until it stops altogether. This is due to the dissipation of energy caused by the air resistance, the friction, etc. The dissipative phenomenon, in itself quite complex, is schematized considering present viscous actions, proportional to the variation of position in time, that is to the speed $\dot{u}$ (derived before the displacement), and therefore equal to $-c\dot{u}$. The proportionality coefficient c is called viscous damping coefficient. The equation of dynamic equilibrium becomes in this case

$$m\ddot{u}(t) + c\dot{u}(t) + ku(t) = 0$$

and can also be written as

$$m\ddot{u}(t) + 2\xi\omega\dot{u}(t) + \omega^2 u(t) = 0$$

having placed

$$\xi = \frac{c}{2\sqrt{km}}$$

The solution of the equation depends on the value of ξ. If this parameter is less than 1, there will be a periodic motion with a decreasing amplitude. With the condition of having an initial displacement u_0, the solution is

$$u(t) = [u_0 \cos(\omega_d t) + \frac{\xi\omega u_0}{\omega_d} \sin(\omega_d t)]e^{-\xi\omega t}$$

which has an angular frequency lower than that of the non-damped motion

$$\omega_d = \omega\sqrt{1-\xi^2}$$

and so a major period

$$T_d = \frac{T}{\sqrt{1-\xi^2}}$$

If, on the other hand, parameter ξ has a value greater than or equal to 1, the system will reach the quiet position without oscillating. The value of the viscous damping coefficient which corresponds to ξ = 1 is called critical damping. The parameter ξ then represents the damping as a percentage of the critical value.

In reinforced concrete structures, damping is mainly due to non-structural elements, such as partitions and infill walls; to a lesser extent also the non-linearity inherent in the behavior of the concrete contributes to the growth of deformations; the value normally used for the percentage damping in the structures in r.c. is 5%. In any case, however, the period T_d is very close to that corresponding to free oscillations in the absence of damping T and the reduction of the amplitude of the motion in subsequent cycles is not very strong.

Basing on these considerations, characteristics of a simple elastic-plastic oscillator, with mass *m*, rigidity *k* and length *l,* are defined. Mass is assigned at the top node using the lumped (concentrated) mass element (Table 4.2a).

m **[kg]**	***l*** **[m]**	***T*** **[s]**	u_y **[m]**	***ξ***	ω_n **[Hz]**	***k*** **[kN/m]**	***c***	***r***	***h***	k_u
1	1	1	0.075	0.05	6.283	39.478	0.682	0	0	0

Table 4.2a Oscillator's properties

The system has been modeled as simple as possible, assigning a priori the oscillation period *T*; once *T* is known, the frequency ω_n, the rigidity *k* and the viscous damping coefficient *c* are obtained basing on equations previously written:

$$\omega_n = \frac{2\pi}{T} \qquad k = \omega_n^2 m \qquad c = 2m\xi\omega_n$$

It is linear elastic-perfectly plastic, as seen previously, so there's no hardening and the stiffness ratio *r* (the inclination of the hardening part), the stiffness ratio for series model *h* and the ultimate stiffness in the hardening part k_u are all equal to 0, infact

$$h = k\frac{r}{1-r} \qquad\qquad k_u = r\,k$$

The yield displacement u_y is set up to 0.075 m; also in ths case, to determine u_y for the system, no pushover analyzes are executed because, as for the period *T*, it's easier to fix a value of yield displacement rather than finding it through the construction of the capacity curve, and verify afterwards the correctness of the choice by checking results.
It is directly implemented in the software MATLAB, infact parameters described above represent input data on which all analyzes, also conducted in MATLAB, are based.

4.3 Structural Response Evaluation: Approach 1

The IDA analysis described in Section 3.2 is set up in MATLAB and the structural response (the maximum displacement of the lumped mass) is recorded with a non-linear integration function; infact it's a duty to remember that a non linear dynamic analysis is an integration of the equation of the dynamic equilibrium in canonical form, and the integration is non linear because of the geometric non linearity of the system

$$F(t) = m\ddot{u}(t) + 2\xi\omega\dot{u}(t) + \omega^2 u(t)$$

Where *m* is the lumped mass and $\ddot{u}(t)$ is the ground motion scaled to a specific value in the range [0,2g], reason for which this integration is executed for records and for all sampled Intensities; the sing minus means that *F* is a reaction opposed to the soil movement. Obviously this non linear ntegration is made with the help of MATLAB.
The ground motion $\ddot{u}(t)$ is function of time, infact each ground motion is characterized by a personal duration *dt*, that is the instant of time which defines how often shocks have been carried out by seismic stations; so *t* is the range of time for the integration of *F*, from 0 to the final time equal to the lenght of the time series (see Figure 4.3a) multiplied by the *dt*, with steps of *dt*.

This is a non-linear integration because, as previously sayd, there's a geometric non-linearity due to the elastic-perfectly plastic costitutive law of the system, but also because *a(t)* is not a linear function of time, infact it is a time series with casual trend, as seen in Figure 4.3a

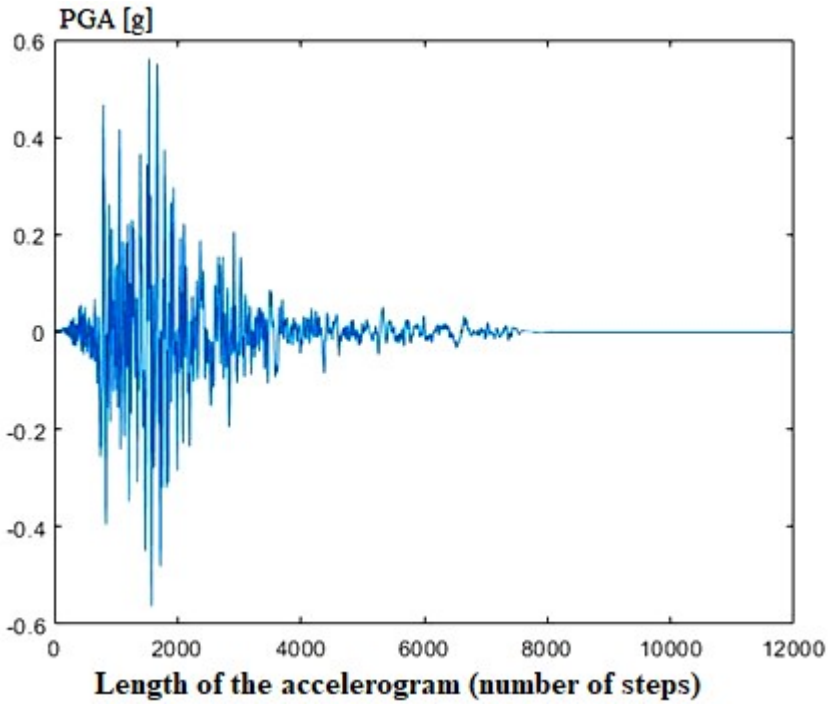

Figure 4.3a Time Series for the 1979 Imperial Valley (Cucapah), scaled to 0.2g of Intensity

The integration of the dynamic equation also needs of other boundary conditions for each sample motion, such as displacement $u(0)$ and velocity $\dot{u}(0)$ initial conditions both equal to 0, the rigidity k of the system and the yield displacement u_y (useful for defining ω), the stiffness ratio r and the viscous damping ratio ξ.

4.3.1 Mainshock Scenarios

To quantify the structural response in an intact configuration, IDA analysis is carried out on the nonlinear model of the system using the set of 30 ground motions (see Section 3.7) acting as mainshocks (Raghunandan et al., 2015).

In Figure 4.3.1a IDA results for the SDOF system are illustrated, showing the relationship between ground motion intensity and the maximum displacement generated at the top mass.

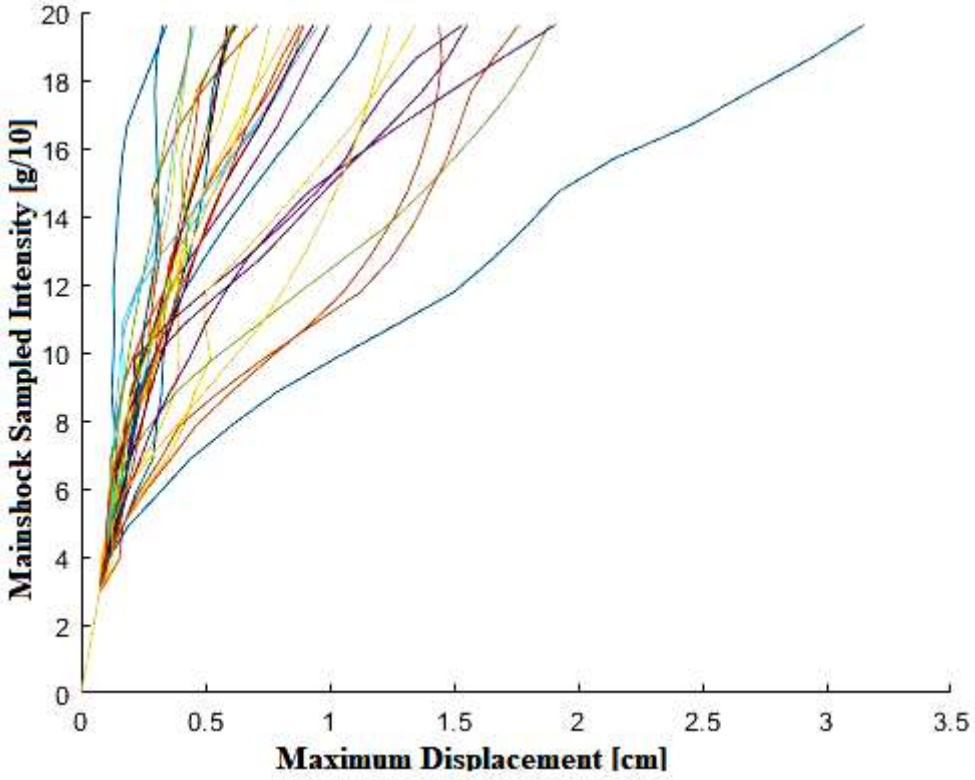

Figure 4.3.1a Incremental dynamic analysis results of the intact system

Mainshock IDA is carried out with closely spaced scale factors (steps of 0.1g, as described in Section 3.2) on the input ground motion, in order to obtain a good estimate of the relationship between ground motion intensity and structural response for each of the records (Raghunandan et al., 2015).

The non linearity is confirmed looking the Figure, infact all IDA curves have the same trend until the reaching of the yield displacement equal to 0.075 m, over that there is substantial variation in structural response as a function of ground motion intensity among the 30 records, due to differences in frequency content, duration, and other ground motion characteristics. About the final purpose, this is the starting point for evaluating the collapse fragility in a system previously damaged by the mainshock.

4.3.2 Mainshock-Aftershock Scenarios

In this case the structural response is recorded with the same non-linear integration function used for the Mainshock analysis, but with some differences in input values: the non-linear integration requires that each mainshock-aftershock sequence must have

a unique value of *dt*, infact for the mainshock analysis this problem is not born because each sequence was formed by a unique ground motion with a specific *dt*; in this case the sequence is formed by two earthquakes, the mainshock and the subsequent aftershock, randomly combined to obtain 500 artificial sequences, and both mainshock and aftershock have a characteristic value of *dt*; so, because not all combinations provide two records having the same duration, the 30 ground motions have been interpolated so that, for each mainshock-aftershock sequence randomly created, there's a unique *dt* given by the average value of the two characteristic ones.

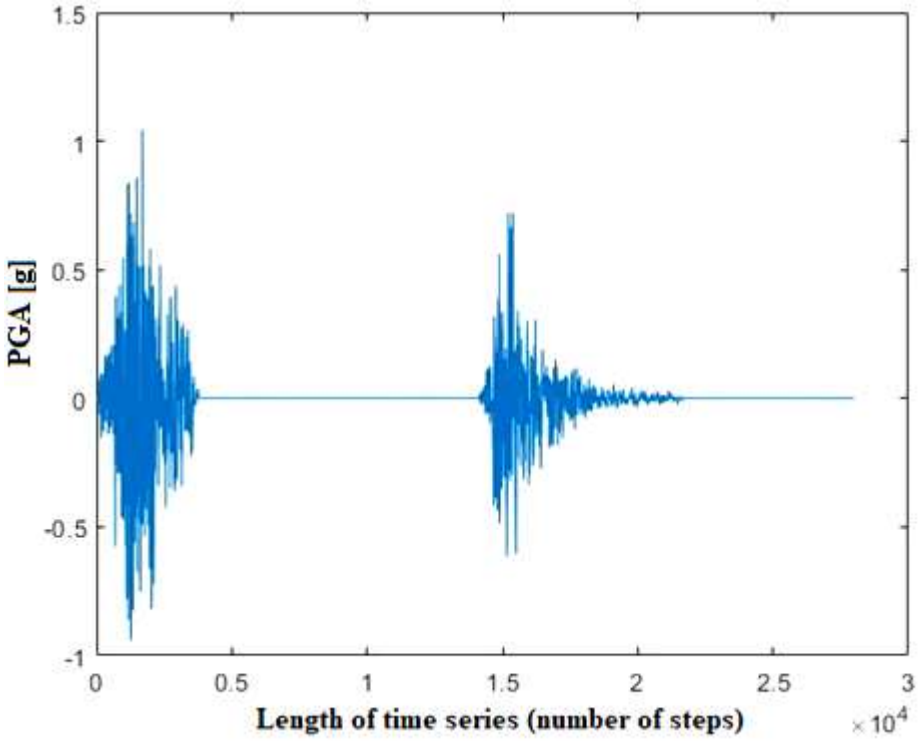

Figure 4.3.2a A mainshock–aftershock sequence randomly created and applied to analyze a mainshock-damaged building; the aftershock is scaled to 0.2g; the unique dt is equal to 0.01s

This operation is repeated for all 500 combinations; *t* is the range of time for the integration of *F*, from 0 to the final time equal to the lenght of the time series (see Figure 4.3.2a) multiplied by the average value of *dt*, with steps of the same entity.

The response time histories *u(t)* of the system under the mainshock–aftershock sequence-type ground motions are obtained through non linear integration of the dynamic equation, as shown in Figure 4.3.2b

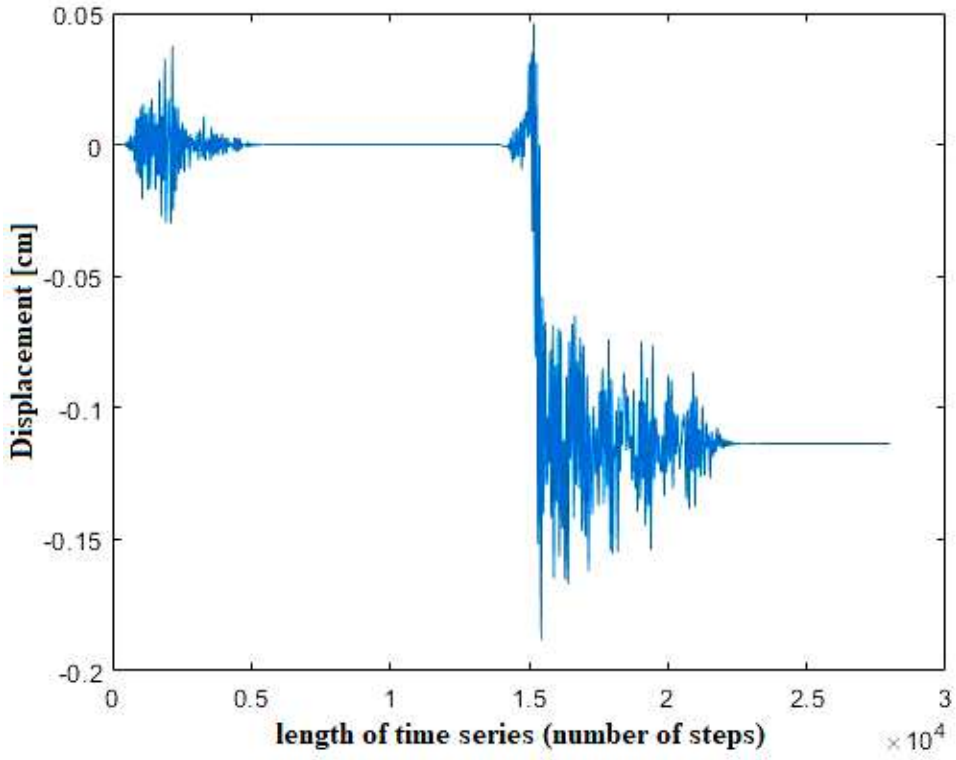

Figure 4.3.2b The displacement time history obtained for an aftershock scale factor of 0.2g: mainshock displacement time history (*left*) and aftershock displacement time history (*right*)

IDA is carried out on the nonlinear model of the system using the set of artificial sequences; the maximum displacement recorded is to be attributed to the system damaged by aftershock, when it's already damaged by mainshocks (Raghunandan et al., 2015).

4.4 Analytical Collapse Fragility Curves: Approach 1

Remembering the definition of fragility curves, they express the probability of overcoming or equaling a certain damage level conditioned to the extent of the earthquake intensity, naturally expressed through the PGA.

The main parameter for the evaluation of the structural damage is the *required ductility*. The required ductility means a maximum displacement at which the collapse of the structure occurs, and it is determined through IDAs previously explained. In this part of the thesis work, as an indicator of damage, the kinematic ductility is assumed

$$D = \mu = \frac{u_{max}}{u_y}$$

where:

-u_{max} is the maximum displacement of the lumped mass during the seismic simulation (either in mainshock or aftershock analyzes)

-u_y is the yield displacement of the same mass

The critical aspect, as sayd, is the division of damage levels, because the SDOF system does not represent any existing building; it's not possible to determine them, for this system, because there's no real structure equal to the modeled SDOF system which it's possible to compare the non-linear analysis of the system with the analysis of the damage suffered for the real structure as a result of the same earthquakes really occurred for.

Given the lack of information on damage of buildings found in real cases following the artificial sequences created, it is decided to adopt the three ductility values as damage indices, for relatives Performance Levels

$d_{PL,1} : \mu = 0.5$ *Slight Damage*

$d_{PL,2} : \mu = 2$ *Moderate Damage*

$d_{PL,3} : \mu = 4$ *Extended Damage*

So, with this approach, the fragility is considered as the probability, conditioned to the intensity of the earthquake, that the function of damage *D* exceeds or equals a given *PL* (or *structural capacity*).

4.4.1 Mainshock Collapse Fragility Curve

The damage level d_{PL} is related to the damage function *D* (or *seismic demand*), in the case in question represented by the maximum ductility required by the system in the undamaged configuration (mainshock). A ductility value as damage index, associated to the relative performance level, is defined

$$d_{PL} : \mu = 0.5 \quad \textit{Slight Damage}$$

Remembering the definition of the cumulative probability of the occurrence of damage *D*, equal to or higher than damage level d_{PL} (Zekeriya Polat, 2006)

$$P[D > d_{PL}/X] = \Phi\left(\frac{lnX - \lambda}{\xi}\right)$$

λ and ξ are respectively the mean and the standard deviation of intensities corresponding to the damage level d_{PL}: $\mu = 0.5$ and extracted by interpolating the vector of mainshock sampled intensities with vectors of the damage D (the required ductility, or the *seismic demand*), obtained through IDA for each sampled value of intensity and for each ground motion; X are mainshock sampled intensities [0:0.1g:2g]

λ	ξ
1.4806	0.0017

For the damage level d_{PL} : $\mu = 0.5$ the probability that D equals or exceed d_{PL} is graphically represented in function of X to obtain the fragility curve (Figure 4.4.1a)

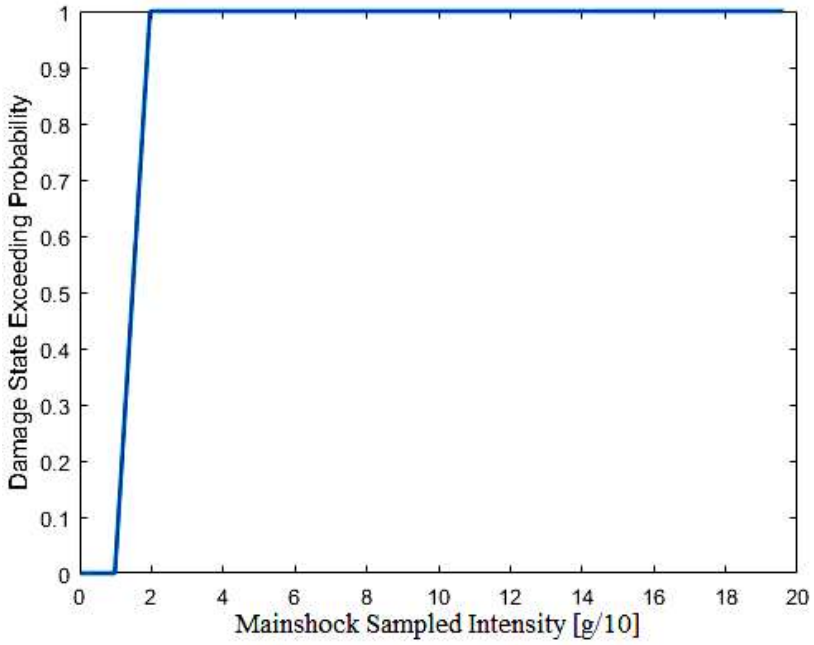

Figure 4.4.1a Collapse Fragility Curve for the Mainshock IDA Analysis $d_{PL} = 0.5$

A first consideration could regard the modality which the system reaches the collapse with: the trend of the curve could make us think that, for the specific d_{PL}, the collapse has been reached for a low value of intensity (0.2g) without giving the possibility to the system to go through a progressive damage phase before. Infact the system is in

linear field for intensities going from 0 to 0.1g, after 0.1g it reaches the failure at 0.2g almost rapidly, and the plastic transition, useful to the system for damaging itself before the collapse, is very small; consequently it's not possible to predict its failure.

4.4.2 Aftershock Collapse Fragility Curves

The collapse fragility, in this case, is evaluated for the damaged system and calculated referring to the aftershock collapse capacity defined for each of the 500 mainshock–aftershock sequences. The mainshock damage corresponds to an initial damage level for the system $d_{PL,in}$: $\mu = 0.5$, the same applied as limit ductility in the construction of the mainshock fragility curve.

In this case D is the damage function (or *seismic demand*), represented by the maximum ductility required by the system in the damaged configuration (aftershock). Given an initial damage and subsequent damage levels

$$d_{PL,in} : \mu = 0.5 \qquad d_{PL,1} : \mu = 0.5 \qquad d_{PL,2} : \mu = 2 \qquad d_{PL,3} : \mu = 4$$

the probability that the damage D equals or exceeds damage levels $d_{PL,i}$ (Zekeriya Polat, 2006)

$$P_i[D > d_{PL,i}/X] = \Phi\left(\frac{lnX - \lambda_i}{\xi_i}\right)$$

λ_i and ξ_i are respectively the mean and the standard deviation of intensities corresponding to damage levels $d_{PL,i}$ and extracted by interpolating the vector of aftershock sampled intensities with vectors of the damage D (the required ductility, or the *seismic demand*), obtained through IDA for each sampled value of intensity and for each artificial sequence; X are aftershock sampled intensities [0:0.1g:2g]

	$d_{PL,1}$	$d_{PL,2}$	$d_{PL,3}$
λ	1.4808	6.3215	10.2279
ξ	0.0019	1.9982	2.7036

For each damage level $d_{PL,i}$ fragility curve is obtained plotting P in function of aftershock sampled intensities (Figure 4.4.2a)

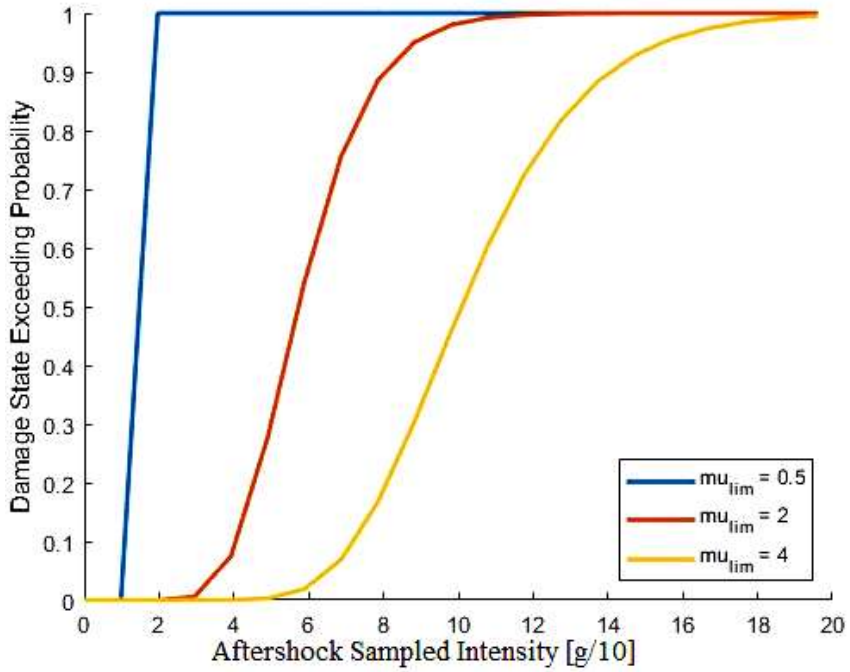

Figure 4.4.2a Collapse Fragility Curves for the Aftershock IDA Analysis

For an initial damage level equal to 0.5, the situation is the same as in the case of intact building if the system reaches the collapse for a damage level μ = 0.5. The more it increases the more the plastic transition increases an the more it's possible to predict the failure, because the probability of occurrence decreases and, passing from mainshock to aftershock, the system has the time to damage itself further but without collapsing.

4.5 Structural Response Evaluation: Approach 3

Also in this case the dynamic analysis is carried out on the nonlinear model of the system using the set of artificial sequences, and the final response is represented by the maximum displacement recorded in the damaged configuration (or in the aftershock), when the system is already damaged by past earthquakes (or by mainshocks).

The non linear dynamic analysis is set up in MATLAB and the structural response is recorded with the same non-linear integration function used for the Approach 1: each

mainshock-aftershock sequence has a unique value of *dt*, although the sequence is formed by two distinct earthquakes, the mainshock and the subsequent aftershock, with a characteristic value of *dt*; infact the 30 ground motions have been interpolated with the same procedure applied in Approach 1, so that, for each mainshock-aftershock sequence randomly created, there's a unique average value of *dt*.

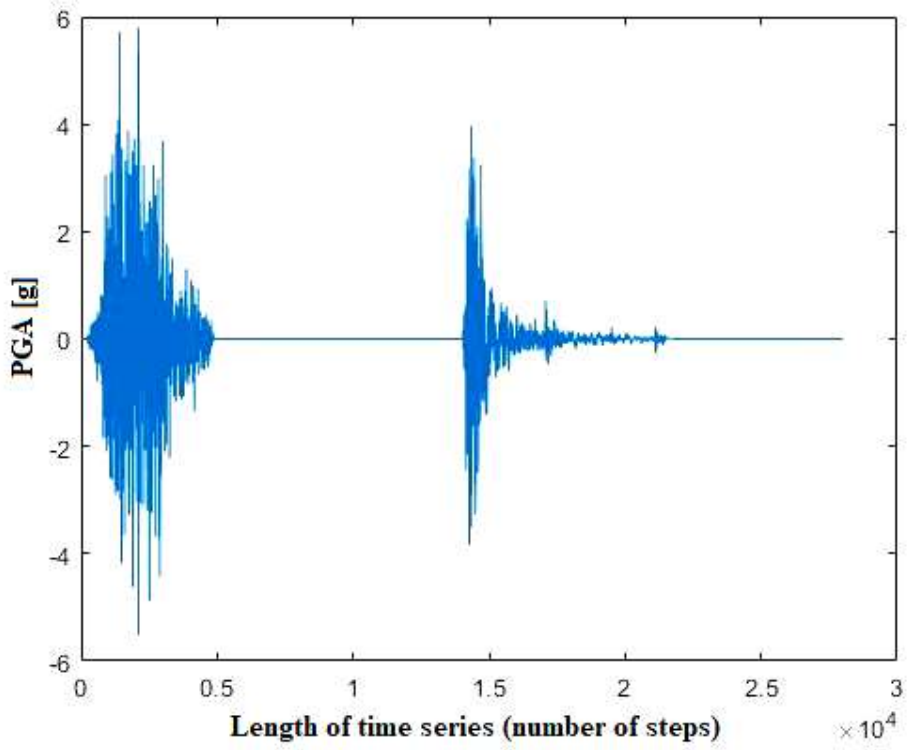

Figure 4.5a 1989 Loma Prieta earthquake (Hollister Differential Array station, *left*), 1989 Loma Prieta earthquake (Anderson Dam Downstream station, right)

In Figure 4.5a the time series of a mainshock-aftershock artificial sequence is shown, in which the 1989 Loma Prieta earthquake (recorded from the Hollister Differential Array station), scaled with an intensity of 0.583g and applied as mainshock, is casually combined with the 1989 Loma Prieta earthquake (recorded from the Anderson Dam Downstream station), scaled with an intensity of 1.305g and applied as aftershock.

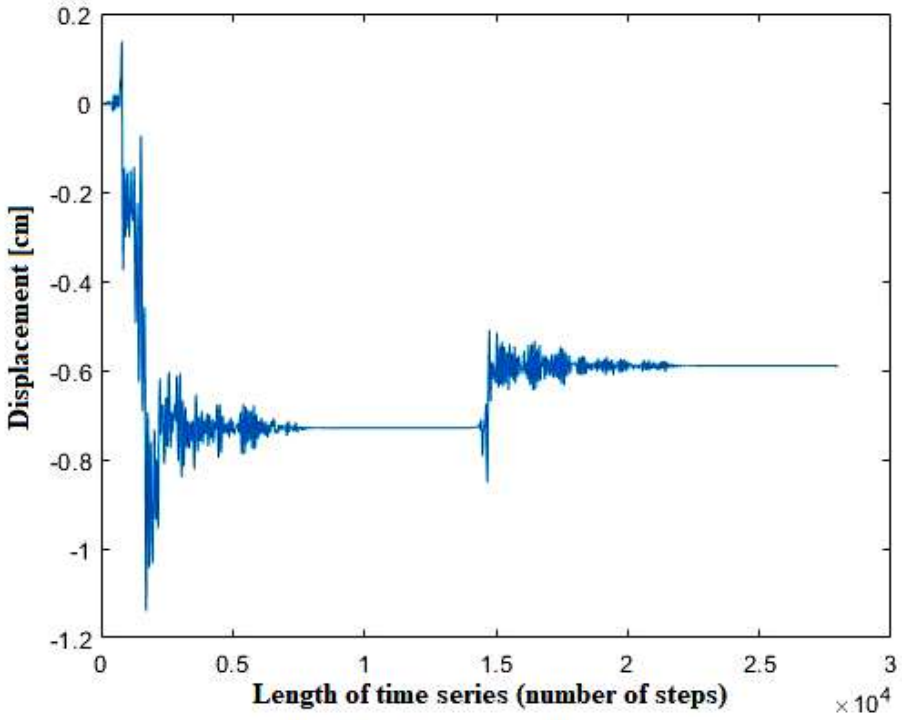

Figure 4.5b Mainshock displacement time history (*left*) and aftershock displacement time history (*right*)

Also in this case the response time histories of the system under the mainshock–aftershock sequence-type ground motions *u(t)* are obtained through the non linear integration of the dynamic equation, as shown in Figure 4.5b. This is the non linear dynamic response history, which it's possible to evaluate the structural response from.

4.6 Analytical Collapse Fragility Curves: Approach 3

For this kind of approach the construction of fragility curves is preceeded by the definition of a *Probabilistic Seismic Demand Model (PSDM)*, an advanced probabilistic approach which is needed to obtain a reliable estimate of the risk of impact (Tubaldi et al., 2016), for both for single shocks and mainshock-aftershock scenarios.

4.6.1 Mainshock Collapse Fragility Curve

The *seismic demand* is represented by the maximum ductility required by the system, obtained as the ratio between the maximum displacement of the lumped mass under mainshocks effects and the yield displacement; the maximum displacement is

calculated through non linear dynamic analysis (see Section 3.3) exploiting the non linear integration described in Section 4.5; so the kinematic ductility is considered as an index of damage.

Considering Intensity Measures *IM* as intensities which mainshocks are scaled with, for a single shock event the *EDP* (the damage *D* or the *seismic demand*) is calculated as (J. Ghosh, J. E. Padgett, and M. Sànchez-Silva, 2015):

$$EDP = a\ IM^{b}$$

In the bilogarithmic plane, this espression defines a linear *PSDM* (J. Ghosh, J. E. Padgett, and M. Sànchez-Silva, 2015):

$$ln(EDP) = ln(a) + b\ ln(IM)$$

coefficients a and b are calculated by linear regression, as well as the standard deviation β of demand values. Graphically the linear regression line presents the trend reported in Figure 4.6.1a

a	***b***	***β***
0.301	1.176	0.451

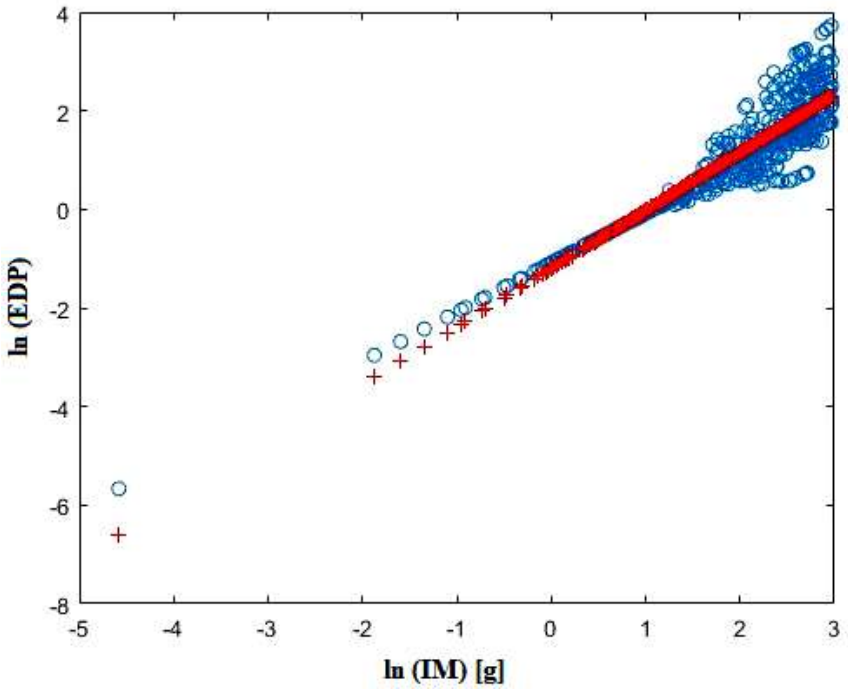

Figure 4.6.1a Linear Regression in the *ln (IM) – ln (EDP)* plane

In Figure 4.6.1a the blue dots represent the bilogarithmic distribution of *IM* and *EDP* for the 500 mainshock samples, in particular the red line is the regression one, which defines average values for each *IM* (the straight line defined by the equation *ln (a) + b ln (IM)*); most of samples exceed the elastic phase entering in the plastic one, and this is easy to understand because, up to a value of ln (*IM*) more or lesse qual to 1, there's a linear data distribution, over which there's a light dispersion from the regression line; however the precision obtained in fitting quantities confirms that this demand model is suitable to predict the damage index for single shock scenarios.
The probability of exceeding each *PL* given the seismic action is:

$$P_{f,PL}(IM) = P[EDP > d_{PL}/IM]$$

IM are intensities which mainshocks are scaled for; for single shock scenarios, a unique limit damage (structural capacity), associated to the Performance Level, is defined for the system, corresponding to a limit ductility d_{PL}: $\mu = 0.5$; so, using the closed form developed by Tubaldi et al. 2016 (Section 3.5.2 *i*)), and plotting the probability that the damage *D* (or *EDP*) equals or exceeds d_{PL} in function of mainshock intensities, the fragility curve is represented in Figure 4.6.1b

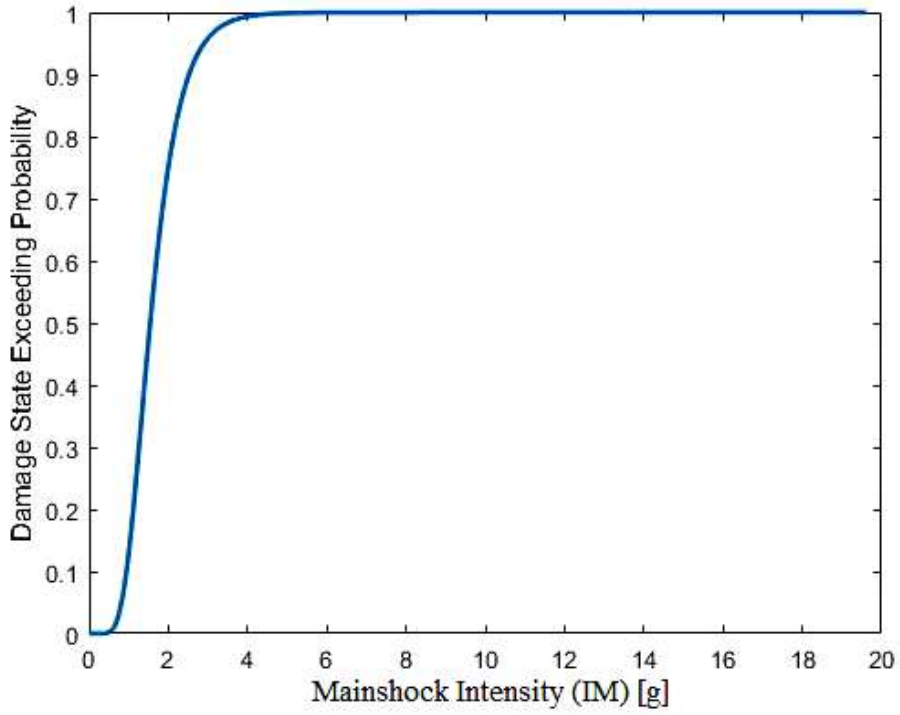

Figure 4.6.1b Collapse Fragility Curve for the Mainshock Non-Linear Dynamic Analysis $d_{PL} = 0.5$

4.6.2 Aftershock Collapse Fragility Curves

The damage is represented by the maximum ductility required by the damaged system, obtained as the ratio between the maximum displacement of the lumped mass under the effect of aftershock sequences and the yield displacement; the maximum displacement is calculated through non linear dynamic analysis (see Section 3.3) exploiting the non linear integration described in Section 4.5; so the kinematic ductility is always considered as an index of damage.

Knowing that the only parameter that can be considered strictly cumulative is total Energy dissipated E_h (J. Ghosh, J. E. Padgett, and M. Sànchez-Silva, 2015), for the kinematic ductility the maximum value is important, which could be reached either during the most imminent earthquake or in any of the previous shakes, this depends on the nature of the earthquake shocks. Thus it is expected that μ_2 should always be greater than μ_1 (J. Ghosh, J. E. Padgett, and M. Sànchez-Silva, 2015), but this is not always true.

Infact, in this approach, the damage function is a random one, but randomness, besides uncertainties about materials and seismic actions, derive from the choice to combine earthquakes in random mainshock-aftershock sequences, so a mainshock may have an intensity smaller than the aftershock one and viceversa; the fortuity is further amplified from the assumption that each earthquake of the sequence is multiplied for a scale factor whose value is randomly taken from the range [0;2g], and also in this case there could be the possibility that the first shock is more harmful than its subsequent one. Consequently this may lead to a case where $\mu_1 > \mu_2$. The ductility depends on the strongest shock, but regardless of this, the seismic demand model for a mainshock-aftershock sequence is built considering that

$$D_2 = f(D_1, IM_2)$$

IM_2 are intensities which aftershocks are scaled with, D_1 is the damage index evaluated after the system has been subjected to mainshocks and D_2 is the required ductility for the aftershock; D_2 is evaluated with a multilinear regression model

$$ln(D_2) = a + b\, ln(IM_2) + c\, ln(D_1) + d\, ln(D_1)\, ln(IM_2) \qquad (1)$$

(J. Ghosh, J. E. Padgett, and M. Sànchez-Silva, 2015) where *a, b, c, d* are regression coefficients, in particular *d* is the coefficient defining the interaction. Before applying this multilinear regression and finding regression coefficients there's a fundamental consideration to do about the Eqn (1): the construction of the most appropriate demand model to fit damage indexes D_1, D_2 and IM_2 intensities is based on the observation of IM_2/D_2 distribution in a Cartesian plane (Figure 4.6.2a). The trend is rather unusual because, for relatively low seismic excitation levels (more or less up to 0.55g) the distribution of samples (mainshock-aftershock sequences) is linear, but their presence is quite poor, and at the same time these few samples require a ductility (D_2) to the system almost equal to 0, which means that the few sequences present are able to keep the system in the elastic phase even though it is damaged by the previous shock (D_1).

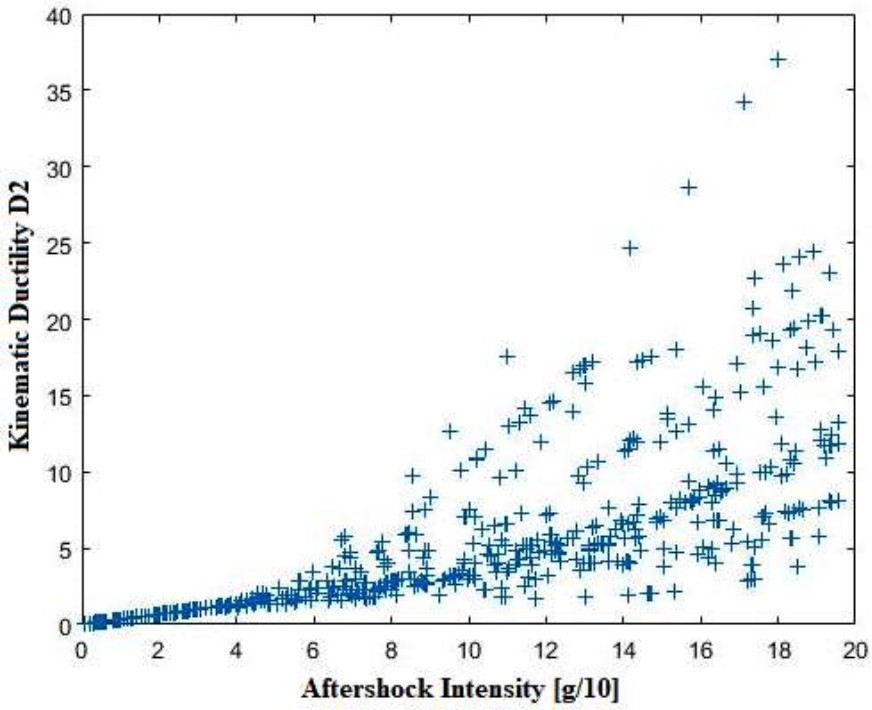

Figure 4.6.2a Seismic demand distribution at the 2nd erthquake shock (for all 500 mainshock-aftershock sequence) in function of aftershock scale factors

For increasing levels of IM_2 the presence of samples becomes thicker, the linearity of the distribution is lost and the related ductility demand increases significantly, this means that most of the sequences require a ductility that leads the damaged system into the plastic phase.

So the nonlinear behavior is expected to induce an increased dispersion of the *EDPs* (D_2) values, because of the reduced efficiency of an IM_2 that is based on the elastic system properties; thus, also the assumption of homoscedasticity could be not satisfied (Tubaldi et al., 2016). The difference in behavior between one phase and the other is further marked by the increase in data dispersion, as possible to see in Figure 4.6.2a, consequently a linear relationship in the log–log plane between the IM_2 and the median response could be not valid for the entire IM_2 range of interest: this is a situation in which a linear *PSDM* can fail in properly describing the seismic demand (Tubaldi et al., 2016).

For accurately describing the *EDP*, or seismic demand, many alternative procedures exist; for example a *bilinear PSDM* is considered because of its simplicity and the small number of parameters involved in the fitting (Figure 4.6.2b)

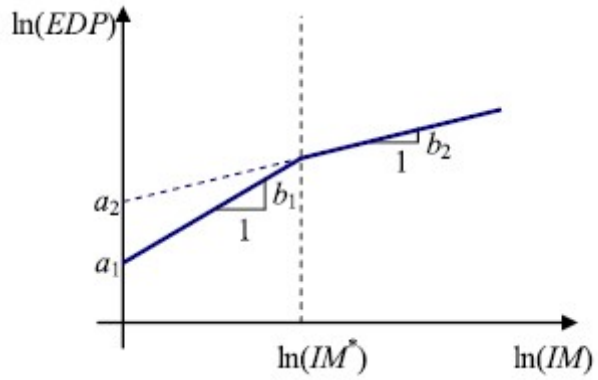

Figure 4.6.2b Bilinear regression model and parameters involved (Tubaldi et al., 2016).

This bilinear regression model is described by the expression (Tubaldi et al., 2016):

$$ln\,(EDP/IM) = [a_1 + b_1\,ln(IM)]\,H_1 + [a_2 + b_2\,ln(IM)](1 - H_1)$$

in which a_i and b_i (i = 1, 2) represent intercepts and slopes of the i-th segment, respectively, and H_1 denotes the step function (i.e. $H_1 = 1$ for $IM \leq IM^*$, and $H_1 = 0$ for $IM > IM^*$); the parameter IM^* identifies the breakpoint, the point of intersection of the two segments, representing on average the yielding of the building. The value of IM^* is obtained by solving the following equation (Tubaldi et al., 2016):

$$a_1 + b_1\,ln(IM^*) = a_2 + b_2\,ln(IM^*)$$

by substituting this relation into previous one, with the appropriate parameters, the following alternative expression is obtained (Tubaldi et al., 2016):

$$ln\,(D_2/IM_2) = [a_1 + b_1\,ln(IM_2)]\,H_1 + [a_1 + (b_1 - b_2)\,ln(IM^*) + b_2\,ln(IM_2)](1 - H_1) \quad (2)$$

The yellow relation defines the 1st segment, the green one defines the 2nd segment. Considering that the seismic demand D_2 and relatives intensities IM_2 have a bilinear distribution (Eqn (2)), and knowing that, in mainshock-aftershock scenarios, the same seismic demand not only depends on aftershock intensities IM_2 but also on the damage the structure suffers during the first shock D_1 (Eqn (1)), a *multi-bilinear regression* has been performed (Figure 4.6.2c)

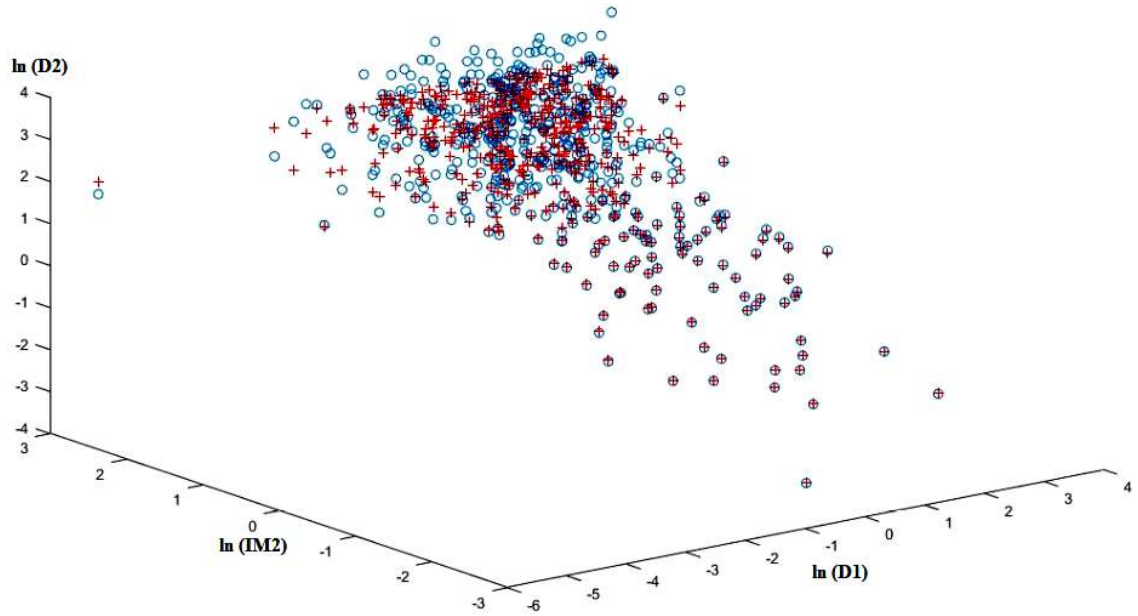

Figure 4.6.2c *Multi-bilinear* regression model, with interaction, for the case of study

Described by the following expression

$$ln(D_2) = H_1\,[a_1 + b_1\,ln(IM_2) + c\,ln(D_1) + d\,ln(D_1)\,ln(IM_2)] + \\ + (1 - H_1)\,[a_1 + b_1\,ln(IM^*) + b_2\,ln(IM_2 - IM^*) + c\,ln(D_1) + d\,ln(D_1)\,ln(IM_2 - IM^*)] \quad (3)$$

Where H_1 is the step function

$$H_1 = IM^* - IM_2$$

a_1, b_1, b_2, c, d are estimated with the regression just performed.

The first coefficients are used in the representation of the *bilinear PSDM* for D_2 and

IM_2, infact, referring to Figure 4.6.2b, it is developed by semplifying the Eqn (3)

$$ln(D_2) = H_1 [a_1+b_1 ln(IM_2)] + (1-H_1) [a_1+b_1 ln(IM^*)+b_2 ln(IM_2-IM^*)]$$

The Figure 4.6.2d confirms the presence of most of sequences after IM* remarking the predominantly non linear behavior of the system, as sayd before; the red bilinear straight line is the regression one, which defines median values for each IM_2 (defined by the Eqn (3)). Coefficients *c, d* are properly of the interaction, infact *c* expresses the D_2 dipendence on D_1 while *d* quantifies the dipendence on coupling between D_1 and IM_2.

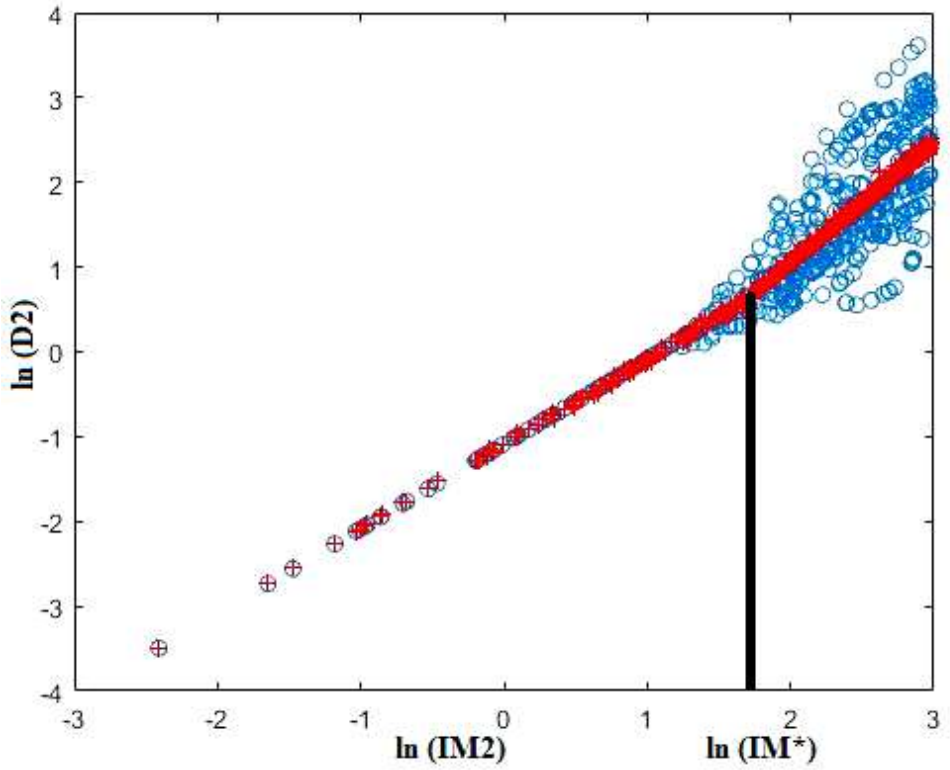

Figure 4.6.2d Bilinear demand model for D_2 and IM_2

a_1	b_1	b_2	$ln(IM^*)$ [g]
-1.0623	1.0091	1.4252	1.709

c	*d*
-0.0183	-0.0117

From these results it seems obvious that the damage index D_2 is slightly influenced by the damage occurred after the first shock D_1: the collapse fragility final for the system is almost all attributable to the effects of the aftershock; this is confirmed by fact that d is more or less equal to c, so the poor influence of D_1 on D_2 is verifiable also in the coupling with IM_2.

It is noteworthy that the use of a bilinear model permits to consider two different dispersions for the linear (first segment) and nonlinear (second segment) range of behavior, i.e. the assumption of homoscedasticity is not worth anymore (Tubaldi et al., 2016). As sayd, the two dispersions represent standard deviations of the seismic demand D_2 respect to the median value given by the regression surface for each value of IM_2 and D_1, respectively β_1 for $IM_2 < IM^*$, and β_2 for $IM_2 > IM^*$

β_1	β_2
0.0841	0.5028

The two dispersions confirms the goodness of fit measures: looking the Figure 4.6.2d and 4.6.2c the median response (red distribution) is perfectly osculatory with the ductility demand (blue distribution) until IM^*, infact the dispersion in the 1st segment β_1 is very small; after IM^* the dispersion between the median response and the ductility demand increases, due to the non linearity of the system, and this explains the increasing value from β_1 to β_2, but β_2 is however a more than acceptable value because in this case it's impossible to improve further the fitting, given this dispersion.

Collapse fragility curves are calculated by considering aftershock collapse capacities referring to the 500 mainshock–aftershock sequences; the initial damage level for the structure corresponds to a limit ductility $d_{PL,in}$: $\mu = 0.5$.

Given the initial limit damage and subsequent limit damages

$$d_{PL,in} : \mu = 0.5 \qquad d_{PL,1} : \mu = 0.5 \qquad d_{PL,2} : \mu = 2 \qquad d_{PL,3} : \mu = 4$$

the probability that the damage D_2 equals to or exceeds damage levels $d_{PL,i}$ is obtained with the following relation

$$P_i[D_2 > d_{PL,i}/IM_s] = \Phi\left(\frac{ln(median/d_{PL,in},IM_s) - ln(d_{PL,i})}{\beta_1}\right) \qquad for\ IM_s < IM^*$$

$$P_i[D_2 > d_{PL,i}/IM_s] = \Phi\left(\frac{ln(median/d_{PL,in},IM_s) - ln(d_{PL,i})}{\beta_2}\right) \qquad for\ IM_s > IM^*$$

In orded to make a fragility comparison with the other two approaches used, intensities used for representing fragility curves must be the same; in previous approaches the intensity was sampled with steps of 0.1g in a range from 0 to 2g, in this approach they are casually extracted from a range with the same dimension [0;2g] so, for having a correct comparison, also in this approach they are sampled in the same range with the same step, and IM_2 become IM_s. Consequently IM_2 are subtituted with sampled values IM_s in Eqn.(3), as well as $d_{PL,in}$ substitutes D_1 as representive of the damage limit state for the first shock. $ln(median/d_{PL,in}, IM_s)$ is the expected median value of the seismic demand D_2 calculated on the regression surface (Eqn.(3)) for each IM_s and referring to $d_{PL,in}$. Fragility curves are obtained by plotting the probability calculated for each subsequent limit damage in function of IM_s (Figure 4.6.2e)

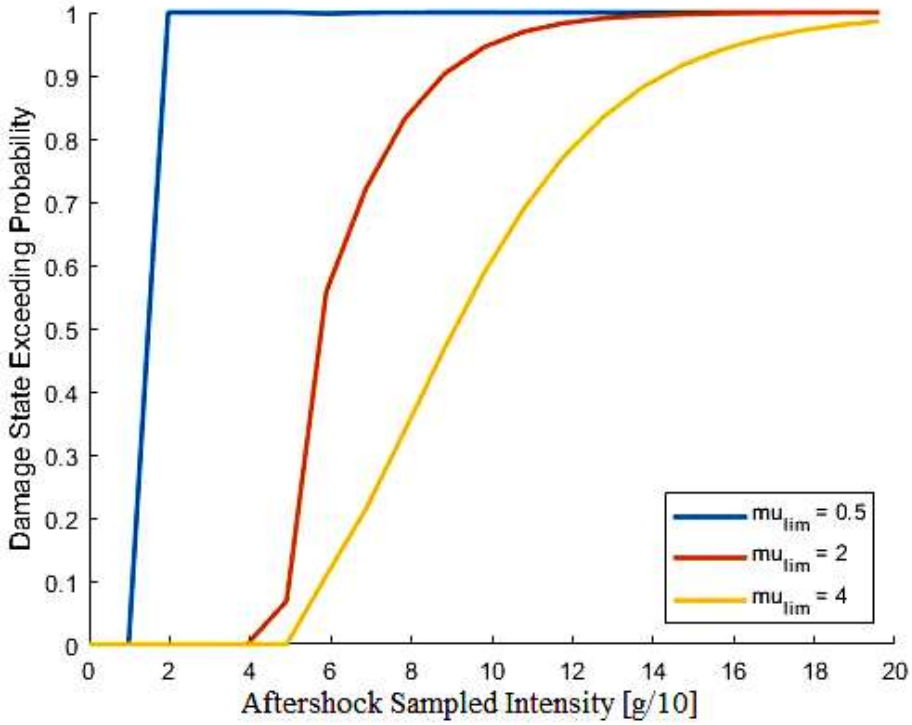

Figure 4.6.2e Collapse Fragility Curves for the Aftershock Non-Linear Dynamic Analysis

Also in this case the subsequent limit damages are the same of those chosen for the first approach, because the damage index is the same (the required ductility). The same considerations for this approach can be done: the more the limit ductility increases the more the more it's possible to protect the structure from the failure because its behavior becomes more plastic and, passing from mainshock to aftershock, the system has the time to accumulate damage without collapsing.

4.7 Empirical Collapse Fragility Curves: Approach 2

Collapse fragility curves are calculated by considering non linear IDA results (Section 4.3) exploiting the classical definition of *mathematical* probability referred to an event, the number of all possible cases for that event and the number of favorable cases, i.e. those cases which verify the event for which the probability is to be calculated.

4.7.1 Mainshock Collapse Fragility Curve

D is the damage function (or *seismic demand*) represented by the maximum ductility required to the system in the undamaged configuration (mainshock) and calculated as the ratio between the maximum displacement obtained through non linear IDA and the yield displacement, for each sampled value of mainshock intensities. The limit ductility value, associated to the relative performance level, is fixed $d_{PL} : \mu = 0.5$.

$$P = \frac{1}{N} P\ (D \geq d_{PL})$$

The number of possible cases which this event may realize is given by the total number N of earthquake which the system is subjected to; in this case it is equal to 30. Numerically the damage D is a table with 30 rows (the number of earthquakes) and 21 columns (the number of steps equal to 0.1g included in the range [0;2g]), each cell contains the required ductility calculated for the specific shock and for the specific scale factor; the number of favorable cases is evaluated by counting how many values of this table satysfy the event: if the event is satisfied for the specific value of ductility, then the probability of the event is sure and the value of ductility is substituted by 1; if

not, the probability of the event is not possible and the value of ductility is substituted by 0. For each column the sum of favorable cases is done, obtaining a unique row representing the mathematical probability. This last one is grafically represented in function of mainshock sampled intensities for obtaining the fragility curve (Figure 4.7.1a)

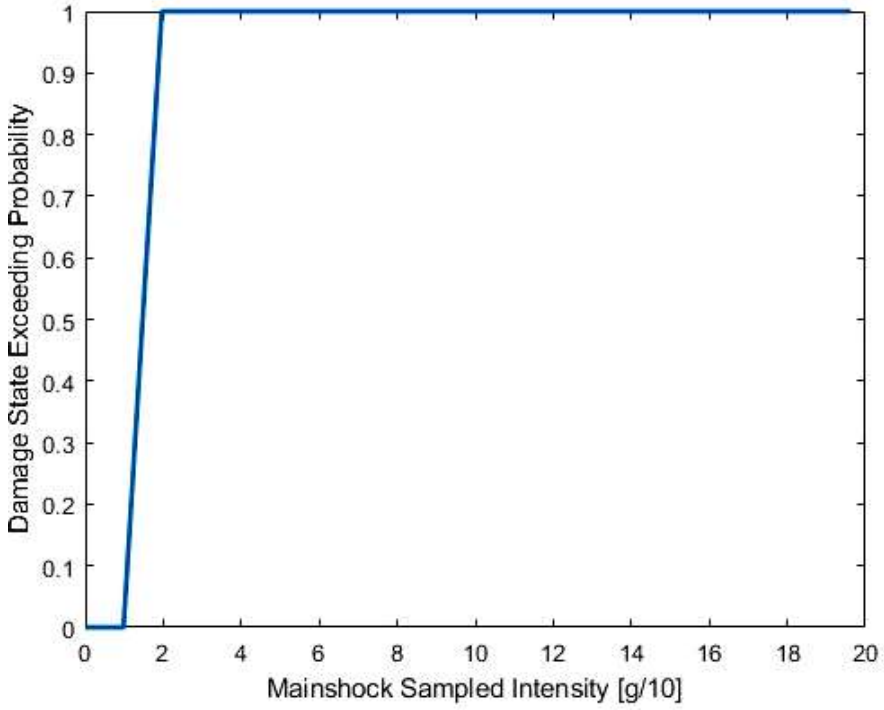

Figure 4.7.1a Collapse Fragility Curve for the mainshock Non Linear IDA analysis, evaluated through the mathematical probability, $d_{PL} = 0.5$

4.7.2 Aftershock Collapse Fragility Curves

The damage level reached by the structure during the first shock (the initial Performance Pevel) corresponds to a limit ductility $d_{PL,in}$: $\mu = 0.5$. Given the initial limit damage and subsequent limit damages

$$d_{PL,in} : \mu = 0.5 \qquad d_{PL,1} : \mu = 0.5 \qquad d_{PL,2} : \mu = 2 \qquad d_{PL,3} : \mu = 4$$

the mathematical probability of the occurrence of damage D, equal to or higher than damage levels $d_{PL,i}$, is calculated with the same expression exposed in the previous Section, considering that the number N of possible cases is given by the total number of sequences the system is subjected, i.e. 500. D is the seismic demand represented by the maximum ductility required to the system in the damaged configuration

(aftershock), i.e. the ratio between the maximum displacement obtained through non linear IDA and the yield displacement, for each sampled value of aftershock intensities. The counting procedure is the same as described in the previous Section, with the unique difference that rows are 500 and the procedure is repeated three times, one for each subsequent damage level. Fragility curves are obtained plotting the probability in function of aftershock sampled intensities and d_{PL} (Figure 4.7.2a)

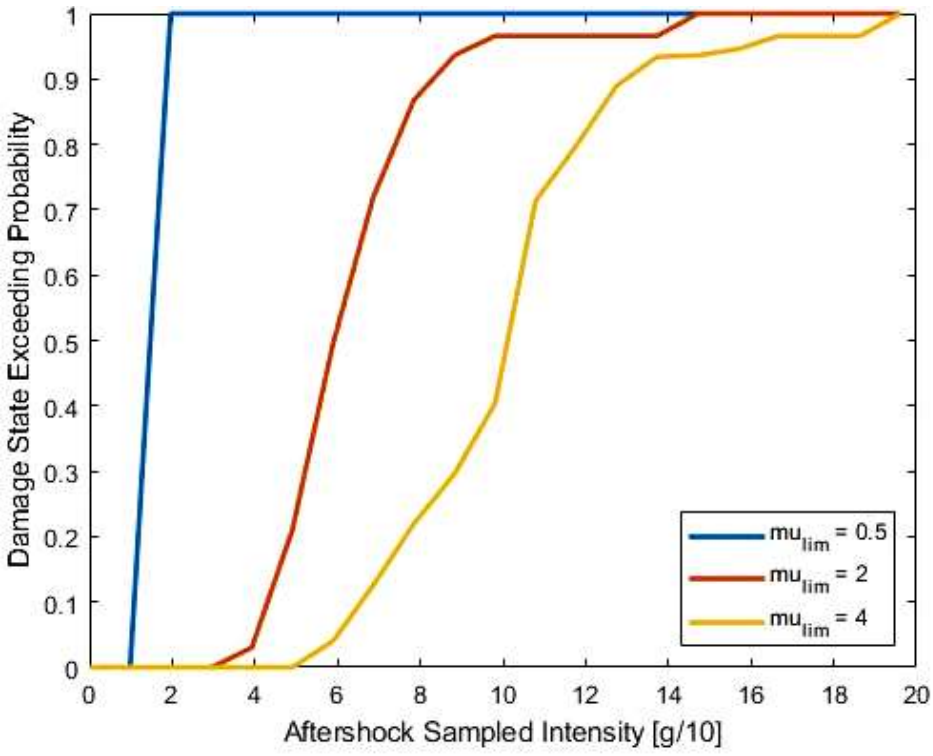

Figure 4.7.1a Collapse Fragility Curves evaluated through the mathematical probability

Looking the curves in Figure 4.7.1a it's possible to notice the discrete character of their trends, this due to the fact that the mathematical probability, or empirical or cumulative one, in this case is a function of distribution of the discrete random variable D that associates to each value of d_{PL} the probability that $D \geq d_{PL}$. D is considered as a discrete random variable because it is the one that is extracted from the favorable case counting procedure, in fact 21 D values are defined, one for each column representing an aftershock scale factor in which the favorable cases are counted and added in a single value. Consequently, the cumulative probability function will not have a continuous trend but piecewise or discrete one.

CHAPTER 5 APPLICATIONS TO THE CASE OF STUDY: DEGRADING SYSTEM

5.1 Introduction

In this Chapter, the structural response of the degrading system under the effect of multiple earthquake loadings is evaluated, basing on the same methodologies described in Chapter 3 and using different procedures for the non linear dynamic response history evaluation; the degrading system is a structure which accumulates damage, in the form of degradation referred to construction materials, due to application of cycle loadings . The software MATLAB is not the only tool used for this purpose, because it does not take into account, for a system, his material properties as part of modeling: the complementary use of the software OpenSees is needed.

About this, the first part of the Chapter describes modalities which the model of the system is implemented and analyzes are launched in Opensees with, subsequently the interaction with the software MATLAB; the use of OpenSees is fundamental as well as MATLAB because it is directly related to the development of methodologies used for the collapse fragility evaluation: this is also explained in this Section. Design implications about the degrading SDOF system are the same set-up for the non degrading one, as well as dynamic and geometric characteristics.

The same Ground motions represented in Section 3.7 are used and response is provided, both when it's subjected only to one shock and to the effect of mainshock-aftershock sequences; the response of the system to this last case is evaluated with the Park & Ang Damage Index (besides the maximum displacement), which considers the increasing dissipated energy, with a following stiffness reduction, passing from the first to the second shock. Finally fragility curves are built with the same approaches used for the non-degrading system.

5.2 Degrading system: OpenSees

OpenSees is the acronym of *Open System for Earthquake Engineering Simulation*, it is a software with free license, (open-source), object-oriented, used in the field of seismic

engineering for the simulation of the action of the earthquake on numerical models of structures or geotechnical systems. It is a program funded by the PEER institute (University of California, Berkley) but with free access. In fact, the great potential of this code is that, until today, many researchers have enriched it with additional components that allow performing sophisticated simulation of the response of structures to seismic action. These additional implementations mainly concern the model construction phase, the analytical formulation of each element, material models, analysis procedures, sub-programs that deal with the numeric resolution of non-linear equations, tools for data management. OpenSees is mainly written in C ++ language, but if necessary it invokes libraries implemented in Fortran or C language, it is composed of a modular structure and developers can insert or modify specific modules individually.

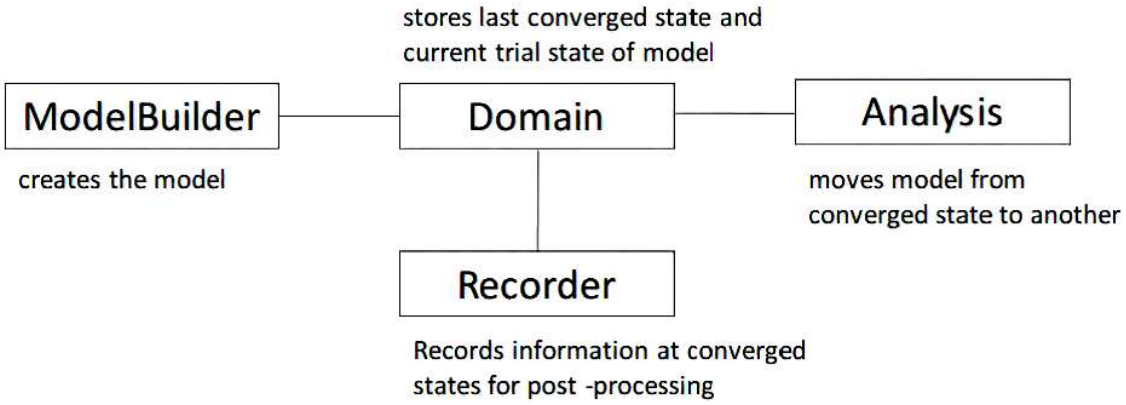

Figure 5.2a Main objects of the software OpenSees (Diego Debortoli, 2013)

Figure 5.2a shows the main objects and their organization in a hierarchical structure within the software. For example, the *Domain* object, created in turn by the *ModelBuilder* object, provides the status of the finite element and varies as the changing object of *Analysis*. Instead, the *Recorder* object takes care of retrieving appropriate useful information for the post-processor and for the display of the results on the screen. The *Domain* object is consequently formed by other elements, as shown in Figure 5.2b: the type of finite element, the nodes, the boundary conditions, the loads, the internal and external constraint conditions.

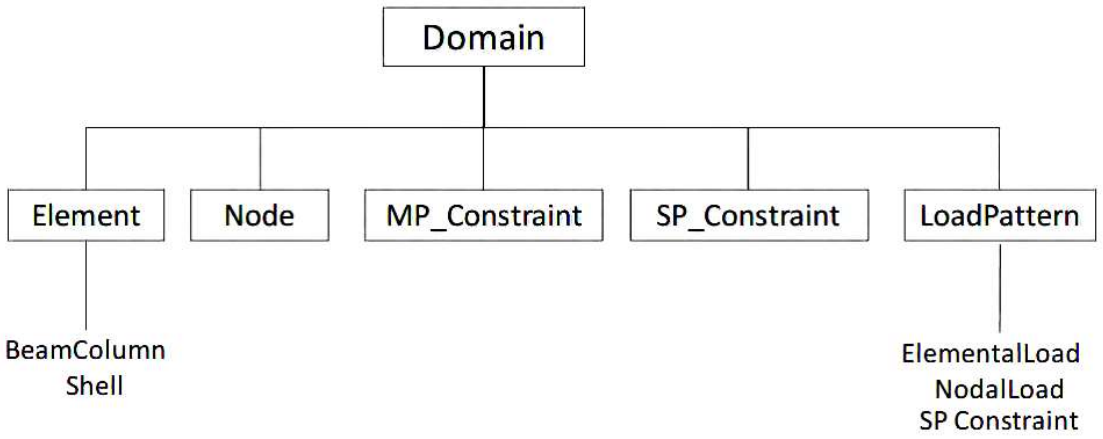

Figure 5.2b Hierarchical structure of the *Domain* object (Diego Debortoli, 2013)

On the site http://opensees.berkeley.edu/ it is very easy to find information about the correct syntax for constructing objects, also through examples of pre-packaged models, or discussions within the community of the Opensees forum.

5.2.1 Creation of command files for the degrading system

This is the step in which the system is modeled in OpenSees in order to make a seismic simulation, through non linear (IDA and not) dynamic analyzes described in Chapter 3, that considers also the material degradation. The necessary *.tcl* are multiple, for the compilation of each of which an appropriate program called *Notepad++* has been used. Let's see, in detail, for each OpenSees command file used, its function and its characteristics:

- NodeCoord.tcl is the file that contains the numbering of all the nodes with the relative coordinates along the x, y and z axes. In this case the system has been thought as a simple oscillator, as schematized in Chapter 4 and, considering that analyzes are conducted only in one direction (regardless x or y direction), the representation is in a plane, so it is schematized as 2 points, the first one with coordinates 0,0 and the second one placed at a distance equal to the length of the oscillator, i.e. 1m, representing the lumped mass; to guarantee dimensional homogeneity with the rest of the sizes, it was necessary to express the coordinates of the points in meters.
- Materials.tcl in this command file the choose of the nature of the materials is needed, starting from the types present in the OpenSees library, and then specify the properties.

For the system, properties of materials suitable for depicting degradation are assigned (Table 5.2.1a)

```
uniaxialMaterial Hysteretic $matTag $s1p $e1p $s2p $e2p <$s3p $e3p> $s1n
$e1n $s2n $e2n <$s3n $e3n> $pinchX $pinchY $damage1 $damage2 <$beta>
```

Table 5.2.1a The Command "UniaxialMaterial - Hysteretic" assigned to the SDOF system (http://opensees.berkeley.edu/OpenSees/manuals/usermanual/174.htm)

According to the definition provided by OpenSees Wiki (URL: http://opensees.berkeley.edu/wiki/index.php/Hysteretic_Material), the Command UniaxialMaterial – Hysteretic << *is used to construct a uniaxial bilinear hysteretic material object with pinching of force and deformation, damage due to ductility and energy, and degrading unloading stiffness based on ductility* >>. This Command is associated to the steel; each coefficient characterizing this command represents a different property assigned to the SDOF system and, considering the schematized envelope of the force-displacement curve in Figure 5.2.1a

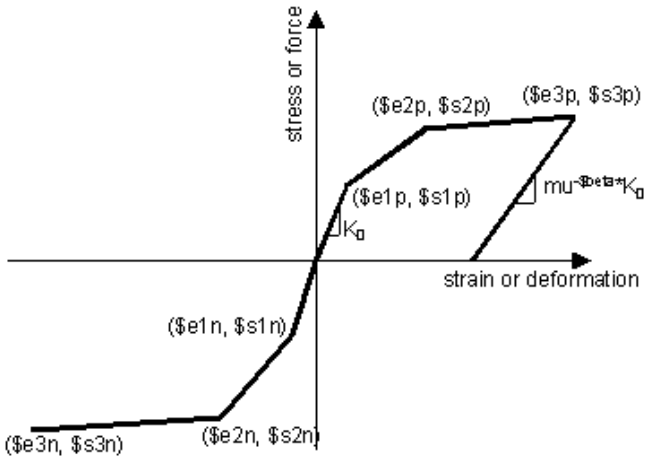

Figure 5.2.1a Schematized envelope of the force-displacement curve for Hysteretic UniaxialMaterial (http://opensees.berkeley.edu/OpenSees/manuals/usermanual/174.htm)

Their meaning is summarized in the following Table 5.2.1b

Basing on design hypotheses, the system suffers an accumulation of damage, due to repeated stresses, which develops over time; this accumulation of damage is synonymous with structural deterioration, but a degradation afflicting only the

stiffness, taking into account the Pinching effect and assuming that the system, between a stress and the other (in other words in an unload-reload cycle), has the time to relax but not to be repaired, so assuming that the resistance is not altered.

$matTag	integer tag identifying material
$s1p $e1p	stress and strain (or force & deformation) at *first* point of the envelope in the *positive* direction
$s2p $e2p	stress and strain (or force & deformation) at *second* point of the envelope in the *positive* direction
$s3p $e3p	stress and strain (or force & deformation) at *third* point of the envelope in the *positive* direction
$s1n $e1n	stress and strain (or force & deformation) at *first* point of the envelope in the *negative* direction
$s2n $e2n	stress and strain (or force & deformation) at *second* point of the envelope in the *negative* direction
$s3n $e3n	stress and strain (or force & deformation) at *third* point of the envelope in the *negative* direction
$pinchx	pinching factor for strain (or deformation) during reloading
$pinchy	pinching factor for stress (or force) during reloading
$damage1	damage due to ductility: D_1(mu-1)
$damage2	damage due to energy: $D_2(E_{ii}/E_{ult})$
$beta	power used to determine the degraded unloading stiffness based on ductility mu^{-beta}

Table 5.2.1b "UniaxialMaterial - Hysteretic" Command and properties (http://opensees.berkeley.edu/OpenSees/manuals/usermanual/174.htm)

In numerical terms, and based on Table 5.2.1b, these hypotheses have been transcribed assuming unit values for the Pinching effect, null values for damages due to ductility and energy ($damage1 and $damage2) because representative of resistance degradation (this latter assumed constant during load cycles) and a value equal to 0.7 for the coefficient indicating the stiffness degradation in the second unloading phase, function of ductility; in other words it is the intial stiffness k_0 ($\omega_n^2 m$) multiplied by this coefficient which expresses the inclination of the straight line after the reloading phase mu^{-beta}. Other coefficients are shape parameters and have been chosen in such a way that the final envelope of the force-displacement curve assumes the trend shown in Figure 5.2.1b

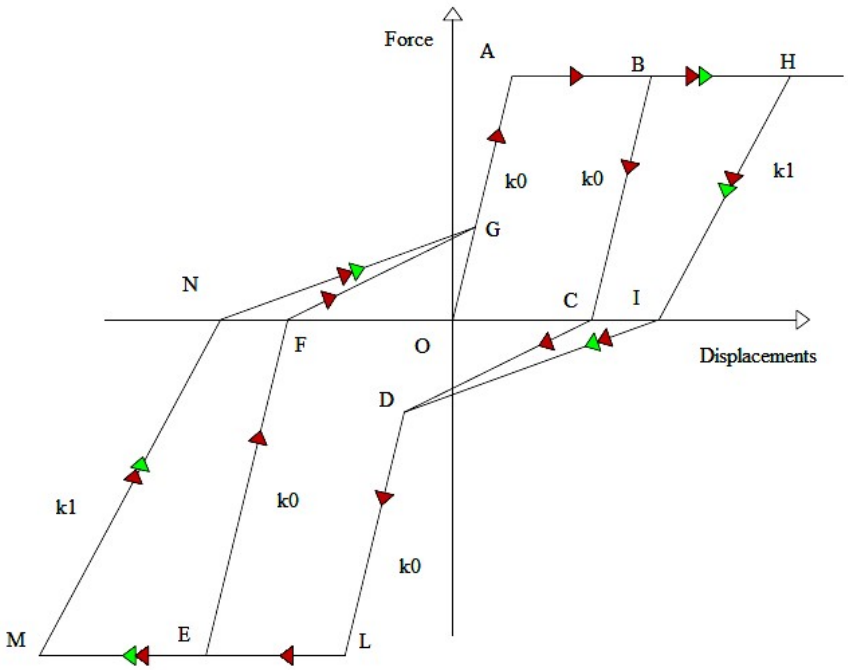

Figure 5.2.1b Stiffness Degradation, with Pinchng Effect, for the SDOF System

Also in this case there's the presence of geometric non-linearity due to elastic-plastic costitutive law. The cyclic load simply follows the O-A-B-C-D-L-E-F-G-H-I-L-M-N-G-A-H path and, as it's possibe to observe, the Pinching effect is well evident in the NG-FG-DC-DI sections; the loss of stiffness increases passing from the first load cycle (k_0) to the next ($k_1 = 0.7k_0$); consequently the energy dissipated for hysteresis increases, it's possible to observe this expansion because, graphically, the dissipated energy is the area contained in each cycle load, so, when the inclination decreases (from 1 to 0.7), the area increases; the resistance, instead, keeps unaltered.

- SPconstraint.tcl, in this command the constraints attributed to the each nodes are declared, in the case under consideration the simple oscillator is stuck only at the base, because at the opposite side the lumped mass is free to translate horizontally, referring to the hypothesis of this kind of system, described in Section 4.2.
- NodeMass.tcl, this file specifies the nodal mass. In this case the nodal mass is the same of the non degrading system, equal to 1 kg.
- Elements.tcl, it's the file in which the characteristics of each structural element are specified, in a view to automate the process of compiling command files, the Script Editor declares all objects in order, grouping them by type. Type Truss is specified, with an area of transversal section equal to $1m^2$.

- AnalysisRecorder.tcl, this command specifies what are the results that OpenSees should provide on output for each type of analysis that is being launched. Referring to the lumped mass, the displacement is required, as well as the reaction at the base, for each mainshock-aftershock sequence and for each increasing step of intensity.
- LoadPattern.tcl, these. Tcl specify the entity and distribution of the load for each type of analysis that is launched. An UniformExcitation LoadPattern is used, which allows to apply a uniform excitation to a model acting in a certain direction (http://opensees.berkeley.edu/wiki/index.php/Uniform_Excitation_Pattern); in this case the direction is arbitrarily chosen along x, but this is not relevant for the purpose of analyzes because ground motions applied to the system have been selected referring to the direction they developed the maximum PGA, regardless if that direction is along x or y. Each LoadPattern has a TimeSeries associated with it.
- TimeSeries.tcl, it represents the relationship between the time in the domain, *t*, and the load factor applied to the loads, λ, in the load pattern with which the Time Series object is associated, i.e. $\lambda = F(t)$. In this case λ is the ground motion applied to the system, and t is its relative dt. A Path TimeSeries object is created, in which the relationship between load factor (ground motion) and time (dt) is input by the user as a series of discrete points in the 2d space (load factor, time). The input points come from a list in the MATLAB script of the analysis; in particular this is described better in the Section 5.3 *i)*, now it's only mentioned that the input points are all ground motions (and their relatives dt) taken as single shocks or in mainshock-aftershock sequences, with the characteristics design criteria of each analysis described in Chapter 3.
- AnalysisOptions.tcl, this command encloses all non linear dynamic analysis settings, i.e. modalities which methodologies described in Chapter 3 are solved with, such as sub-programs that deal with the numeric resolution of non-linear equations, tools for data management, the algorithm used for the resolution of these non linear equations, integrators and other parameters not object of discussion in this treatment. In other words this is what the non linear integration function is for the non degrading system: for the degrading system the structural response is evaluated by launching the analysis through OpenSees according to the settings defined in this *.tcl* file. These options obviously take into account, for each ground motion (single shock) or sequence

(mainshock-aftershock), its length (the number of steps) and its *dt* and, about this, if two records concatenated of a sequence have two different *dt*, as well as for the non linear integration described in Section 4.3.2, a linear interpolation is used to obtain a unique *dt* for the unique sequence; this is repeated for all sequences administrated to the system.

- sdof.tcl, this is the main command file, the file created in *Notepad++* including all *.tcl* files just described and the only one that needs to be loaded and analyzed by the OpenSees prompt. During its execution it invokes, with appropriate order, all the *.tcl* files written above and allows to obtain, for the degrading system, the structural response basing on methodologies exposed in Chapter 3 and using the analysis options set up. All the command files described above are compiled in a completely automatic way from the code connected to the interface (*Notepad++*), when the *write file .tcl* button is pressed. This modeling procedure is more complex than the non degrading system, but however it's the most suitable for this kind of problem.

5.3 Structural Response Evaluation: Approach 1

The Non Linear IDA analysis described in Section 3.2 is set up in MATLAB, but the structural response (the maximum displacement of the lumped mass), as sayd in the previous paragraph, in this case is not recorded with a non-linear integration function as in the case of the non degrading system. The non linear integration function applied to the non degrading system is all implemented in MATLAB; here there's a certain number of steps which is needed to follow because the model has been implemented in OpenSees.

5.3.1 Mainshock Non Linear Incremental Dynamic Analysis

Once IDA analysis described in Section 3.2 *i)* is carried out by using the set of 30 ground motions only as mainshocks, within the same MATLAB script many steps, needed to follow for obtaining the structural response, are defined:

- Creating, for each 0.1g of the scale factor range [0, 2g], a work folder with the same content including first of all the main command file created in *Notepad++* with all *.tcl*

files describing the degrading system model, and also the executable *OpenSees.exe* needed for loading the file of the model and launching analyzes.

-Defining, within each folder created in the first step, input files for the Ground Motion's selection, in the form of text file; the specific command to create a generic text file is *fopen* (*'filename'*, *'w'*), the *'w'* (*writable*) flag, used to make it accessible and editable, later , to write within this file use the command *fprintf* (*fileID*, *'body of the text'*). In a practical way the *filenames* will represent all 30 ground motions scaled with the specific mainshock sampled intensity, which are *written* in a form of a text file inside the work folder and *printed* with a number from 1 to 30. Once the text file has been compiled, it must be closed, by means of the instruction: *fclose*(*fileID*) it is also automatically saved in the current MATLAB work folder. This operation is repeated for all sampled value of the mainshock intensity range.

- Writing the input files for the analysis: for each ground motion text file, included in a specific work folder, an input text file is created with the same command *fopen* (*'filename'*, *'w'*), *fprintf* (*fileID*, *'set'*, *'body of the text'*); in this case the *filenames* are inputs going from 1 to 30 which are always *written* in a form of a text file; the *body of the text* is a string which recalls and allow the writing, for each input text file, of all parameters useful for launching non linear dynamic analyzes such as F_y, k_y, *dt* and *c*; *'set'* is a series of instructions for determining the spacing and distribution of the parameters reported in the body of the text. Once the text file has been compiled, it must be closed by using the instruction: *fclose*(*fileID*). Also this operation is repeated for all sampled value of the mainshock intensity range.

- Ensuring the presence of the executable *OpenSees.exe*, the non linear dynamic analyzes is launched for each work folder, one by one, taking into account, for that specific sampled value, all ground motions and inputs that are transcripted in a text file. The progress of OpenSees can be monitored at any time through the *CommandWindow*, in the MATLAB environment. Outputs defined in the *.tcl* file of recorders will be generated in the same work folder for each shock. They are represented by the displacement time histories of the lumped mass and the reaction time histories of the system for each mainshocks and for each scale factor.

- Outputs needs to be converted from data of text file into arrays available for post-processing studies of the structural response, so first of all they are read by using the command *fopen* (*'filename'*, *'r'*), infact the *'r'* (*readable*) flag is used to make it accessible and only readable; then, with the command *fscanf* (*fileID*, *format*), it's possible to read and convert displacements and reactions from a text file into array basing on instruction included in the *format*. Once the procedure has been compiled, it must be closed by using the instruction *fclose*(*fileID*).
Structural response are represented by the maximum displacement and the maximum reaction recorded in the intact configuration (or in the mainshock) for the system.

5.3.2 Mainshock-Aftershock Non Linear Incremental Dynamic Analysis

Once IDA analysis described in Section 3.2 *ii)* is carried out, the same steps applied for mainshock scenarios are defined for the set of 500 artificial mainshock-aftershock sequences, within the same MATLAB script, with little differences: the number of work folders, equal to the number of sampled values of aftershock intensities, is the same, but in this case the input files generated in each work folder are not 30, they are 500, i.e. one for each mainshock-aftershock sequence. Furthermore the non linear dynamic analysis set up in *AnalysisOptions.tcl* is executed by considering a unique *dt* for the whole sequence, given by the average value between two; this is repeated for all 500 sequences.
Outputs are represented by the displacement time histories of the lumped mass and the reaction time histories at the base of the system for each mainshock-aftershock sequence and for each scale factor.
The structural response is evaluated in two different ways:
1) the maximum displacement and the maximum reaction at the base in a damaged configuration (aftershock) when the system is already damaged by the previous earthquake (mainshock);
2) the maximum displacement and the maximum reaction at the base calculated on the whole sequence, useful in considering the damage accumulated from the system passing from the mainshock to the aftershock. Infact this will allow to understand if

methodologies created to evaluate the response under multiple earthquakes are also suitable to best represent the case in which the system accumulates damage in the form of degradion of construction materials after a mainshock-aftershock cycle load. For this purpose, fragility estimation will be based on the structural damage evaluated by the Park & Ang Damage Index, as explained in next paragraphes.

5.4 Analytical Collapse Fragility Curves: Approach 1

The main parameters for the evaluation of the structural damage are two: the first one is the *required displacement*, while the second is the *Park & Ang* Damage Index. The *required displacement* u_{max} is the maximum displacement of the lumped mass during the seismic simulation (either in mainshock or aftershock analyzes), while the *Park and Ang* Damage Index is used to develop regression models for statistically predicting damage accumulation based on earthquake intensity and damage history. For damage measurement, it results from a combination of ductility demand induced by the earthquake and the dissipated hysteretic energy (J. Ghosh, J. E. Padgett, and M. Sànchez-Silva, 2015)

$$D = \frac{\mu_m}{\mu_u} + \beta \frac{E_h}{F_y u_y \mu_u}$$

where:

- D is the *Park & Ang* Damage Index
- μ_m is the maximum ductility required to the system by earthquakes (u_{max} / u_y)
- μ_u is the ultimate ductility capacity under monotonic loading
- E_h is the total hysteretic energy dissipated
- F_y and u_y are respectively the yielding force and the yielding displacement
- β is a dimensionless constant usually equal to 0.05 for reinforced concrete structures

For both damage indexes the problem is always the division of damage levels: building fragility curves considering the structural damage with the *Park & Ang* Damage Index means to calculate the probability that D equals or exceeds many values of damage levels D_{PL} so it's necessary to define them being aware of the lack of information on damage of buildings found in real cases following the artificial

sequences created, it is decided to adopt the three *Park & Ang* damage values asdamage indices, for relatives Performance Levels

$D_{PL,1} = 1$ *Slight Damage*
$D_{PL,2} = 2$ *Moderate Damage*
$D_{PL,3} = 3$ *Extended Damage*

Damage levels related to the *required displacement* are defined by adopting three ductility values and multiplying them with the yield displacement u_y. These three values are the same adopted as damage levels for the non degrading issue, infact

$\mu = 0.5$ → $d_{PL,1} : u = 0.5u_y$ *Slight Damage*
$\mu = 2$ → $d_{PL,2} : u = 2u_y$ *Moderate Damage*
$\mu = 4$ → $d_{PL,3} : u = 4u_y$ *Extended Damage*

So the fragility is considered as the probability, conditioned to the intensity of the earthquake, that the function of damage *D, Park & Ang* Damage Index or required displacement, exceeds or equals a given *PL* (or *structural capacity*).

5.4.1 Case 1: Required Displacement

i) Mainshock Collapse Fragility Curve

As first case, the damage level d_{PL} is related to the damage function *D* (or *seismic demand*) represented by the maximum displacement required by the system in the undamaged configuration (mainshock). A ductility value is assumed, so the consequent displacement as damage index, associated to the relative performance level, is defined

$$\mu = 0.5 \quad \rightarrow \quad d_{PL} : u = 0.5u_y \quad \text{Slight Damage}$$

The cumulative probability of the occurrence of damage *D*, equal to or higher than damage level d_{PL} (Zekeriya Polat, 2006)

$$P[D > d_{PL}/X] = \Phi\left(\frac{lnX - \lambda}{\xi}\right) \qquad (1)$$

λ and ξ are respectively the mean and the standard deviation of intensities corresponding to the damage level d_{PL} and extracted by interpolating the vector of mainshock sampled intensities with vectors of the damage D (the required displacement, or the *seismic demand*), obtained through IDA for each sampled value of intensity and for each ground motion; X are mainshock sampled intensities

λ	ξ
1.4806	0.0018

The probability that D equals or exceeds d_{PL} is graphically represented in function of X to obtain the fragility curve (Figure 5.4.1a)

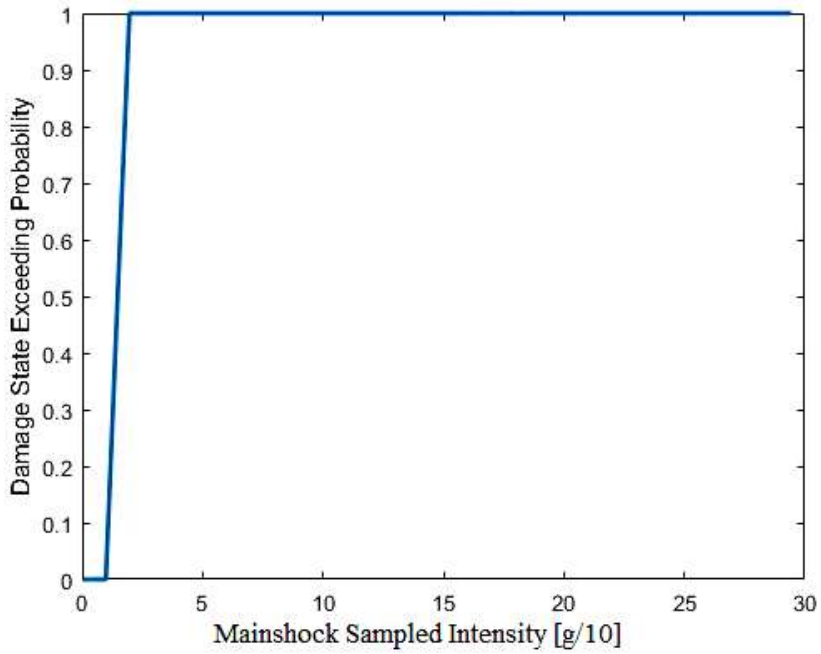

Figure 5.4.1a Collapse Fragility Curve for the Mainshock IDA Analysis $d_{PL} = 0.5u_y$

As the non degrading issue, in this case the mean and the standard deviation of intensities corresponding to the damage level d_{PL} are the same recorded for the same analysis referred to the non degrading issue, this means that the damage D (the *required ductility* or the *required displacement*) exceeds the damage d_{PL} (ductility 0.5 and displacement $0.5u_y$) in the same way if the system is a non degrading one or degrading one.

ii) Aftershock Collapse Fragility Curves

The collapse fragility is calculated referring to the aftershock collapse capacity defined for each of the 500 mainshock–aftershock sequences. The mainshock damage corresponds to an initial damage level for the system $d_{PL,in}$: $u = 0.5u_y$, the same applied as limit displacement in the construction of the mainshock fragility curve.

D is the damage function (or *seismic demand*), represented by the maximum displacement required by the system in the damaged configuration (aftershock). Given an initial damage and subsequent damage levels

$$d_{PL,in} : u = 0.5u_y \qquad d_{PL,1} : u = 0.5u_y \qquad d_{PL,2} : u = 2u_y \qquad d_{PL,3} : u = 4u_y$$

the probability that the damage *D* equals or exceeds damage levels $d_{PL,i}$ (Zekeriya Polat, 2006)

$$P_i[D > d_{PL,i}/X] = \Phi\left(\frac{lnX - \lambda_i}{\xi_i}\right) \tag{2}$$

λ_i and ξ_i are respectively the mean and the standard deviation of intensities corresponding to damage levels $d_{PL,i}$ and extracted by interpolating the vector of aftershock sampled intensities with vectors of the damage *D* (the required displacement, or the *seismic demand*), obtained through IDA for each sampled value of intensity and for each artificial sequence; *X* are aftershock sampled intensities

	$d_{PL,1}$	$d_{PL,2}$	$d_{PL,3}$
λ	1.4805	5.2157	9.6033
ξ	0.0023	1.1335	2.9795

Plotting P in function of aftershock sampled intensities, fragility curves are built, for each damage level d_{PL} (Figure 5.4.1b)

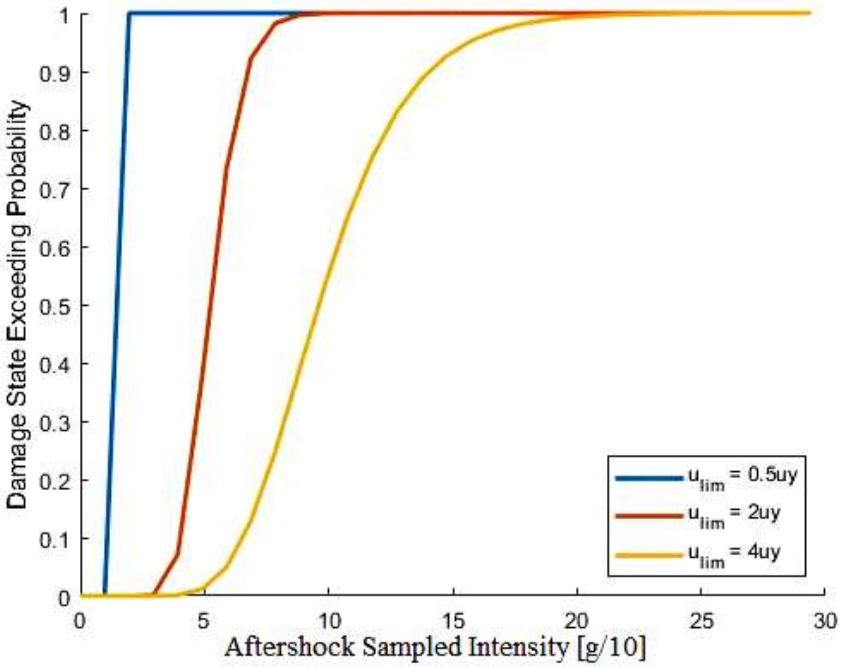

Figure 5.4.1b Collapse Fragility Curves for the Aftershock IDA Analysis

5.4.2 Case 2: *Park & Ang* Damage Index

i) Mainshock Collapse Fragility Curve

As second case, the damage level d_{PL} is related to the damage function D (or *seismic demand*) represented by the Park & Ang Damage Index (J. Ghosh, J. E. Padgett, and M. Sànchez-Silva, 2015)

$$D = \frac{\mu_m}{\mu_u} + \beta \frac{E_h}{F_y u_y \mu_u}$$

It allows to understand how the damage accumulates in the degrading system when subjected only to mainshocks. The two unknowns of this relation are the ultimate ductility capacity μ_u and the total hysteretic energy dissipated E_h, in particular this last one is calculated as the area subtended by the envelope force-displacement for each cycle load. In this case the structural response is not only represented by the displacement of the lumped mass, but also by the reaction (see Section 5.3.1), infact the hysteretic energy is calculated by considering enclosed areas given by each value of displacement an the respective value of force. A value of ultimate ductility is assumed $\mu_u = 4$, μ_m is obtained as the ratio between the maximum displacement of the

lumped mass under the effect of mainshocks and the yield displacement, the other parameters are known

Fy **[kN]**	***β***
2.9609	0.05

A damage value, associated to the relative Performance Level, is assumed

$$D_{PL} = 0.5 \qquad Slight\ Damage$$

The cumulative probability of the occurrence of damage D, equal to or higher than damage level D_{PL}, is calculated with the same relation used in the previous case (Eqn.(1)); λ and ξ are respectively the mean and the standard deviation of intensities corresponding to the damage level D_{PL} and extracted by interpolating the vector of mainshock sampled intensities with vectors of the damage D (the *Park & Ang* Damage Index for mainshock scenarios, or the *seismic demand*), obtained for each sampled value of intensity and for each ground motion;

λ	**ξ**
5.0954	0.9903

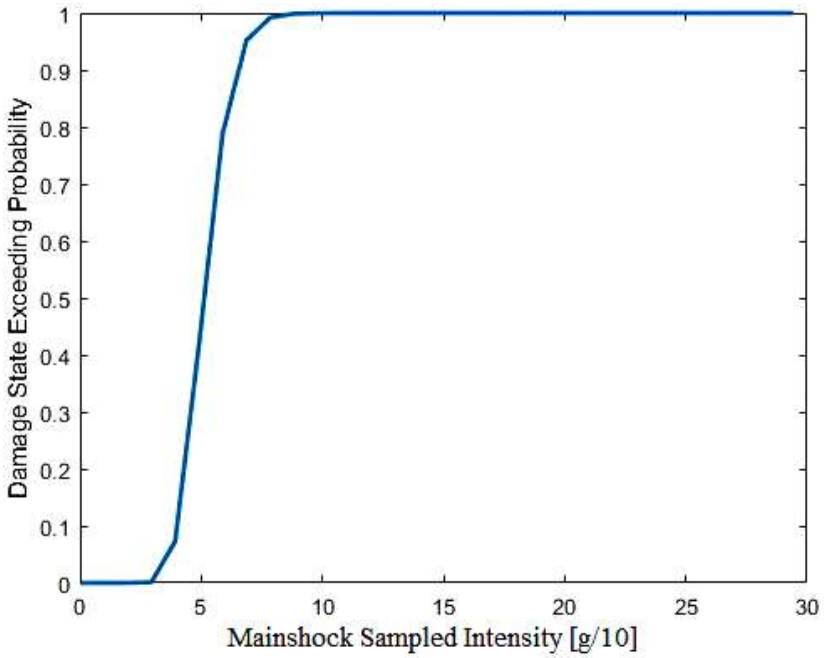

Figure 5.4.2a Collapse Fragility Curve for the Mainshock IDA Analysis $D_{PL} = 0.5$

The probability that D equals or exceeds D_{PL} is graphically represented in function of X to obtain the fragility curve (Figure 5.4.2a). Here it's possible to observe a first difference between the behavior of the non degrading system and the degrading one in the same configuration (mainshock): if the collapse is reached by exceeding a limit displacement (or a limit ductility), the behavior is the same regardless the nature of the system (degrading or not); if we consider the hysteretic energy dissipated during mainshocks for the system as damage indicator (so describing the damage accumulated with the *Park & Ang* relation), the collapse is reached for higher intensity levels, more or less 0.8g respect 0.2g for the limit displacement, this means that in this case the system, after it has been hit by the shock, crosses a first "relaxing" phase in which it accumulates damage and which allow to exceed the D_{PL} with major delay.

ii) Mainshock-Aftershock Collapse Fragility Curves

The fragility is estimated by referring to the collapse capacity of the whole sequence, defined for each of the 500 artificial sequences. In other words this is the case in which the total hysteretic energy dissipated in a complete cycle load (mainshock-aftershock sequence) is used as main parameter for evaluating the structural damage D (or *seismic demand*) (J. Ghosh, J. E. Padgett, and M. Sànchez-Silva, 2015)

$$D = \frac{\mu_m}{\mu_u} + \beta \frac{E_h}{F_y u_y \mu_u}$$

μ_m is the maximum ductility required to the system by a complete cycle load (mainshock-aftershock), obtained as the ratio between the maximum displacement in the whole sequence and the yield displacement; $\mu_u = 4$; E_h is the total hysteretic energy dissipated, i.e. the area below the force-displacement curve obtained for each one of the 500 artificial sequences and for each sampled value of aftershock intensity (forces and displacements calculated on the whole mainshock-aftershock sequence).
The mainshock damage corresponds to an initial damage level for the system $D_{PL,in} = 0.5$, the same applied as limit damage in the construction of the mainshock fragility curve. Given an initial damage and subsequent damage levels

$$D_{PL,in} = 0.5 \qquad D_{PL,1} = 1 \qquad D_{PL,2} = 2 \qquad D_{PL,3} = 3$$

The probability that the damage D equals or exceeds damage levels $d_{PL,i}$ is calculated with the Eqn.(2), λ_i and ξ_i are respectively the mean and the standard deviation of intensities corresponding to damage levels $D_{PL,i}$ and extracted by interpolating the vector of aftershock sampled intensities with vectors of the damage D (the Park & Ang Damage Index for mainshock-aftershock scenarios, or the *seismic demand*), obtained for each sampled value of intensity and for each artificial sequence;

	$D_{PL,1}$	$D_{PL,2}$	$D_{PL,3}$
λ	8.0144	13.1731	18.1014
ξ	56.1190	5.7142	9.0084

Fragility curves are built, for each damage level D_{PL} (Figure 5.4.2b)

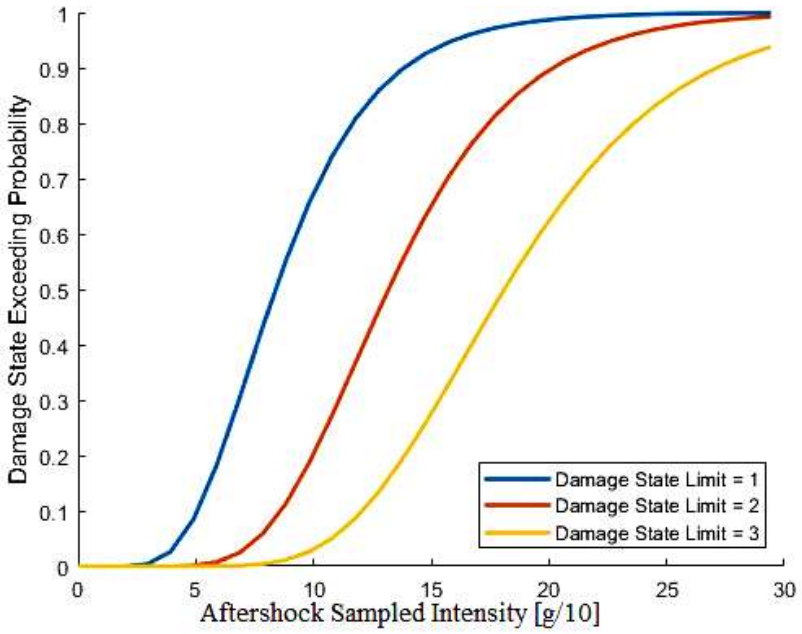

Figure 5.4.2b Collapse Fragility Curves for the Mainshock-Aftershock IDA Analysis

iii) Aftershock Collapse Fragility Curves

The damage index is defined by the *Park & Ang* relation, but in this case the total hysteretc energy dissipated only in the second cycle load (aftershock) is examined. So the collapse fragility is calculated referring to the aftershock collapse capacity defined

for each of the 500 mainshock–aftershock sequences. the damage D (or *seismic demand*) is obtained as difference between Park & Ang Damage Indexes calculated for the whole load sequence and for mainshock scenarios. Given an initial damage and subsequent damage levels

$$D_{PL,in} = 0.5 \qquad D_{PL,1} = 1 \qquad D_{PL,2} = 2 \qquad D_{PL,3} = 3$$

The probability that the damage D equals or exceeds damage levels $d_{PL,i}$ is calculated with the Eqn.(2), λ_i and ξ_i are respectively the mean and the standard deviation of intensities corresponding to damage levels $D_{PL,i}$ extracted by interpolating the vector of aftershock sampled intensities with vectors of the damage D (the Park & Ang Damage Index for aftershock scenarios, or the *seismic demand*), obtained for each sampled value of intensity and for each artificial sequence;

	$D_{PL,1}$	$D_{PL,2}$	$D_{PL,3}$
λ	11.2858	15.8031	20.2552
ξ	4.3154	7.4539	12.0790

Fragility curves are built by plotting P in function of aftershock sampled intensities, for each damage level D_{PL} (Figure 5.4.2c)

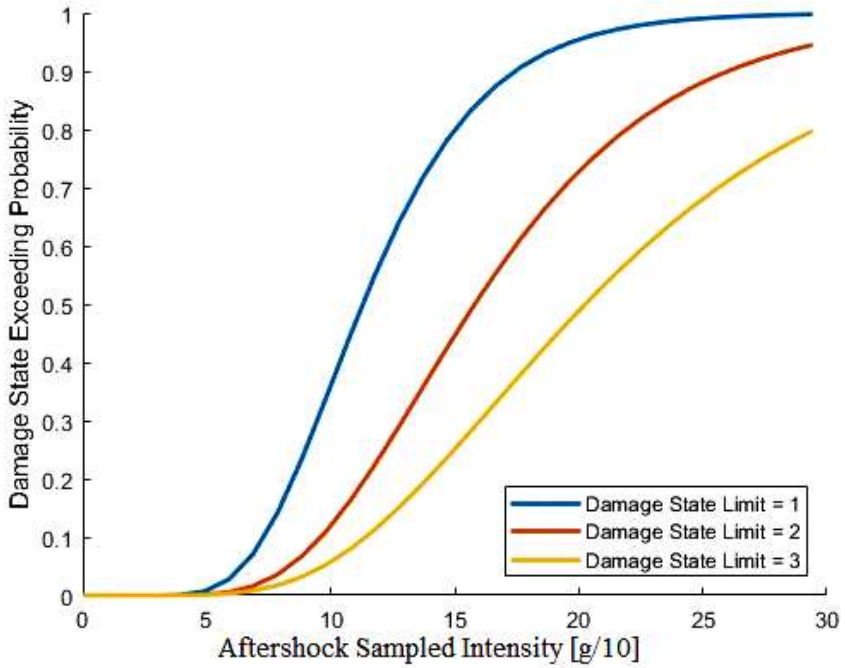

Figure 5.4.2c Collapse Fragility Curves for the Mainshock-Aftershock IDA Analysis

5.5 Structural Response Evaluation: Approach 3

The Non Linear Dynamic analysis described in Section 3.4 is set up in MATLAB, but also in this case the structural response (the maximum displacement of the lumped mass) is not recorded with a non-linear integration function as in the case of the non degrading system. Infact also here there's a certain number of steps which is needed to follow because the model has been implemented in OpenSees: they are briefly described below.

5.5.1 Mainshock-Aftershock Non Linear Dynamic Analysis

Once Non Linear Dynamic Analysis described in Section 3.4 is carried out, the same steps applied for the IDA Mainshock Analysis (see Section 5.3.1) and for the IDA Mainshock-Aftershock Analysis (see Section 5.3.2) are defined for the set of 500 artificial mainshock-aftershock sequences, within the same MATLAB script, with little differences: the work folder is only one because this is not an IDA and each shock of each artificial sequence is scaled by an intensity casually extracted from the range [0, 2g], so there's no a work folder for each sampled value. The non linear dynamic analysis set up in *AnalysisOptions.tcl* is executed by considering a unique *dt* for the whole sequence, given by the average value between two; this is repeated for all 500 sequences.

Outputs are represented by the displacement time histories of the lumped mass and the reaction time histories at the base of the system for each mainshock-aftershock sequence and for each scale factor.

Also in this case the structural response is evaluated in two different ways:

1) the maximum displacement and the maximum reaction at the base in a damaged configuration (aftershock) when the system is already damaged by the previous earthquake (mainshock);

2) the maximum displacement and the maximum reaction at the base calculated on the whole sequence, useful in considering the damage accumulated from the system passing from the mainshock to the aftershock.

5.6 Analytical Collapse Fragility Curves: Approach 3

As sayd in Section 3.5.1, the construction of fragility curves is preceeded by the definition of a *Probabilistic Seismic Demand Model (PSDM)* for both for single shocks and mainshock-aftershock scenarios. In this case the study is conducted by analyzing the two damage parameters, i.e. the required displacement and the Park & Ang Damage Index, as well as for the first approach.

5.6.1 Case 1: Required Displacement

i) Mainshock Collapse Fragility Curve

The *seismic demand* is represented by the maximum displacement required by the system; the maximum displacement is calculated through non linear dynamic analysis (see Section 3.3) exploiting the procedure described in Section 5.5.
Considering Intensity Measures *IM* as intensities which mainshocks are scaled with, for a single shock event the *EDP* (the damage *D* or the *seismic demand*) is calculated as (J. Ghosh, J. E. Padgett, and M. Sànchez-Silva, 2015):

$$EDP = a\, IM^{b} \tag{3}$$

In the bilogarithmic plane, this espression defines a linear *PSDM* (J. Ghosh, J. E. Padgett, and M. Sànchez-Silva, 2015):

$$ln(EDP) = ln(a) + b\, ln(IM) \tag{4}$$

coefficients a and b are calculated by linear regression, as well as the standard deviation β of the demand values. Graphically the linear regression line presents the trend reported in Figure 4.6.1a

a	***b***	***β***
0.020	1.2783	0.544

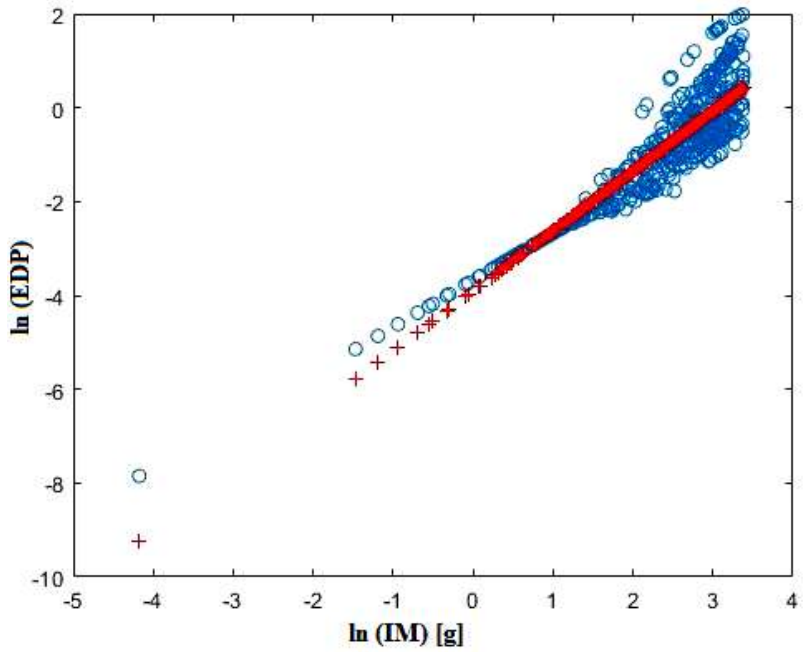

Figure 5.6.1a Linear Regression in the *ln (IM) – ln (EDP)* plane

Also here it's possible to observe that most of samples exceed the elastic phase entering in the plastic one, and this is easy to understand because, up to a value of *ln* (*IM*) more or lesse qual to 1, there's a linear data distribution, over which there's a light dispersion from the regression line; however the precision obtained in fitting quantities confirms that this demand model is suitable to predict the damage index for single shock scenarios. The probability of exceeding each *PL* given the seismic action is calculated with the expression (Tubaldi et al., 2016):

$$P\,[D > d_{PL}/IM] \;= \Phi\left(\frac{ln(a) + b\,ln(IM) - ln\,(d_{PL})}{\beta}\right) \tag{5}$$

IM are intensities which mainshocks are scaled for; the limit damage (*structural capacity*), associated to the Performance Level, is defined d_{PL}: $u = 0.5u_y$; the fragility curve is represented in Figure 5.6.1b

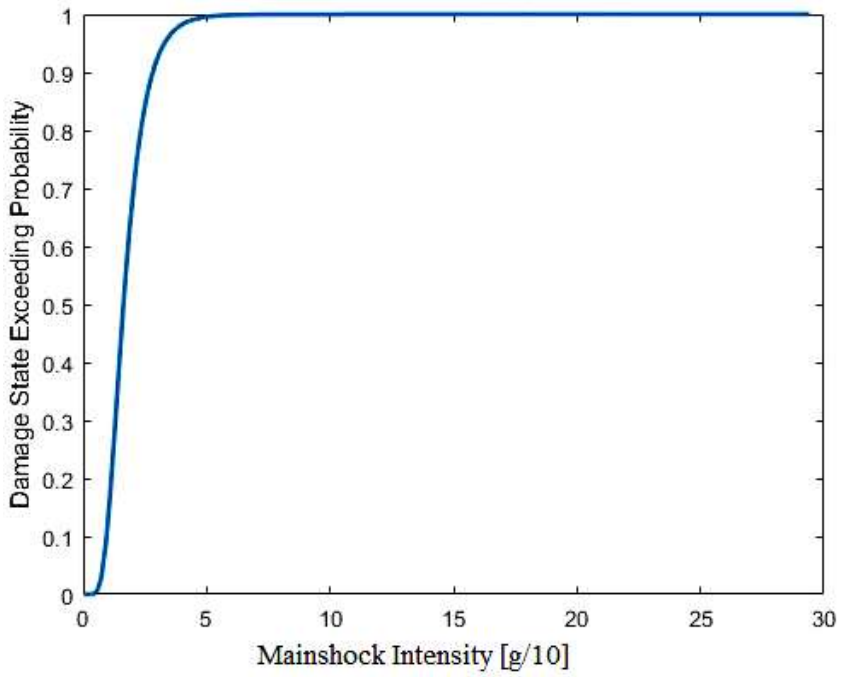

Figure 5.6.1b Collapse Fragility Curve for the Mainshock Non-Linear Dynamic Analysis $d_{PL} = 0.5u_y$

The mean and the standard deviation of intensities corresponding to the damage level d_{PL} are similar to those recorded for the same approach but referred to the non degrading issue, this means that the damage D (the *required ductility* or the *required displacement*) exceeds the damage d_{PL} (ductility 0.5 and displacement $0.5u_y$) in the same way if the system is a non degrading one or degrading one.

ii) Aftershock Collapse Fragility Curves

The damage is represented by the displacement ductility required by the damaged system. Knowing that the only parameter that can be considered strictly cumulative is total Energy dissipated E_h (J. Ghosh, J. E. Padgett, and M. Sànchez-Silva, 2015), for the displacement, as well as for the ductility, the maximum value is important, which could be reached either during the most imminent earthquake or in any of the previous shakes, this depends on the nature of the earthquake shocks (J. Ghosh, J. E. Padgett, and M. Sànchez-Silva, 2015).

Being aware of the randomness of the damage function D, the seismic demand model for a mainshock-aftershock sequence is built considering that

$$D_2 = f(D_1, IM_2)$$

IM_2 are intensities which aftershocks are scaled with, D_1 is the damage index evaluated after the system has been subjected to mainshocks and D_2 is the required displacement for the aftershock; D_2 is evaluated with a multilinear regression model (J. Ghosh, J. E. Padgett, and M. Sànchez-Silva, 2015)

$$ln(D_2) = a + b\ ln(IM_2) + c\ ln(D_1) + d\ ln(D_1)\ ln(IM_2) \tag{6}$$

where *a, b, c, d* are regression coefficients, in particular *d* is the coefficient defining the interaction. In this case, as well as for the non degrading issue, the observation of IM_2/D_2 distribution in a Cartesian plane (Figure 5.6.1c) lead to think that the hypothesis of homoscedasticity is not satisfied, infact for increasing levels of IM_2 the presence of samples becomes thicker, the linearity of the distribution is lost and the related displacement demand increases significantly; this means that most of the sequences require a final displacement that leads the damaged system into the plastic phase, infact the data dispersion increases. The behavioral difference is less marked than the non degrading case, but however a linear relationship in the log–log plane between IM_2 and median response is not valid for the entire IM_2 range. So, for describing the *EDP*, a bilinear *PSDM* is adopted

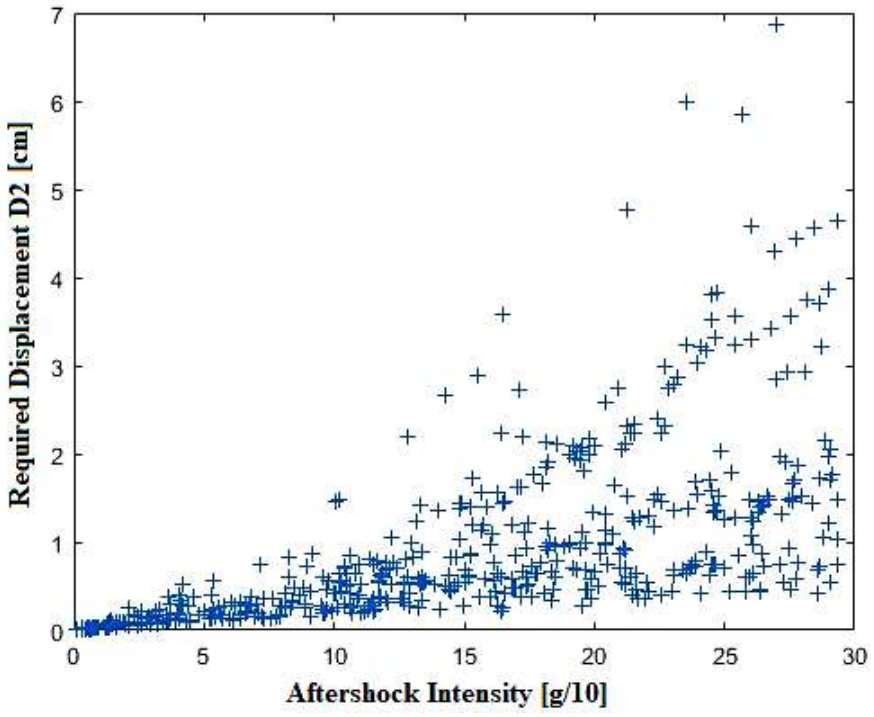

Figure 5.6.1b Seismic demand distribution at the 2nd erthquake shock (for all 500 mainshock-aftershock sequence) in function of aftershock scale factors

Considering that the seismic demand D_2 and relatives intensities IM_2 have a bilinear distribution, and knowing that, in mainshock-aftershock scenarios, the same seismic demand not only depends on aftershock intensities IM_2 but also on the damage the structure suffers during the first shock D_1 (Eqn (6)), a *multi-bilinear regression* has been performed (Figure 5.6.1c)

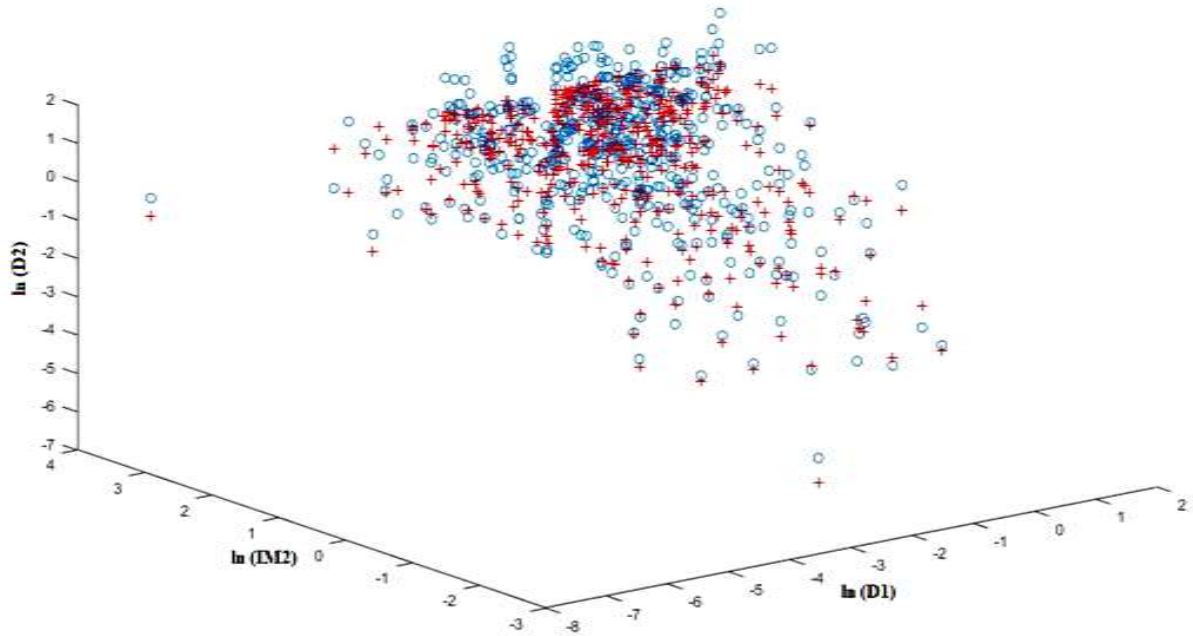

Figure 5.6.1c Bilinear regression model, with interaction, for the case of study

Described by the following expression

$$ln(D_2) = H_1\,[a_1+b_1\,ln(IM_2)+c\,ln(D_1)+d\,ln(D_1)\,ln(IM_2)] + \\ +(1-H_1)\,[a_1+b_1\,ln(IM^*)+b_2\,ln(IM_2-IM^*)+c\,ln(D_1)+d\,ln(D_1)\,ln(IM_2-IM^*)] \quad (7)$$

H_1 is the step function

$$H_1 = IM^* - IM_2$$

a_1, b_1, b_2, c, d are estimated with the regression just performed; the first three coefficients are used in the representation of the bilinear *PSDM* for D_2 and IM_2, graphically described by a simplified demand model (Eqn.(2))

$$ln(D_2) = H_1\,[a_1+b_1\,ln(IM_2)] + (1-H_1)\,[a_1+b_1\,ln(IM^*)+b_2\,ln(IM_2-IM^*)] \quad (8)$$

The Figure 5.6.1d confirms the presence of most of sequences after IM* remarking the predominantly non linear behavior of the system, as sayd before; there's a particular difference respect to the non degrading case, which is possible to observe both in Figure 5.6.1d and in Figure 5.6.1b: even if the regression between D_2 and IM_2 is described by the equation of a bilinear straight line in a log-log plane (Eqn.(8)), a strongly non linear behavior of the system is highlighted also for low intensitiy values.

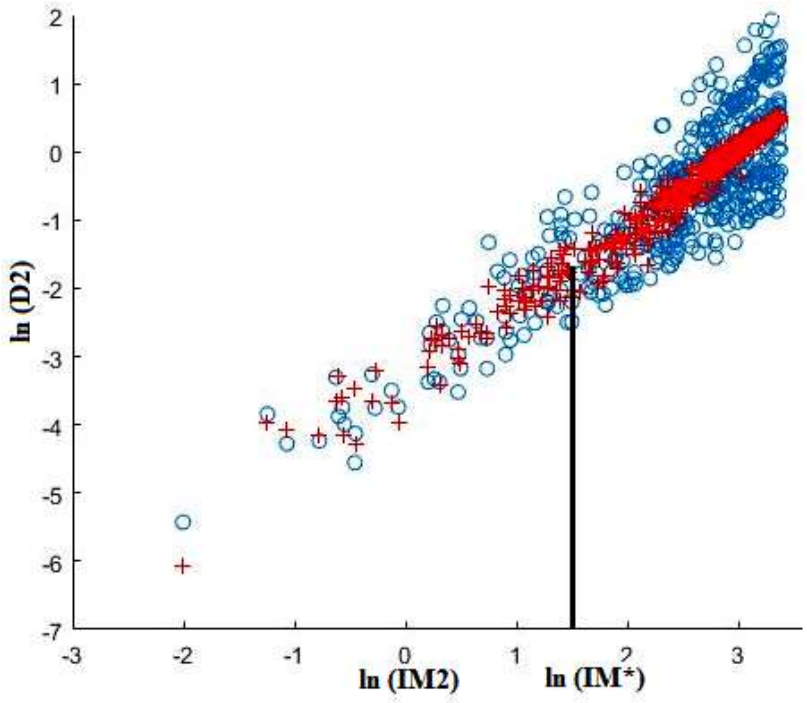

Figure 5.6.1d Bilinear *demand* model for D_2 and IM_2

This means that the degrading properties have a great influence on the structural response, infact graphically the trend is however bilinear, but the linear elasticity of the system is almost inexistent, due to the degradation of materials, so the system reaches aleady the plastic transition during the mainshock and before being subjected to the aftershock, for most sequences after the value of *IM**; this is demonstrated by the fact that both median values for each IM_2 (defined by the Eqn (8), red points) and the couple of data $ln(IM_2)–ln(D_2)$ (blue points) follow a straightaway trend but they are more dispersed. Coefficients *c, d* are properly of the interaction: *c* expresses the D_2 dipendence on D_1, *d* quantifies the dipendence on coupling between D_1 and IM_2.

a_1	b_1	b_2	$ln(IM^*)$ [g]
-3.0152	0.9105	1.13	1.2755

c	d
0.2675	-0.1159

The damage index D_2 is slightly influenced by the damage occurred after the first shock D_1: the collapse fragility final for the system is almost all attributable to the effects of the aftershock; the light influence of D_1 on D_2 is verifiable also in the coupling with IM_2. The two dispersions represent standard deviations of the seismic demand D_2 respect to the median value given by the regression surface for each value of IM_2 and D_1, respectively β_1 for $IM_2 < IM^*$, and β_2 for $IM_2 > IM^*$

β_1	β_2
0.3723	0.5900

The two values are higher than the non degrading case, but however the cloud of points is sufficiently fitted. β_1 and β_2 are more than acceptable values because in this case it's impossible to improve further the fitting, given this dispersion.

Fragility curves are calculated by considering the aftershock collapse capacities for each of the 500 mainshock–aftershock sequences; given the initial limit damage and subsequent limit damages

$$d_{PL,in} : u = 0.5u_y \qquad d_{PL,1} : u = 0.5u_y \qquad d_{PL,2} : u = 0.5u_y \qquad d_{PL,3} : u = 0.5u_y$$

the probability that the damage D_2 equals to or exceeds damage levels $d_{PL,i}$ is obtained with the following relation

$$P_i[D_2 > d_{PL,i}/IM_s] = \Phi\left(\frac{ln(median/d_{PL,in}, IM_s) - ln(d_{PL,i})}{\beta_1}\right) \quad for\ IM_s < IM^* \quad (9)$$

$$P_i[D_2 > d_{PL,i}/IM_s] = \Phi\left(\frac{ln(median/d_{PL,in}, IM_s) - ln(d_{PL,i})}{\beta_2}\right) \quad for\ IM_s > IM^* \quad (10)$$

In orded to make a fragility comparison with the other two approaches used, intensities used for representing fragility curves must be the same; consequently IM_2 are subtituted with sampled values IM_s in Eqn.(8), as well as $d_{PL,in}$ substitutes D_1 as representive of the damage limit state for the first shock. $ln(median/d_{PL,in}, IM_s)$ is the expected median value of the seismic demand D_2 calculated on the regression surface (Eqn.(8)) for each IM_s and referring to $d_{PL,in}$. Plotting the probability calculated for each subsequent limit damage in function of IM_s (Figure 5.6.1e), fragility curves are obtained

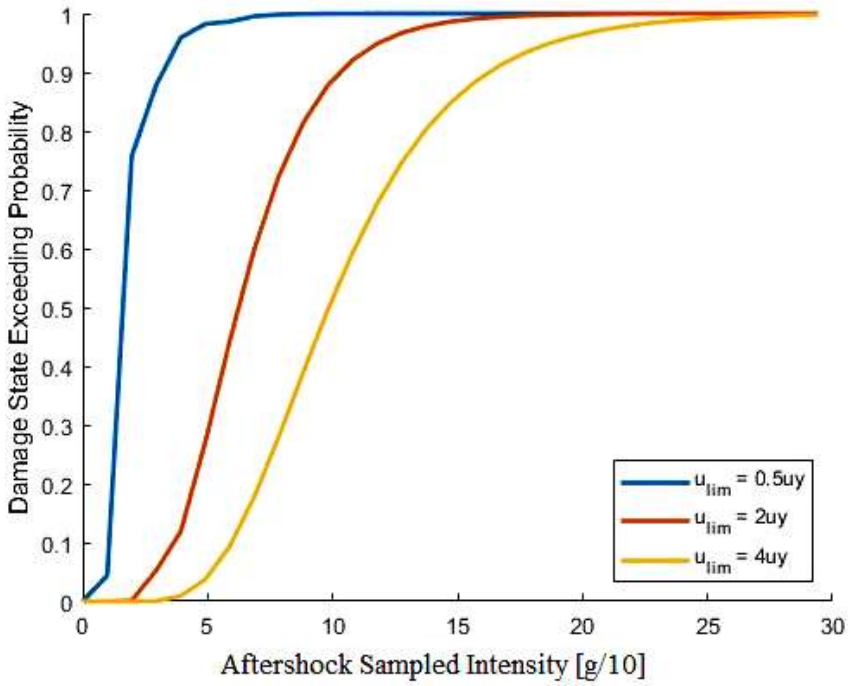

Figure 5.6.1e Collapse Fragility Curves for the Aftershock Non-Linear Dynamic Analysis

5.6.2 Case 2: *Park & Ang* Damage Index

i) Mainshock Collapse Fragility Curve

The damage function D (or *seismic demand*) is represented by the Park & Ang Damage Index (J. Ghosh, J. E. Padgett, and M. Sànchez-Silva, 2015)

$$D = \frac{\mu_m}{\mu_u} + \beta \frac{E_h}{F_y u_y \mu_u} \tag{11}$$

It allows to understand how the damage accumulates in the degrading system when

subjected only to mainshocks. A value of ultimate ductility is assumed $\mu_u = 4$, μ_m is obtained as the ratio between the maximum displacement of the lumped mass under the effect of mainshocks and the yield displacement, the other parameters are known. The *EDP* (the damage *D* or the *seismic demand*) is calculated with the Eqn.(3), which define, in the bilogarithmic plane, a linear *PSDM* in the form of the Eqn.(4). Graphically the linear regression line presents the trend reported in Figure 5.6.2a

a	***b***	***β***
0.065	1.340	0.557

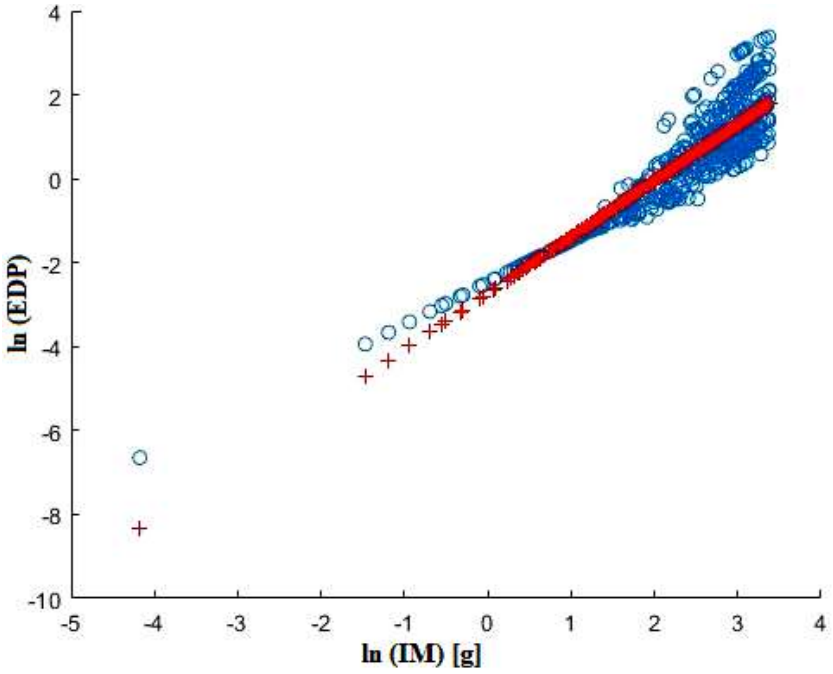

Figure 5.6.2a Linear Regression in the *ln (IM) – ln (EDP)* plane

As well as for the required displacement, similar considerations are made for the regression in the log-log plane between the *Park & Ang* Damage Index and *IM*.

The probability of exceeding each *PL* given the seismic action is calculated with the expression given by the Eqn.(5); the limit damage (*structural capacity*), associated to the Performance Level, is defined $D_{PL} = 0.5$; the fragility curve is represented in Figure 5.6.2b

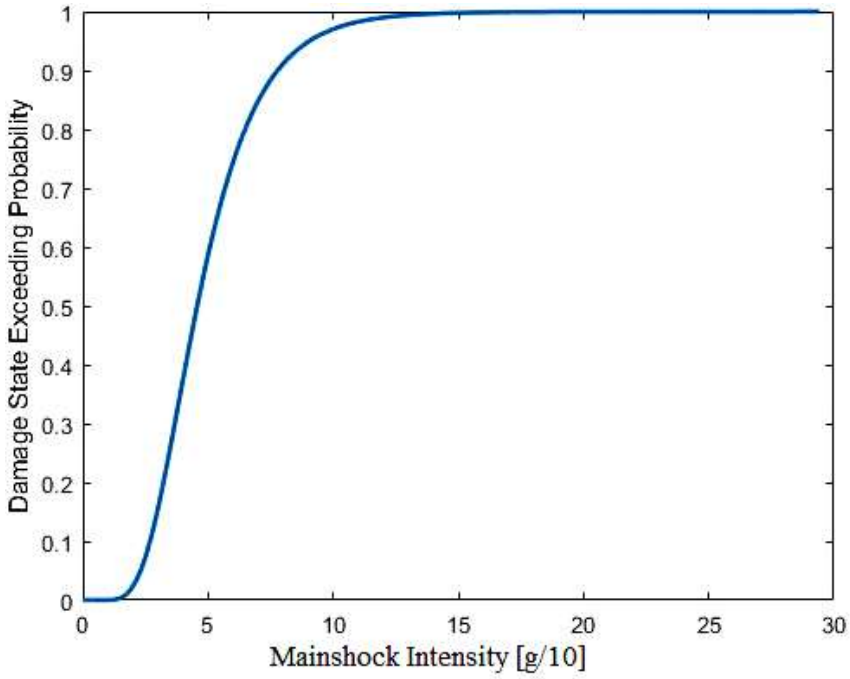

Figure 5.6.2b Collapse Fragility Curve for the Mainshock Non-Linear Dynamic Analysis $D_{PL} = 0.5$

The behavioral difference between the non degrading system and de degrading one is highlighted also in this case because, if the collapse is reached by exceeding a limit displacement (or a limit ductility), the fragility is the same regardless the nature of the system (degrading or not); if we consider the hysteretic energy dissipated during mainshocks for the system as damage indicator (so describing the damage accumulated with the *Park & Ang* relation), the collapse is reached for higher intensity levels, more or less 1.5g respect 0.5g for the limit displacement, this means that the system, after having been hit by the shock, crosses a first "relaxing" phase in which it accumulates damage and which allow to exceed the D_{PL} with major delay.

ii) Mainshock-Aftershock Collapse Fragility Curves

The total hysteretic energy dissipated in a complete cycle load (mainshock-aftershock sequence) is used as main parameter for evaluating the structural damage D_2 (or *seismic demand*). Referring to the Park & Ang Damage Index (Eqn.(11)), μ_m is the maximum ductility required to the system by a complete cycle load (mainshock-aftershock), obtained as the ratio between the maximum displacement in the whole sequence and the yield displacement; $\mu_u = 4$; E_h is the total hysteretic energy

dissipated, i.e. the area below the force-displacement curve obtained for each one of the 500 artificial sequences and for each sampled value of aftershock intensity (forces and displacements calculated on the whole mainshock-aftershock sequence). Being aware of the randomness of the damage function D, the seismic demand model for a mainshock-aftershock sequence is built considering that

$$D_2 = f(D_1, IM_2)$$

IM_2 are intensities which aftershocks are scaled with, D_1 is the damage index evaluated after the system has been subjected to mainshocks (see Section 5.6.2 *i*)) and D_2 is the *Park & Ang* Damage Index calculated on the whole load cycle; D_2 is evaluated with a multilinear regression model, referring to the Eqn.(6). Knowing that, in mainshock-aftershock scenarios, the same seismic demand not only depends on aftershock intensities IM_2 but also on the damage the structure suffers during the first shock D_1 (Eqn (6)), the *multi-bilinear regression* has been performed (Figure 5.6.2c)

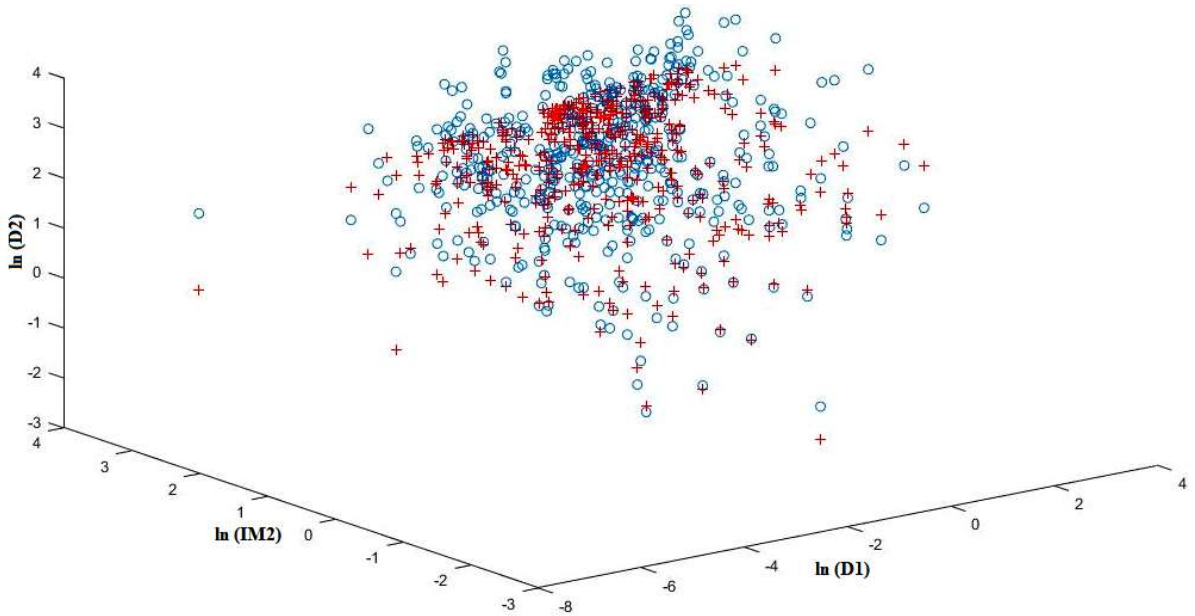

Figure 5.6.2c Bilinear regression model, with interaction, for the case of study

described by the Eqn.(7); the *bilinear PSDM* for D_2 and IM_2 is described by a simplified demand model (Eqn.(8)). The Figure 5.6.2d remarks the predominantly non linear behavior of the system.

There's a great behavioral difference respect to the case in which the required displacement is studied (Section 5.6.1 *ii*)): first of all the data distribution doesn't allow to define a specific *PSDM* for evaluating the damage, neither linear nor bilinear, but however it's assumed that the demand model follows a bilinear configuration because, despite their great uncertainty in the distribution, this choice provides smaller dispersions in fitting data (i.e. values of β are acceptable) than the linear one

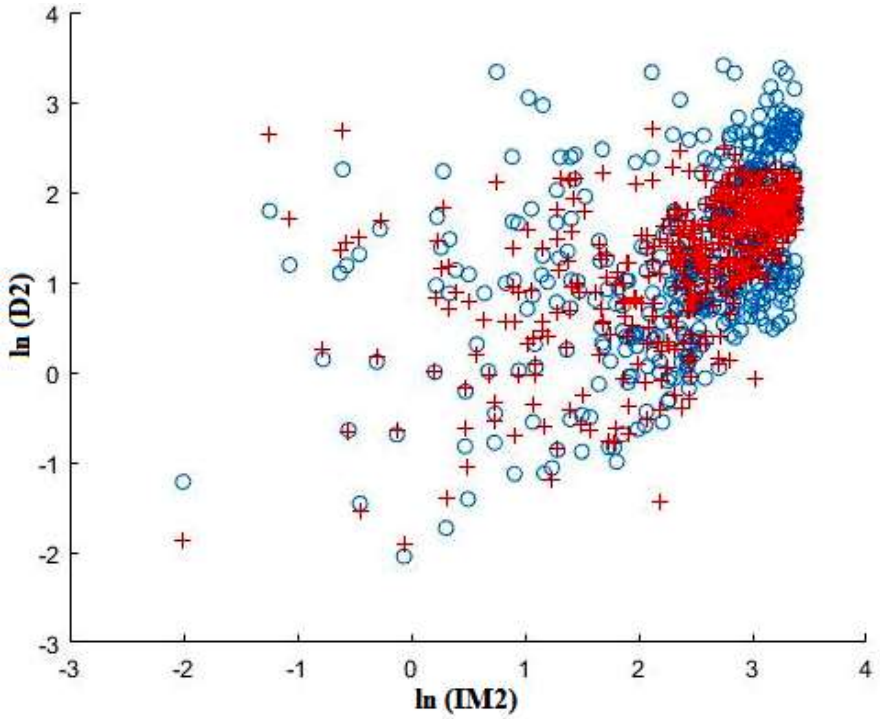

Figure 5.6.2d Bilinear *demand* model for D_2 and IM_2

Median values for each IM_2 (defined by the Eqn (8), red points) and the couple of data $ln(IM_2)–ln(D_2)$ (blue points) have a casual distribution with high dispersion, the system enters already in the plastic phase when subjected to potentially dangerous aftershocks with low intensities.

In any case, having adopted a multi-bilinear regression, all coefficients are obtained, in particular coefficients *c, d* are properly of the interaction: *c* expresses the D_2 dipendence on D_1, *d* quantifies the dipendence on coupling between D_1 and IM_2.

a_1	b_1	b_2	$ln(IM^*)$ [g]
0.0266	-0.0781	0.9026	1.2755

c	*d*
0.9273	-0.3800

The damage index D_2 is strongly influenced by the damage occurred after the first shock D_1: the final collapse fragility for the system is attributable to the effects of the whole mainshock-aftershock sequence; the coupling of D_1 with IM_2 is less influent. The two dispersions represent standard deviations of the seismic demand D_2 respect to the median value given by the regression surface for each value of IM_2 and D_1, respectively β_1 for $IM_2 < IM^*$, and β_2 for $IM_2 > IM^*$

β_1	β_2
0.5402	0.5447

The two values are higher than the non degrading case, but however the cloud of points is sufficiently fitted. β_1 and β_2 are more than acceptable values because in this case it's impossible to improve further the fitting, given this dispersion.
The fragility is estimated by referring to the collapse capacity of the whole sequence, defined for each of the 500 artificial sequences.; given the initial limit damage and subsequent limit damages

$$D_{PL,in} = 0.5 \qquad D_{PL,1} = 1 \qquad D_{PL,2} = 2 \qquad D_{PL,3} = 3$$

the probability that the damage D_2 equals to or exceeds damage levels $D_{PL,i}$ is obtained with Eqn.(9) and Eqn.(10). In orded to make a fragility comparison with the other two approaches used, intensities used for representing fragility curves must be the same; consequently IM_2 are subtituted with sampled values IM_s in Eqn.(8), as well as $D_{PL,in}$ substitutes D_1 as representive of the damage limit state for the first shock. $ln(median/D_{PL,in}\ ,IM_s\ )$ is the expected median value of the seismic demand D_2 calculated on the regression surface (Eqn.(8)) for each IM_s and referring to $D_{PL,in}$. The probability calculated for each subsequent limit damage is represented in function of IM_s (Figure 5.6.2e) for obtaining fragility curves

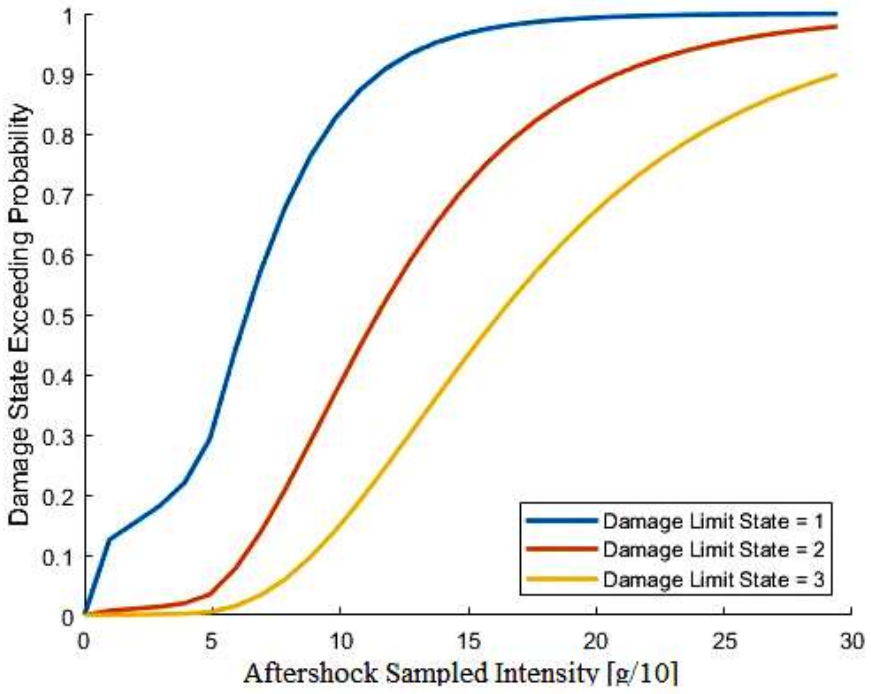

Figure 5.6.2e Collapse Fragility Curves for the Mainshock-Aftershock Non-Linear Dynamic Analysis

iii) Aftershock Collapse Fragility Curves

The damage index is defined by the *Park & Ang* relation, but in this case the total hysteretc energy dissipated only in the second cycle load (aftershock) is examined. The damage D_2 (or *seismic demand*) is obtained as difference between Park & Ang Damage Indexes calculated for the whole load sequence (Section 5.6.2 *ii*)) and for mainshock scenarios (Section 5.6.2 *i*)). The seismic demand model for a mainshock-aftershock sequence is built considering that

$$D_2 = f(D_1, IM_2)$$

IM_2 are intensities which aftershocks are scaled with, D_1 is the damage index evaluated after the system has been subjected to mainshocks (see Section 5.6.2 *i*)); D_2 is evaluated with a multilinear regression model, referring to the Eqn.(6). Knowing that, in mainshock-aftershock scenarios, the same seismic demand not only depends on aftershock intensities IM_2 but also on the damage the structure suffers during the first shock D_1 (Eqn (6)), the *multi-bilinear regression* has been performed (Figure 5.6.2f)

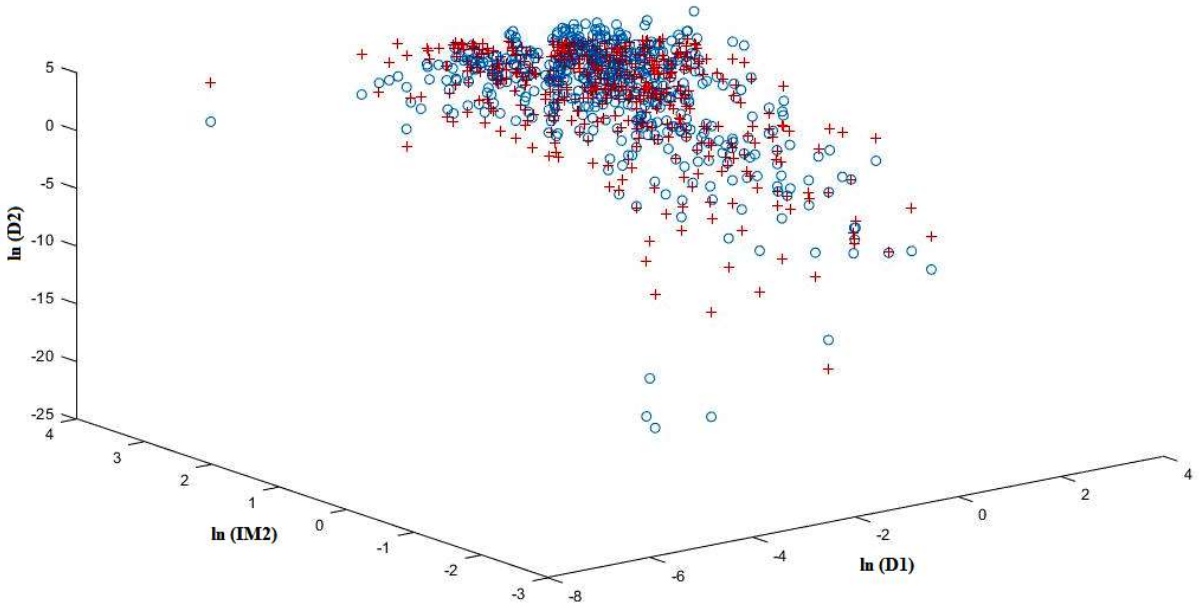

Figure 5.6.2f Bilinear regression model, with interaction, for the case of study

described by the Eqn.(7); the bilinear *PSDM* for D_2 and IM_2 is described by a simplified demand model (Eqn.(8)).

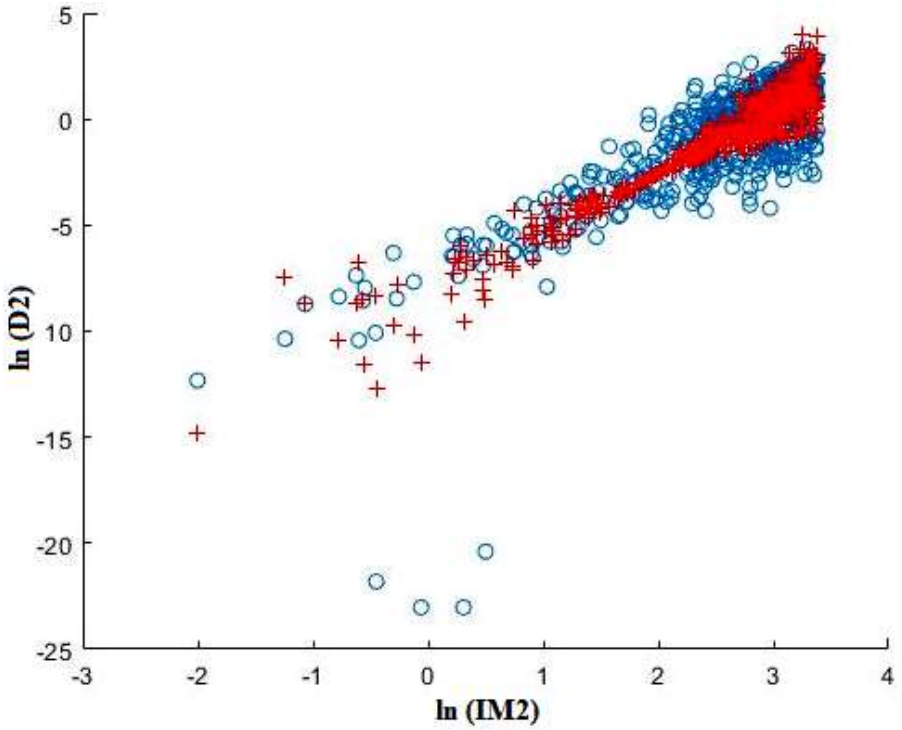

Figure 5.6.2g Bilinear *demand* model for D_2 and IM_2

The Figure 5.6.2g remarks the predominantly non linear behavior of the system but,

unlike the damage evaluated in the overall sequence (Section 5.6.2 *ii*)), the damage accumulated in the second load cycle is well represented by a *bilinear PSDM*, even if the data dispersion leads to suppose that the system crosses always the plastic phase, for each mainshock-aftershock sequence.

a_1	b_1	b_2	$ln(IM^*)$ [g]
-9.9837	0.9254	3.2136	-0.4507

c	d
1.3439	-0.5606

The damage index D_2 is strongly influenced by the damage occurred after the first shock D_1: although the fragility is calculated by referring to the aftershock collapse capacity, the system will be strongely damaged by the first shock; the coupling of D_1 with IM_2 is less influent. The two dispersions β_1 for $IM_2 < IM^*$ and β_2 for $IM_2 > IM^*$

β_1	β_2
4.0738	1.6206

The two values are very high, infact for $IM_2 < IM^*$ the presence of samples is almost null, and those few sequence left have a great dispersion from median values; for $IM_2 > IM^*$ the dispersion is less elevated, but however the four points which the fitting is not able to cover (in the bottom centre of the graph) contribute to increase the margin of error of the distribution. Also in this case it's impossible to improve further the fitting, given this dispersion. Given an initial damage and subsequent damage levels

$$D_{PL,in} = 0.5 \qquad D_{PL,1} = 1 \qquad D_{PL,2} = 2 \qquad D_{PL,3} = 3$$

the probability that the damage D_2 equals to or exceeds damage levels $D_{PL,i}$ is obtained with Eqn.(9) and Eqn.(10). In orded to make a fragility comparison with the other two approaches used, intensities used for representing fragility curves must be the same; consequently IM_2 are subtituted with sampled values IM_s in Eqn.(8), as well as $D_{PL,in}$

substitutes D_1 as representive of the damage limit state for the first shock. $ln(median/D_{PL,in}\ ,IM_s\ )$ is the expected median value of the seismic demand D_2 calculated on the regression surface (Eqn.(8)) for each IM_s and referring to $D_{PL,in}$. fragility curves are represented in Figure 5.6.2h

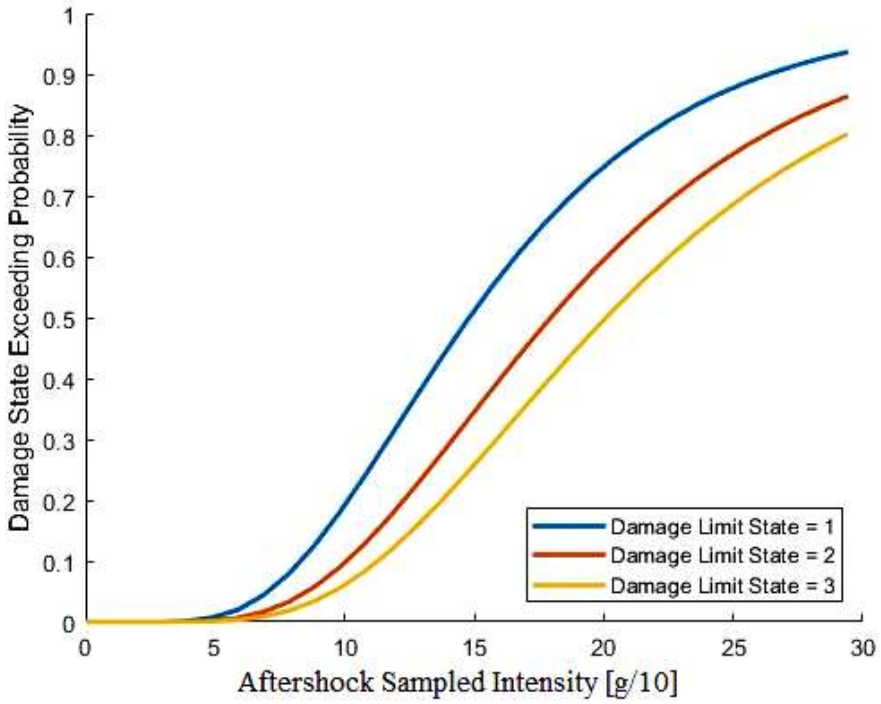

Figure 5.6.2h Collapse Fragility Curves for the Aftershock Non-Linear Dynamic Analysis

5.7 Empirical Collapse Fragility Curves: Approach 2

Collapse fragility curves are calculated by considering non linear IDA results (Section 5.3) exploiting the classical definition of *mathematical* probability referred to an event, the number of all possible cases for that event and the number of favorable cases, i.e. those cases which verify the event for which the probability is to be calculated.

5.7.1 Case 1: Required Dispacement

i) Mainshock Collapse Fragility Curves

D is the damage function (or *seismic demand*) represented by the maximum displacement required to the system in the undamaged configuration (mainshock) calculated for each ground motion and for each sampled value of mainshock

intensities. The limit damage, associated to the relative performance level, is fixed d_{PL} : $u = 0.5u_y$.

$$P = \frac{1}{N} P\,(D \geq d_{PL}) \tag{1}$$

The number of possible cases which this event may realize is given by the total number N of earthquake which the system is subjected to; in this case it is equal to 30. The number of favorable cases is evaluated by counting how many values of required displacements satysfy the event: if the event is satisfied for the specific value of ductility, then the probability of the event is sure and the value of ductility is substituted by 1; if not, the probability of the event is not possible and the value of ductility is substituted by 0. The mathematical probability is grafically represented in function of mainshock sampled intensities for obtaining the fragility curve (Figure 5.7.1a)

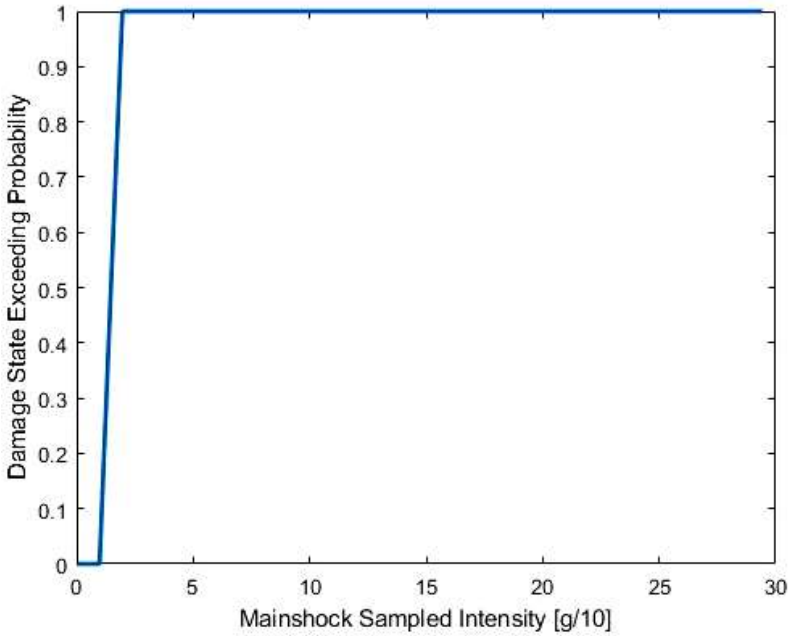

Figure 5.7.1a Collapse Fragility Curve for the Mainshock Non Linear IDA analysis, evaluated through the mathematical probability, $d_{PL} = 0.5u_y$

ii) Aftershock Collapse Fragility Curves

The damage level reached by the structure during the first shock (the initial Performance Pevel) corresponds to a limit displacement $d_{PL,in}$: $\mu = 0.5$. Given the initial limit damage and subsequent limit damages

$d_{PL,in} : \mu = 0.5$ $d_{PL,1} : \mu = 0.5$ $d_{PL,2} : \mu = 2$ $d_{PL,3} : \mu = 4$

the mathematical probability of the occurrence of damage D, equal to or higher than damage levels $d_{PL,i}$, is calculated with the Eqn.(1), considering that the number N of possible cases is given by the total number of sequences the system is subjected, i.e. 500. D is the seismic demand represented by the maximum displacement required to the system in the damaged configuration (aftershock) calculated for each sampled value of aftershock intensities. The counting procedure is the same as described in the previous Section, with the unique difference that N = 500 and the procedure is repeated three times, one for each subsequent damage level. Fragility curves are represented in Figure 5.7.1b

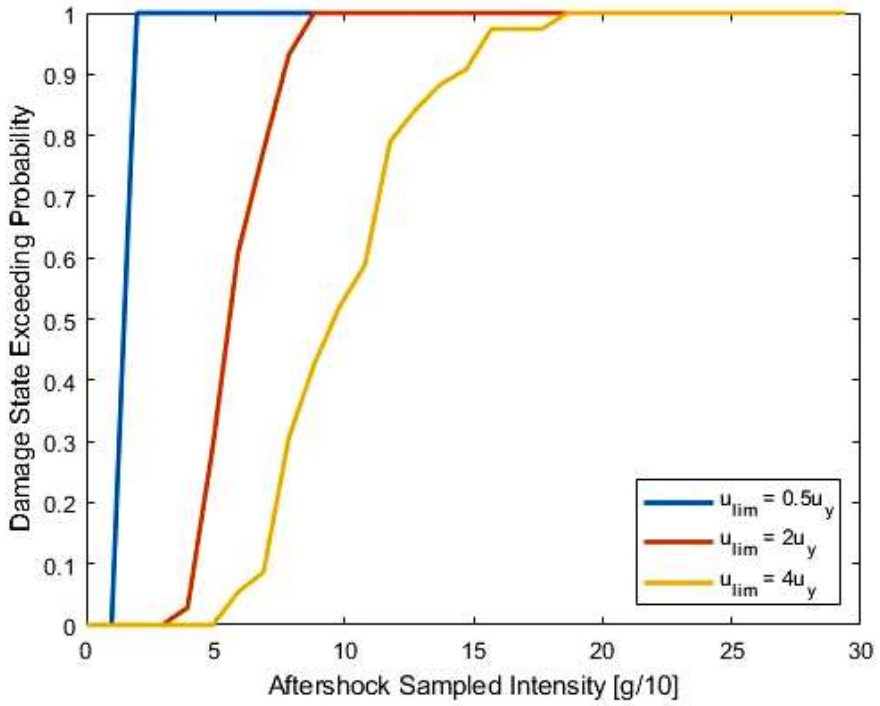

Figure 5.7.1b Collapse Fragility Curve for the Aftershock Non Linear IDA analysis, evaluated through the mathematical probability

5.7.2 Case 2: *Park & Ang* Damage Index

i) Mainshock Collapse Fragility Curves

D is the damage function (or *seismic demand*) represented by the damage accumulated by the system for the undamaged configuration (mainshock) and calculated with the *Park & Ang* Damage Index (Section 5.4.2 *i*)) for each ground motion and for each

mainshock sampled intensity. The limit damage, associated to the relative performance level, is fixed $D_{PL} = 0.5$. The mathematical probability of the occurrence of damage D, equal to or higher than the damage level d_{PL} , is calculated with the Eqn.(1); the number of possible cases which this event may realize is given by the total number N of earthquake which the system is subjected to; in this case it is equal to 30 while the number of favorable cases is evaluated by counting how many values of required displacements satysfy the event $D \geq d_{PL}$. Fragility curves is plotted in Figure 5.7.2a

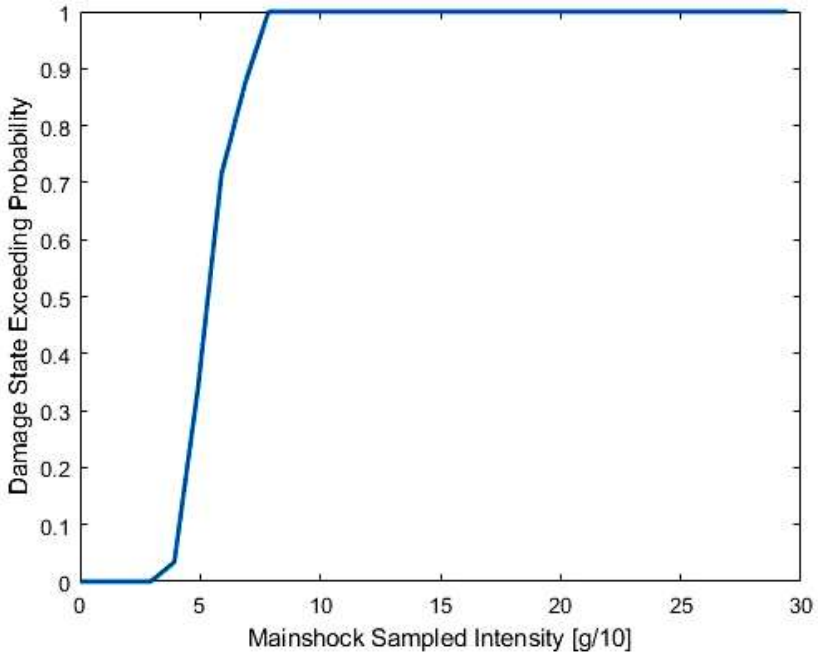

Figure 5.7.2a Collapse Fragility Curve for the Mainshock Non Linear IDA analysis, evaluated through the mathematical probability, $D_{PL} = 0.5$

ii) Mainshock-Aftershock Collapse Fragility Curves

D is the damage function (or *seismic demand*) represented by the damage accumulated by the system in a whole load cycle (mainshock-aftershock sequence) and calculated with the *Park & Ang* Damage Index (Section 5.4.2 *ii*)) for each sequence and for each aftershock sampled intensity. Given an initial damage and subsequent damage levels

$$D_{PL,in} = 0.5 \qquad D_{PL,1} = 1 \qquad D_{PL,2} = 2 \qquad D_{PL,3} = 3$$

the mathematical probability of the occurrence of damage D, equal to or higher than damage levels $D_{PL,i}$, is calculated with the Eqn.(1), considering the number N of

possible cases equal to the total number of sequences the system is subjected, i.e. 500. The counting procedure is the same, with the unique difference that N = 500 and the procedure is repeated three times, one for each subsequent damage level. Fragility curves are represented in Figure 5.7.2b

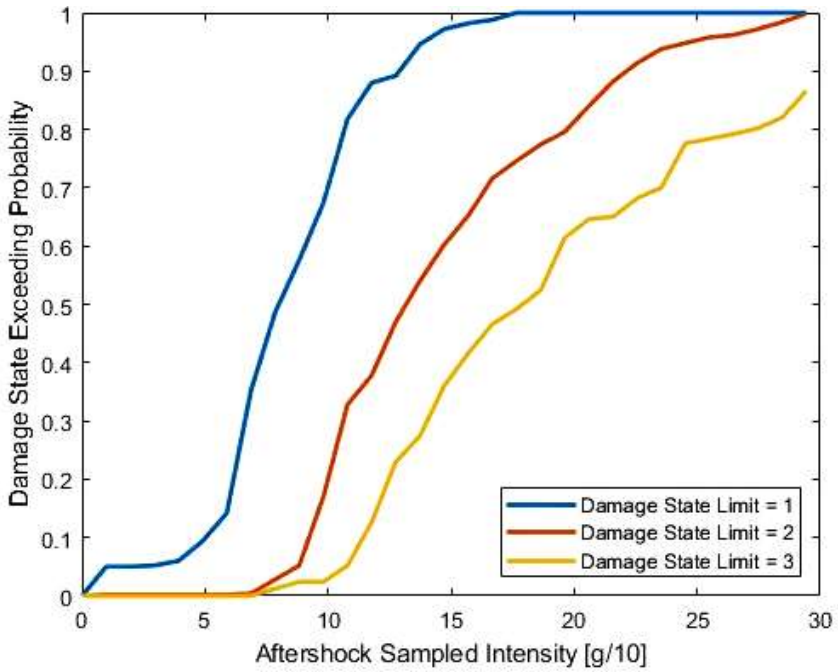

Figure 5.7.2b Collapse Fragility Curve for the Mainshock-Aftershock Non Linear IDA analysis, evaluated through the mathematical probability

iii) Aftershock Collapse Fragility Curves

D is the damage function (or *seismic demand*) represented by the damage accumulated by the system in the second load cycle (aftershock) and calculated with the *Park & Ang* Damage Index as the difference between the damage accumulated by the system in a whole load cycle (mainshock-aftershock sequence) and the damage accumulated in the undamaged configuration (mainshock). Given an initial damage and subsequent damage levels

$$D_{PL,in} = 0.5 \qquad D_{PL,1} = 1 \qquad D_{PL,2} = 2 \qquad D_{PL,3} = 3$$

the mathematical probability of the occurrence of damage D, equal to or higher than damage levels $D_{PL,i}$, is calculated with the Eqn.(1), considering the number N of

possible cases equal to the total number of sequences the system is subjected, i.e. 500. Fragility curves are represented in Figure 5.7.2c

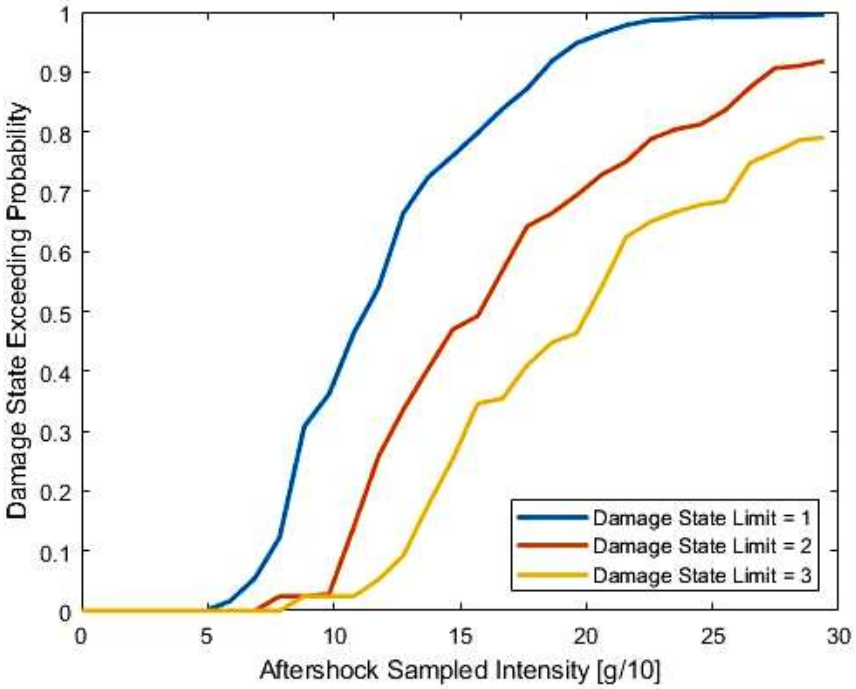

Figure 5.7.2c Collapse Fragility Curve for the Aftershock Non Linear IDA analysis, evaluated through the mathematical probability

CHAPTER 6 DISCUSSION OF RESULTS AND CONCLUSIONS

6.1 Introduction

In this last Chapter all fragility curves previously presented for each case of study will be compared in function of the approach used for obtaining them and of damage levels estabilished. In the first part, fragility estimate based on the aftershock collapse fragility, for the non degrading system, is conducted by comparing fragility curves built with the three methods, in order to verify their reliability and goodness in representation of results; in this case the damage index is the required ductility, as sayd in Chapter 4.

In the second part, fragility estimate based both on aftershock collapse fragility and mainshock-aftershock collapse fragility is conducted for the degrading system by comparing always fragility curves built with the three methods, in order to verify if they are able to effectively simulate also the behavior of the system which accumulates damage in a whole mainshock-aftershock sequence; damage indexes in this case are two: one is the required displacement and the other is the *Park & Ang* Damage Index, as sayd in Capter 5. The final Section will present conclusions about the discussion and suggestions for future works.

6.2 Aftershock Collapse Fragility Curves: Non Degrading System

The damage function D is represented by the *required ductility*, obtained as the ratio between the maximum displacement recorded for the system in the damaged configuration (aftershock), in function of the method used, and the yield displacement, for each of the 500 artificial sequences.

The collapse fragility, in this case, is evaluated for the damaged system and calculated referring to the aftershock collapse capacity defined for each of the 500 mainshock–aftershock sequences. The mainshock damage corresponds to an initial damage level for the system $d_{PL,in}$: $\mu = 0.5$. Given an initial damage and subsequent damage levels

$$d_{PL,in} : \mu = 0.5 \qquad d_{PL,1} : \mu = 0.5 \qquad d_{PL,2} : \mu = 2 \qquad d_{PL,3} : \mu = 4$$

the probability P that D equals or exceeds d_{PL} is calculated for each sampled value of aftershock intensity in function of the method used; consequently fragility curves, for each method, are built by plotting P in function of aftershock sampled intensities. The comparison is represented in Figure 6.2a-6.2b-6.2c

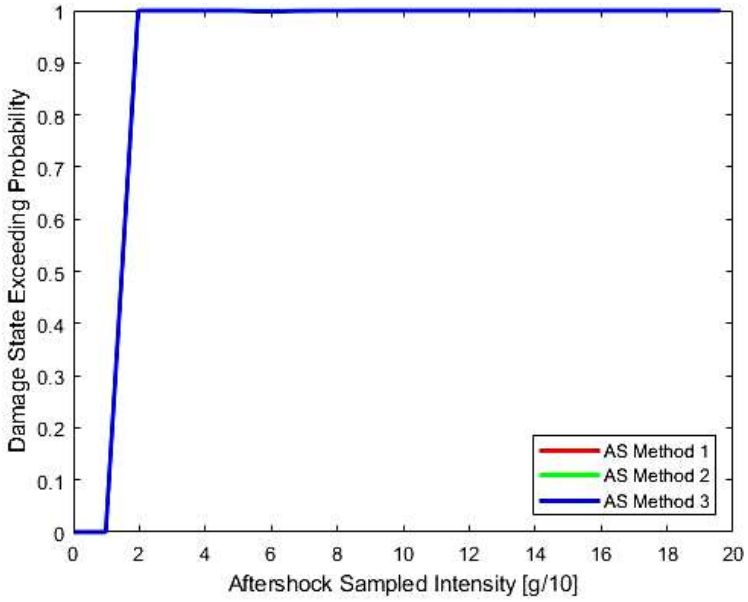

Figure 6.2a Aftershock Collapse Fragility Curves for $d_{PL} = 0.5$

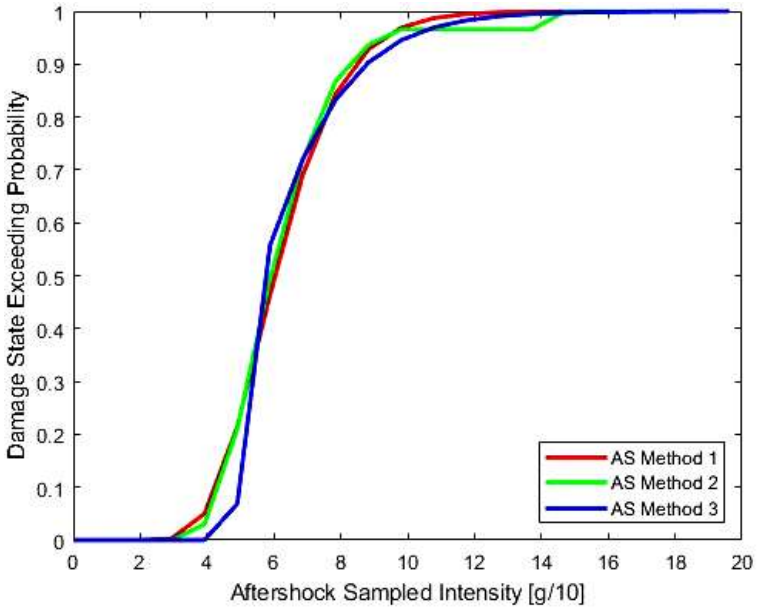

Figure 6.2b Aftershock Collapse Fragility Curves for $d_{PL} = 2$

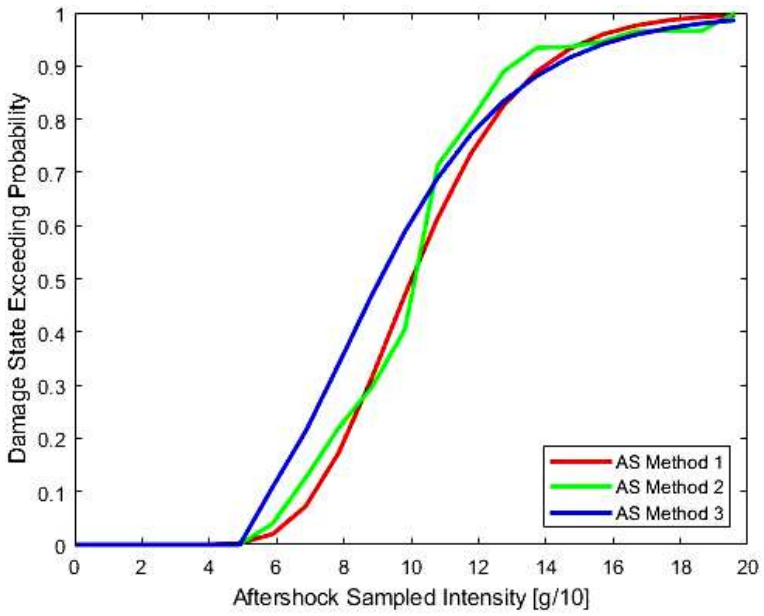

Figure 6.2c Aftershock Collapse Fragility Curves for $d_{PL} = 4$

For a damaged system with a d_{PL}: $\mu = 0.5$ fragility curves fit together perfectly: there's no distinction among them; in this case the collapse has been reached for a low value of intensity (0.2g) without giving the possibility to the system to pass through a progressive damage phase from the mainshock to the aftershock. Infact the system is in linear field for intensities going from 0 to 0.1g, after 0.1g it reaches the failure at 0.2g almost rapidly, and the plastic transition, useful to the system for damaging itself before the collapse, is very small; this is the reason of their linear trend.

Fragility curves becomes more extended by increasing the damage level (Figure 6.2b-6.2c), infact the higher the damage level (the limit ductility or the *structural capacity*), the higher the intensity needed to reach the collapse, with the same required ductility (or *seismic demand*); consequently the plastic transition increases and the more it increases the more the system has the time to damage itself, allowing to monitor it step by step and to predict the failure. Green curves are fragility curves calculated with the mathematical probability, infact it's possible to notice the discrete character of their trends, this due to the fact that the mathematical probability is function of distribution of a discrete random variable, as sayd in Chapter 4.

In general, unless uncertainties on the system response and ground excitations, fragility curves calculated for each damage level match perfectly; this means that a correct fragility analysis has been conducted and that the three methods used for this

purpose have been correctly set up because, for each damage level, fragility curves built by adopting three different approaches returns the same value of intensity in correspondence of which the collapse is reached: 0.2g for d_{PL}: μ = 0.5, 1g for d_{PL}: μ = 2 and 2g for d_{PL}: μ = 4. So in this case, for a fragility estimate conducted under these conditions, the choice of one method rather than another is indifferent because they lead to the same result.

6.3 Aftershock Collapse Fragility Curves for the Degrading System: Case 1

D is represented by the *required displacement*, i.e. the maximum displacement recorded for the system in the damaged configuration (aftershock), in function of the method used, for each of the 500 artificial sequences. The collapse fragility is calculated by referring to the aftershock collapse capacity defined for each of the 500 mainshock–aftershock sequences. The mainshock damage corresponds to the initial damage level for the system $d_{PL,in}$: $u = 0.5u_y$. Given an initial damage and subsequent damage levels $d_{PL,in} : u = 0.5u_y$ $d_{PL,1} : u = 0.5u_y$ $d_{PL,2} : u = 2u_y$ $d_{PL,3} : u = 4u_y$ the probability P that *D* equals or exceeds d_{PL} is calculated always for each sampled value of aftershock intensity in function of the method used; The comparison between the three approaches is represented in Figure 6.3a-6.3b-6.3c

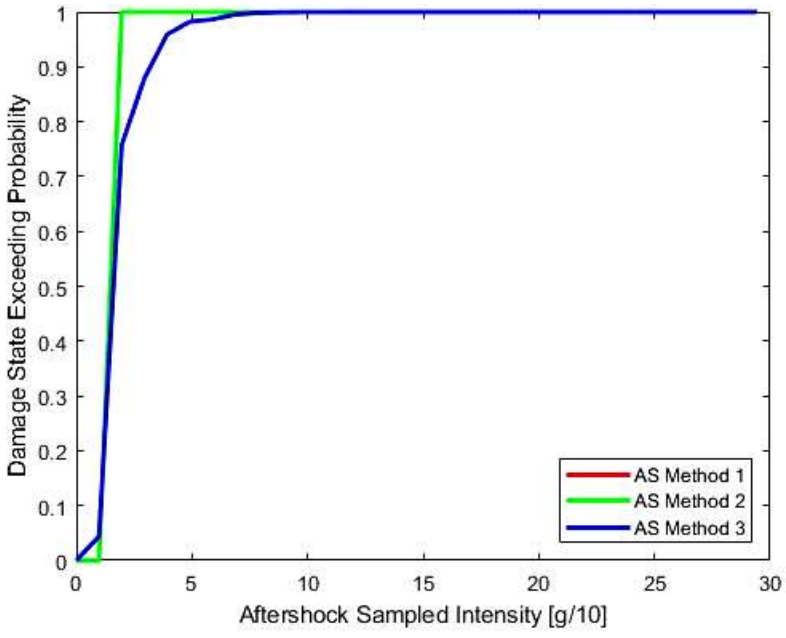

Figure 6.3a Aftershock Collapse Fragility Curves for $d_{PL} : u = 0.5u_y$

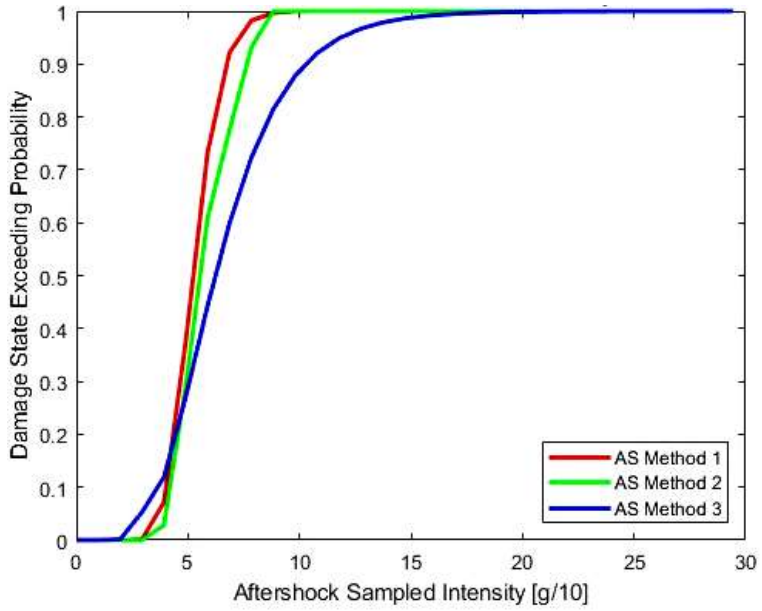

Figure 6.3b Aftershock Collapse Fragility Curves for d_{PL} : $u = 2u_y$

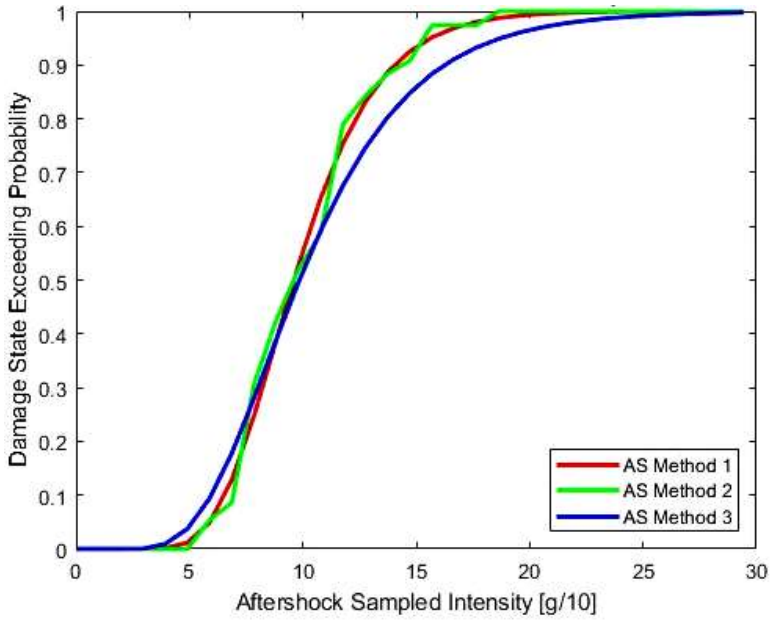

Figure 6.3c Aftershock Collapse Fragility Curves for d_{PL} : $u = 4u_y$

The first point which particular attention is paid on is the aftershock intensity: this is a first consequence of the behavior changing in the system, in which the degradation of materials in terms of stiffness is taken into account, infact analyzes has been extended to a range of aftershock sampled intensities up to 3g (always with steps of 0.1g) because, if the system suffers a stiffness lost due to the application of a cycle load, the collapse is reached for values of intensity higher than the case in which the system is a non degrading one, for the same damage levels (infact the required ductility is the ratio

between the required displacement in the damaged configuration and the yield displacement; the same thing if the required displacement, in the damaged configuration, is the product among the same values of the required ductility and the yield displacement). In other words, analyzes conducted for the degrading system are the same conducted for the non degrading system, with the same damage levels: basing on this consideration, fragility curves obtained with the non linear IDA analysis are slightly more extended than those obtained for the non degrading system, as for those obtained by applying the mathematical probability. This means that values of intensity in correspondence of which the collapse is reached are higher: 0.23g for d_{PL}: $u = 0.5u_y$, 1.2g for d_{PL}: $u = 2u_y$ and 2.4g for d_{PL}: $u = 4u_y$.

On the other hand, considering the damage D evaluated in the aftershock as linked with the damage occurred during the mainshock and the aftershock intensities with a *multi-bilinear PSDM* (blue curves) lead to even lower fragility for the system towards earthquakes: limit values of intensity in correspondence of which the collapse occurs are higher than the previous case and than the one recorded in this case with the IDA, for all three damage levels; infact the collapse is reached for: 0.75g when d_{PL}: $u = 0.5u_y$, 1.8g when d_{PL}: $u = 2u_y$ and 2.8g when d_{PL}: $u = 4u_y$. This means that, unlike the non degrading situation, the system presents less fragile, regardless the method used. Consequently, unless uncertainties on the system response, demand model (the data dispersion which translates in an enlargement among curves) and ground excitations, a correct fragility analysis has been conducted and, although the three methods have been correctly set up, it has been demonstrated that, talking in terms of safety life from collapse, a non linear IDA should be able to better simulate the behavior of a system with stiffness loss than a non linear dynamic analysis based on a probabilistic evaluation of the seismic demand, at the same damage levels.

6.4 Mainshock-Aftershock Collapse Fragility Curves: Degrading System

The total hysteretic energy dissipated in a complete cycle load (mainshock-aftershock sequence) is used as main parameter for evaluating the structural damage D (or *seismic demand*). Referring to the *Park & Ang* Damage Index, μ_m is the maximum ductility

required to the system by a complete cycle load (mainshock-aftershock), obtained as the ratio between the maximum displacement in the whole sequence, calculated for each method, and the yield displacement; μ_u = 4; E_h is the total hysteretic energy dissipated, i.e. the area below the force-displacement curve obtained for each one of the 500 artificial sequences and for each sampled value of aftershock intensity (forces and displacements calculated on the whole mainshock-aftershock sequence, for each method). For each method and for each damage level, comparisons among fragility curves are presented in Figure 6.4a-6.4b-6.4c

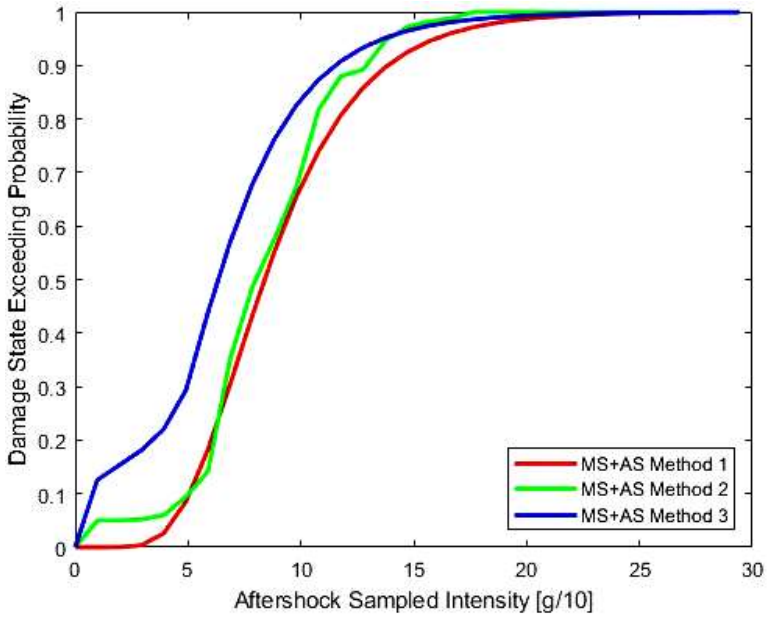

Figure 6.4a Mainshock-Aftershock Collapse Fragility Curves for D_{PL} = 1

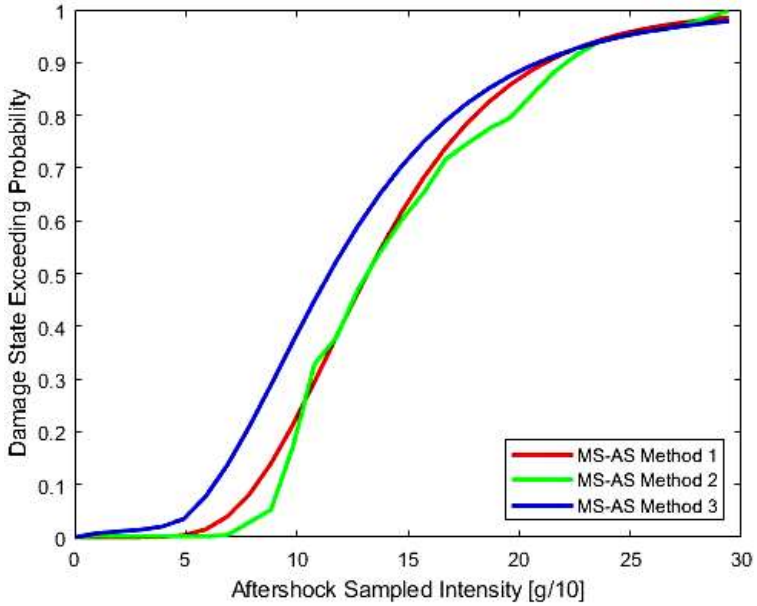

Figure 6.4b Mainshock-Aftershock Collapse Fragility Curves for D_{PL} = 2

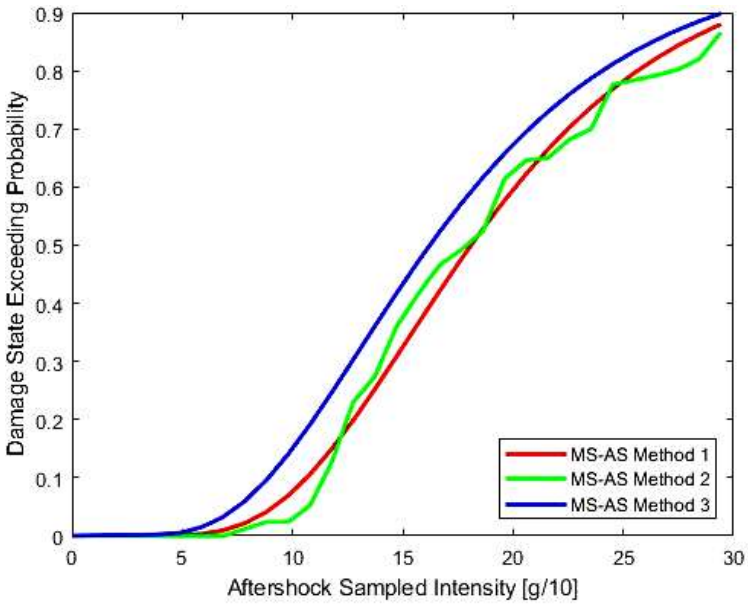

Figure 6.4c Mainshock-Aftershock Collapse Fragility Curves for $D_{PL} = 3$

The fragility is estimated by referring to the collapse capacity of the whole sequence; given the initial limit damage and subsequent limit damages

$$D_{PL,in} = 0.5 \qquad D_{PL,1} = 1 \qquad D_{PL,2} = 2 \qquad D_{PL,3} = 3$$

fragility curves are obtained by plotting the probability that D equals or exceeds D_{PL} in function of aftershock sampled intensities.

If a degrading system is already damaged by a mainshock, it will dissipate energy passing from the first shock to the second one (the aftershock), even if the second shock is less dangerous than the first one; this means an increase of the damage because it directly depends on the total hysteretic energy dissipated, at the same ultimate ductility capacity and maximum ductility required to the system; consequently the system should present itself more vulnerable towards mainshock-aftershock sequences than the case in which the damage accumulated only in aftershock sequence is studied (see next paragraph).

In fragility curves built for $D_{PL} = 2$ the three methods provide an estimate of the failure for a value of intensity equal to 3g, a result perfectly reliable because in this case the damage accumulated in a complete load cycle makes the structure more fragile, from the structural collapse point of view, respect to the one accumulated in aftershock load cycle, i.e. without considering the mainshock contribute to the damage (as we will see

in te next paragraph) . For D_{PL} = 3 the situation is similar, the three methods provide a limit value in correspondence of the failure higher than 3g, as wanted to prove, infact in correspondence of 3g the probability that the damage D equals or exceeds D_{PL} is 90% more or less. For D_{PL} = 1 fragility curves provide all the same result, infact the collapse is reached for a value of intensity more or less equal to 2.3g, obviously less than those needed for exceeding the other two limit capacities; looking these curves they seems to be translated, this phenomenon can be attributed to small implications due to the adoption of a *multi-bilinear PSDM* for the seismic demand evaluation in the third method.

This is not a design mistake because the dispersion between intensities and the seismic demand of the first and second shock, due to the application of this *PSDM*, is very small; this means that they have been fitted in the best way possible. So, following these results, the unique possible conclusion about the three methods regards their adaptability, infact in this case the IDA analysis (the second method is a consequence of the IDA results) underestimates the fragility respect to the one estimated with the non linear dynamic analysis and, given that it's good rule to design in terms of safety life from collapse, the non linear dynamic analysis should be more suitable to conduct a fragility analysis rather than a non linear IDA, with the same conditions.

6.5 Aftershock Collapse Fragility Curves for the Degrading System: Case 2

The damage index is defined by the *Park & Ang* relation, but in this case the total hysteretc energy dissipated only in the second cycle load (aftershock) is examined. The damage D (or *seismic demand*) is obtained as difference between *Park & Ang* Damage Indexes calculated for the whole load sequence (mainshock-aftershock) and for mainshock scenarios. μ_u = 4.

The fragility is estimated by referring to the aftershock collapse capacity; given the initial limit damage and subsequent limit damages

$$D_{PL,in} = 0.5 \qquad D_{PL,1} = 1 \qquad D_{PL,2} = 2 \qquad D_{PL,3} = 3$$

fragility curves are obtained by plotting the probability that D equals or exceeds D_{PL} in function of aftershock sampled intensities; for each method and for each damage level, comparisons among fragility curves are presented in Figure 6.5a-6.5b-6.5c

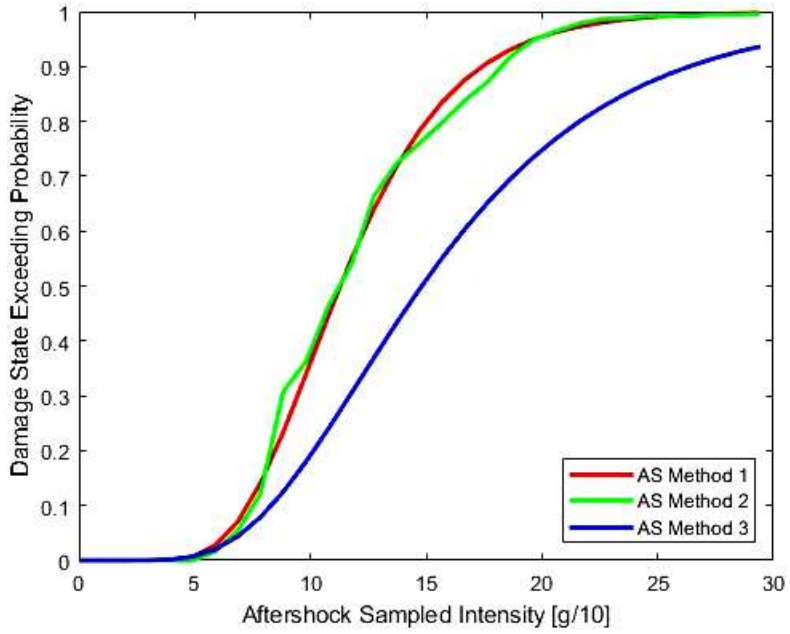

Figure 6.5a Aftershock Collapse Fragility Curves for D_{PL} = 1

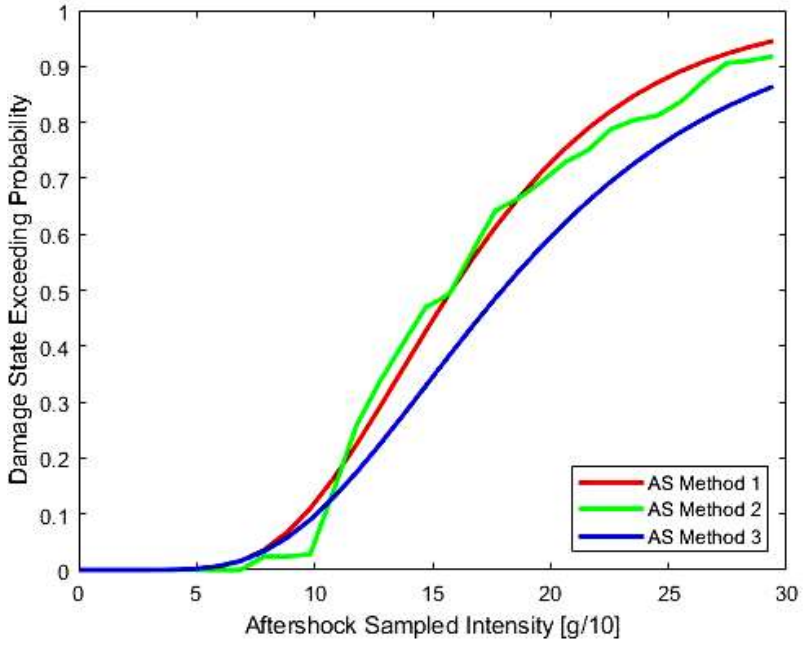

Figure 6.5b Aftershock Collapse Fragility Curves for D_{PL} = 2

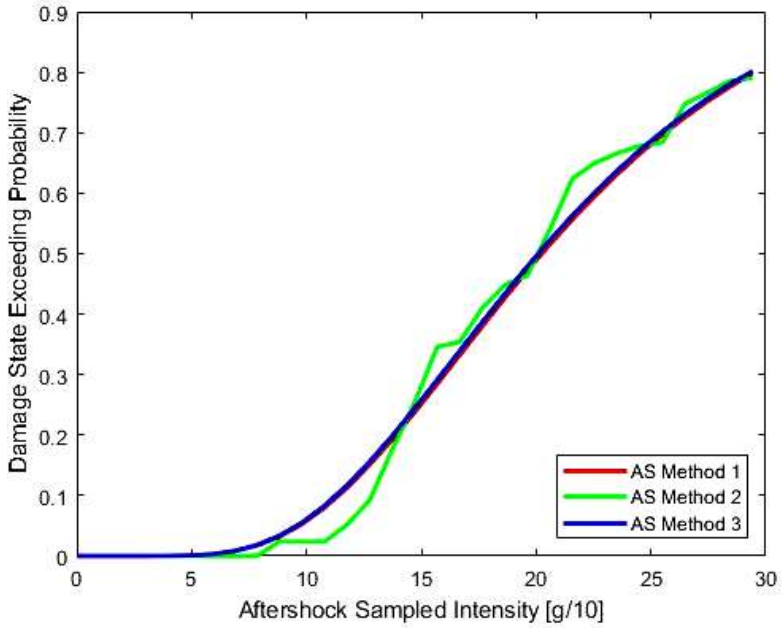

Figure 6.5c Aftershock Collapse Fragility Curves for $D_{PL} = 3$

Regardless the method used, it is obvious that if we consider the damage accumulated only in the second load cycle (aftershock) the system reaches the collapse for higher values of intensities than the case in which the damage accumulated in a complete load cycle is examined, because practically it's like the contribute to the damage given by the first shock is not considered, so the system is less fragile and less vulnerable towards earthquakes; this is confirmed by comparing these results with the results obtained in the previous Section for the mainshock-aftershock sequence.

Knowing that the higher bound of the range of aftershock sampled intensity is 3g, an estimate of limit values which lead the structure to the collapse is conducted

Method 3	$D_{PL,1}$	$D_{PL,2}$	$D_{PL,3}$
MS - AS	2g	3g	≈ 4g
AS	≈ 3.5g	≈ 4g	≈ 4.5g

Method 1-2	$D_{PL,1}$	$D_{PL,2}$	$D_{PL,3}$
MS - AS	2.3g	3g	≈ 4g
AS	3g	≈ 3.5g	≈ 4.5g

This is what was expected: the damage considered in the second load cycle lead the system to exceed a specific damage level for higher intensities, associated to that specific aftershock, than those referred to the entire sequence.

Also in this case, unless uncertainties on the system response, demand model (the data dispersion in this case is strongly marked for the first two damage levels, in which curves are very distant) and ground excitations, a correct fragility analysis has been conducted and, although the three methods have been correctly set up, however it's possible to observe that the IDA analysis (the second method is a consequence of the IDA results) overestimates the fragility respect to the one estimated with the non linear dynamic analysis: this situation is verifiable also in the case in which the required displacement is examined, always for the degrading system and, in a small part, in the non degrading one. The structural collapse capacity in these cases may reduce significantly, probably due to the fact that the building is subjected to a high intensity mainshock and the structure is likely to collapse even if a small aftershock follows the mainshock (Yue Li, M.Asce; Ruiqiang Song, S.M.Asce; and John W. Van De Lindt, M.Asce, 2014); given that it's good rule to design in terms of safety life from collapse, the non linear dynamic analysis should be less suitable to conduct a fragility analysis rather than a non linear IDA, with the same conditions.

6.6 Summary and Concluding Observations

In this thesis the collapse fragility of a system subjected to the effects of mainshock-aftershock sequences has been evaluated, as the properties of the materials and the type of damage caused varied. The impact of the first earthquake and the stiffness lost have been considered for evaluating how the overall damage is influenced and consequently how the collapse fragility changes. Three different approaches have been developed to carry out this evaluation, the first based on the results of a non-linear IDA analysis, the second as a corollary of the first and the third based on a nonlinear dynamic analysis; the latter approach involves a probabilistic evaluation of the seismic demand model. In the mainshock-aftershock non linear IDA the effect of the first shock is already considered in the analysis phase, unlike the third method, infact the

mainshock is scaled with values of intensities in correspondence of which an initial damage for the structure occurs, then the IDA is conducted on the second shock. The structural response is obtained by evaluating the non linear dynamic response history of each method with the help of different analysis tools, in particular a non-linear integration if the system is a non-degrading one and the software OpenSees for the degrading one. Fragility curves are derived on the base of a two-parameter lognormal distribution function useful for calculating the probability of exceeding certain damage limit states, or structural capacities, by the seismic demand. Damages considered are the ductility required to the non-degrading system, the displacement required to the degrading system and the damage accumulated by the degrading system due to the hysteretic energy dissipated in load cycles. Earthquakes used for these analyzes are extracted from the PEER Database, representing seismic events really happened, seismic sequences are randomly and artificially created, including a period of 4s between the first and the second shock. The final outcome of this thesis can be concluded by summarizing the main considerations and observations obtained during the elaboration of the results:

1) In a damaged configuration for the system, when it is subjected to aftershock sequences, it results less fragile (and consequently less vulnerable to earthquakes) as the levels of structural capacity increase (over which collapse occurs), infact intensity values, leading to exceed the probability of failure, grow with the increase of limit damages.
2) Fragility analysis set up in this way helped us to understand what method or what approach is more suitable for best simulating the mainshock-aftershock collapse fragility for a damaged system in function of each specific case studied in this discussion.
3) In a non degrading configuration, the aftershock collapse fragility evaluated for the damaged system lead to results more or less similar regardless the methodology used, even if the IDA analysis (and consequently the empiric approach) provides fragility curves very thin less extended than those obtained by using a *PSDM*, this means that the fragility is slightly overestimated.

4) From the analysis of fragility curves it has been observed that the use of different properties related to the materials of the system significantly influences the seismic performance of a damaged structure; infact, considering the rigidity degradation due to the application of cyclic loads, for the same capacity levels and damage indexes, the collapse fragility for a degrading system is more marked than in the case of a system without degrading properties. Many studies (FEMA-P440A, 2009) have compared the response (in terms of maximum movement achieved) of various structural systems obtained using both hysteretic models with stiffness degradation and with the elastic-plastic models (which do not take into account of stiffness loss). These studies have led to the conclusion that for structural systems with medium-long periods of oscillation, the maximum displacements to which they are subjected are very similar with both types of models. All this suggests that it is possible to use simpler models such as the elastic-plastic one or elastic-hardening which do not take into account the stiffness degradation to estimate lateral displacements for structures with a medium-long period of vibration (systems with a fundamental period greater than 1s). On the other hand, the same studies have shown that for systems with an oscillation period equa or less than 1 second (the case in question, where T = 1s) it is of fundamental importance to use models with stiffness degradation, since the elastic-plastic model generate an underestimation of the displacements; infact, from the non degrading to the degrading situation, maximum displacements reached higher peaks, this leads to an extension of fragility curves and to an increase of collapse intensities . So models that include rigidity degradation more accurately reflect the true behavior of structural elements.
5) In a degrading system, considering aftershock without any previous damage means to obtain the lowest structural vulnerability (and consequently the lowest fragility) for increasing limit capacity levels: this may be because aftershocks usually have lower durations and contain lower range of frequencies. However, considering also the damage accumulated during the first event (i.e. in a complete mainshock-aftershock load cycle), fragility curves show the highest

probability of exceedance in almost all damage levels and earthquake intensities (F. Hosseinpour, A.E. Abdelnaby, 2017), consequently more fragility.

6) For aftershock scenarios, regardless if the damaged system is non degrading or degrading, the IDA analysis overestimates the fragility respect to the one estimated with the Non linear dynamic analysis; this lead in a reduction of the collapse capacity probably due to the fact that the building is subjected to a high intensity mainshock and the structure is likely to collapse even if a small aftershock follows the mainshock (Yue Li, M.Asce; Ruiqiang Song, S.M.Asce; and John W. Van De Lindt, M.Asce, 2014); given that it's good rule to design for the benefit of life safety and taking into account the prevention from the collapse, the non linear dynamic analysis with a *PSDM* should be less suitable to conduct a fragility analysis than a non linear IDA, at the same conditions.
7) All that exposed in the point 6 is confirmed also by the fact that, regardless the nature of the damaged system, probably the assumption of a *multi-bilinear PSDM* for representing the damage recorded in aftershock sequences may be the cause of the detachment between fragility curves; this phenomenon, infact, lead to underestimate the fragility, providing results less reliable than the IDA analysis in terms of collapse; the chaotic distribution of the seismic demands in function of intensities reflects on the graphical development of fragility curves, although their distribution in a regression surface generates small dispersions respect to the median values (measures are fitted very well); consequently results highlight their translation respect the IDA ones, allowing the system to reach the collapse for higher values of intensity, at the same limit capacities.
8) On the other hand, the assumption of the *multi-bilinear PSDM* for representing the damage accumulated in a whole mainshock-aftershock load cycle allows to obtain, for the non linear dynamic analysis, results more reliable than the IDA; also in this case the structural collapse capacity may reduce significantly if the building is subjected to a high intensity mainshock and the structure is likely to collapse even if a small aftershock follows the mainshock; infact the IDA tends to slightly underestimate the mainshock-aftershock collapse fragility.

9) The effect of past earthquakes (mainshocks) in fragility estimation has been considered in all cases, both for the degrading system and non degrading one, in particular the system is supposed to reach an initial damage (during the mainshock) always smaller than limit damage levels in correspondence of which the collapse is reached in aftershock. Obviously, if the initial damage was higher than the subsequent damage levels imposed for reaching the collapse in aftershocks, the system would have shown more vulnerability; in other words the more the initial damage is high, the more fragility curves show the highest probability of exceedance, presenting themselves less extended and less enlarged, and the more the intensity level in correspondence of which the aftershock collapse occurs translates to smaller values, at the same seismic demand and aftershock capacity levels; the more the system is initially damaged and the earlier the system will collapse.

6.7 Suggestions for future works

Conclusions and suggestions for further future developments that can be drawn from the thesis work are the following:

- The current legislation provides for taking into consideration at least a number of three accelerograms for this kind of analysis, but, for semplifying the problem in order to verify the goodness of approaches used, in this work ground motions have not been selected in function of the direction (X or Y), they have been selected in function of the direction in correspondence of which the maximum PGA is developed, regardless the direction which they develop in; no analysys has been performed in X or Y direction. The choice of the number of accelerograms heavily influences the results of the dynamic analysis, and consequently also the trend of the fragility curves, therefore, the greater the number of triads one takes in consideration, the more the estimate of the vulnerability of the building will be correct. However it is not excluded the possibility of a further implementation of the code in order to be able to consider a greater number of three accelerograms.

- In order to have a consistent sample for the probabilistic analysis applied to the results of non linear dynamic analyzes, the system is subjected to the action of 31 PGA values for the IDA analysis, but this does not exclude the possibility of implementing a different type of analysis that includes a greater number of PGA values or different intervals. An application of this type could provide assessments about the sensitivity of the fragility curves, for the same system and for the same ground motions, as the size of the statistical sample varies.
- Non-linear dynamic analysis methods in Time-history are certainly the most correct for this type of problem, that is an IDA for the aftershock collapse fragility or the Non linear dynamic analysis for the mainshock-aftershock collapse fragility. In a real MDOF structure both these approaches requires a non-negligible computational load, it is for this reason that the static schema of the model has been semplified into a SDOF system. However their application could be extended to real structures with higher d.o.f. and, if in some cases it is deemed necessary, it is possible, via OpenSees, to add details to the static scheme, such as: taking into consideration soil-pile interaction, considering the rigidity of the deck in the response of the structure to the seismic action or consider different mechanisms of non-linearity for the batteries, obviously going towards an increase, even important, of the computational burden: making it necessary to evaluate the times required by this type of analysis in relation to the level of accuracy required from the vulnerability investigation.
- To determine the dynamic characteristics in terms of fundamental period of vibration no Eigen value analysis has been conducted; at the same time geometric properties like the mass and the yield displacement are non obtained by applying a Pushover analysis. This is because, for a system like a single degree of freedom one, it’s easier to choose a priori a value of T, mass and yield displacements rather than finding it through a further analyzes, and verify afterwards the correctness of its estimate by checking results. In this way the it can be set up and modified in the best way possible in such a way that the structural response lead to a fragility estimation more similar to what it could be expected in a real case in the same conditions. It’s obvious that, if these

approaches are applied to a more complex structure, Pushover and Eigen analyzes are needed in order to precisely define the building in all its properties; they will influence results of the non linear dynamic analysis, and consequently also the trend of the fragility curves.

- Although mainshock may lead small damages to a structure, subsequent aftershocks have the potential to cause more serious damages and threaten life safety. The magnitude of aftershocks is usually smaller than the mainshocks ones, but for their ground motion intensity is not always the same; infact aftershocks may have a higher peak ground acceleration than the mainshock ones (due for instance to che changing site), even longer duration, and very marked differences in energy content. It is for this reason that, in all approaches used, a certain number of sequences is created randomly in such a way that, in a mainshock-aftershock sequence, the first eartquake may have its recorded peak ground acceleration smaller than the aftershock one and viceversa. This fortuity is confirmed for all collapse fragility estimates. For future works the mainshock-aftershock sequence may be defined in such a way that the first shock has a higher magnitude and is scaled with a higher intensity than the second one, in order to respect the classical intensity hierarchy.

BIBLIOGRAPHY

[1] Adel E. Abdelnaby (2012), *Multiple Earthquake Effects on Degrading Reinforced Concrete Structures*, PhD Thesis, University of Illinois at Urbana-Champaign;

[2] Amadio, C., Fragiacomo, M., and Rajgelj, S. (2003), *The effects of repeated earthquake ground motions on the non-linear response of SDOF systems*, J. Earthquake Engineering and Structural Dynamics;

[3] Aschheim, M., and Black, E. (1999), *Effects of prior earthquake damage on response of simple stiffness-degrading structures*, J. Engineering Spectra;

[4] Christopher Rojahn, Jon A. Heintz, William T. Holmes, Kenneth Elwood, Subhash Goel, Farzad Naeim, Craig Comartin, Eduardo Miranda, Michael Valley, Dimitrios Vamvatsikos (2009), *Effects of Strength and Stiffness Degradation on Seismic Response*, prepared for the Federal Emergency Management Agency (FEMA) P440A, Department of Homeland Security (DHS)

[5] Diego Debortoli (2013), *Procedura Automatizzata per la Valutazione della Vulnerabilità Sismica di tipologie ricorrenti di Ponti e Viadotti*, Department of Civil Engineering, University of Padova;

[6] Dimitrios Vamvatsikos and C.Allin Cornell (2006) *Direct estimation of the seismic demand and capacity of oscillators with multi-linear static pushovers through IDA*, Earthquake Engng Struct. Dyn. 2006; 35:1097–1117, published online in Wiley InterScience;

[7] Donato Sabia (2016), *Elementi di Dinamica*, lesson slides for the Seismic Engineering course, Department of Structural, Building and Geotechnical Engineering, Polytechnic University of Turin;

[8] Enrico Tubaldi, Fabio Freddi and Michele Barbato (2016) *Probabilistic seismic demand model for pounding risk assessment*, Earthquake Engng Struct. Dyn. 2016; 45:1743–1758, published in Wiley Online Library;

[9] F. Hosseinpour, A.E. Abdelnaby (2017), *Fragility curves for RC frames under multiple earthquakes*, Department of Civil Engineering, The University of Memphis, Memphis, TN 38152, USA;

[10] Fragiacomo, M., Amadio, C., and Macorini, L. (2004), *Seismic response of steel frames under repeated earthquake ground motions*, J. Engineering Structures;

[11] Gardoni P., Der Kiureghian A., and Mosalam K. M. (2002), *Probabilistic capacity models and fragility estimates for RC columns based on experimental observations*, J. Eng. Mech.;

[12] George D. Hatzigeorgiou, Dimitri E. Beskos (2009), *Inelastic displacement ratios for SDOF structures subjected to repeated earthquakes*, Engineering Structures 31 (2009) 2744_2755;

[13] Gross J.L. (1998), *A Connection Model for the Seismic Analysis of Welded Steel Moment Frames*, Engineering Structures, Elsevier Science Ltd;

[14] Hatzigeorgious, G. (2010), *Behavior factors for nonlinear structures subjected to mutiple earthquakes*, Computer and Structure;

[15] Hatzigeorgious, G., and Liolios, A. (2010), *Nonlinear behavior of RC frames under repeated strong motions*, Soil Dynamics and Earthquake Engineering;

[16] Hwang H.H.M., and Huo J-R. (1994), *Generation of hazard consistent fragility curves*, Soil Dynamics and Earthquake Engineering;

[17] Jayadipta Ghosh, Jamie E. Padgett and Mauricio Sánchez-Silva (2015), *Seismic Damage Accumulation in Highway Bridges in Earthquake-Prone Regions*, Earthquake Spectra, Volume 31, No.1, Earthquake Engineering Research Institute;

[18] Kaiser, A., Holden, C., Beavan, J., Beetham, D., Benites R., Celentano, A., Collett, D., Cousins, J., Cubrinovskid, M., Dellowa, G., Denyse, P., Fieldingf, E., Frya, B., Gerstenbergera, M., Langridgea, R., Masseya, C., Motaghg, M., Pondarda, N., Krawinkler, H., and Zohrei, M. (1983), *Cumulative damage in steel structures subjected to earthquake ground motions*, Computers and Structures;

[19] Lee K., Foutch D.A.(2004), *Performance evaluation of damaged steel frame buildings subjected to seismic loads*, Journal of Structural Engineering;

[20] Li, Q., and Ellingwood, B. (2007), *Performance evaluation and damage assessment of steel frame buildings under main shock-aftershock earthquake sequences*, J. Earthquake Engineering and Structural Dynamics;

[21] Luco N., Bazzurro P. and Cornell C. A. (2004), *Dynamic versus static computation of the residual capacity of a main shock-damaged building to withstand an aftershock*, 13th World Conference on Earthquake Engineering. Paper No. 2405;

[22] Mahin S.A. (1980), *Effects of Duration and Aftershocks on Inelastic Design Earthquakes*, Proceedings of the Seventh World Conference on Earthquake Engineerng;

[23] Meera Raghunandan, Abbie B. Liel and Nicolas Luco (2015) *Aftershock collapse vulnerability assessment of reinforced concrete frame structures*, Earthquake Engng. Struct. Dyn. 2015; 44:419–439; published in Wiley Online Library;

[24] Murat Serdar, Zekeriya Polat (2006), *Fragility analysis of mid-rise R/C frame buildings*, Department of Civil Engineering, Yıldız Technical University, 34349 Istanbul, Turkey;

[25] Rathje, E., Stewart, J. Baturay, M., and Bardet, J. (2006), *Strong ground motions and damage patterns from the 1999 Duzce Earthquake in Turkey*, J. Earthquake Engineering;

[26] Shinozuka M., Feng M-Q., Lee J., and Naganuma T. (2000), *Statistical analysis of fragility curves*, J. Eng. Mech. 126(12);

[27] Timothy D. Ancheta, Robert B. Darragh, Jonathan P. Stewart, Emel Seyhan, Walter J. Silva, Brian S. J. Chiou, Katie E. Wooddell, Robert W. Graves, Albert R. Kottke, David M. Boore, Tadahiro Kishida, Jennifer L. Donahue (2013), *PEER NGA-West2 Database*, Pacific Earthquake Engineering Research Center, Headquarters at the University of California, Berkeley;

[28] Wen Y.K., Ellingwood B. R., Veneziano D. and Bracci J. M. (2003), *Uncertainty modeling in earthquake engineering*, Mid-America Earthquake Center, University of Illinois, Technical Report No. FD-2, Champaign, Illinois;

[29] Xinyuan Yang (2013) *Seismig fragility of buildings damaged by past earthquakes*, Master Degree Thesis, University of Illinois at Urbana-Champaign;

[30] Yue Li, M.Asce; Ruiqiang Song, S.M.Asce; and John W. Van De Lindt, M.Asce (2014), *Collapse Fragility of Steel Structures Subjected to Earthquake Mainshock-Aftershock Sequences*, J. Struct. Eng.